UNIVERSITA' DEGLI STUDI DI PADOVA

Dipartimento di Geoscienze

SCUOLA DI DOTTORATO DI RICERCA IN SCIENZE DELLA TERRA

CICLO XIX

THE HYPERMOBILITY OF ROCK AVALANCHES

Direttore della Scuola : Ch.mo Prof. Bernardo Cesare

Supervisore : Ch.mo Prof. Rinaldo Genevois

Dottorando : Andrea Maria Deganutti

31 gennaio 2008

UNIVERSITA' DEGLI STUDI DI PADOVA

Sede Amministrativa: Università degli Studi di Padova

Dipartimento di Geoscienze

SCUOLA DI DOTTORATO DI RICERCA IN SCIENZE DELLA TERRA
CICLO XIX

THE HYPERMOBILITY OF ROCK AVALANCHES

Direttore della Scuola : Ch.mo Prof. Bernardo Cesare
Supervisore : Ch.mo Prof. Rinaldo Genevois
(**firma** del Direttore e del Supervisore)

Dottorando : Andrea Maria Deganutti

DATA CONSEGNA TESI
31 gennaio 2008

ACKNOWLEDGEMENTS

I wish to thank Tim Davies of the Geological Sciences Department of the University of Canterbury, Christchurch, New Zealand, who supported this research and bore its author, who worked for a long period at the same Department under his supervision. I thank him also for reviewing the thesis.

Equally I am thankful to Rinaldo Genevois who, in the role of thesis supervisor, followed and sponsored my research work for four long years.

Without the long work and mechanical genius of Rick Diehl the experimental apparatus used for laboratory experiments would have remained just an interesting abstract idea.
Simon Ruddenklau and Mike Evans have been very helpful with experimental apparatus set-up, rock samples preparation, and with testing as well.

Francesco Calvetti of Politecnico di Milano has been a precious advisor for PFC model and simulations.

I thank also Giulio di Toro of Università di Padova with whom I had interesting discussions on low friction geologic processes.

INDEX

ABSTRACT

This study focuses on rock avalanches which are large and very fast landslides characterized by volumes higher (on average) than two to ten million cubic metres with velocities of the order of tens of meter per second and are among the most destructive natural phenomena.
The aim of the research is to increase the knowledge on rock avalanches, putting at scholars community's disposal a new contribution on some long-debated questions related to some aspects of their behaviour that have not been completely understood yet.
In particular the subject of this work is directed to the transport stage of these phenomena, being the motion characteristics of rock avalanches one of the most puzzling questions in present days geological debate and none of the related theories advanced so far has been widely accepted by the scientific community.
The strangest aspect of the behaviour of fast landslides with a volume of at least 10^7 m^3 is that they travel much longer than one would expect by normal Coulomb friction mechanics, which, on the other hand, work rather well for rockslides of small volumes; this behaviour can be called hypermobility of rock avalanches.
In the first chapter of this thesis a general introduction to the rock avalanche theme and related problems is given, followed by the general aims of the present study and the scheme of the adopted methodology.
The second chapter is dedicated to the review of the international literature on the long debate on causes, mechanics and characteristics of rock avalanches, proposed theories for low friction behaviour, stated relations for maximum runout distance forecast and so on. The aim of this chapter is to give a general picture of the knowledge state-of-the-art on the matter.
Then an introductory sub-chapter is given on the novel theory of dynamic fragmentation advanced as an explanation for some geological phenomena characterized by abnormally low friction, among which the hypermobility of rock avalanches.
As an example of how dynamic fragmentation can act on rock avalanches and to give an illustration of the evidence of its effects, three real cases are presented at the end of this chapter. Two of them regard cases of rock avalanches, the third refers to a block slide, all three events happened in New Zealand.
Chapter 3 is on the laboratory part of the present research: a new concept rheometer, capable of high pressure and high shear rate, has been designed and built, in order to obtain an experimental evidence of the effect of the fragmentation in a shearing sample of rock grains. The main constructive difficulties, together with the apparatus capabilities and limitations are

described. The results of the fragmentation rheologic tests are reported and commented with special reference to the effects of fragmentation on rock avalanche behaviour.
The fourth chapter is dedicated to the development of a distinct element method (DEM) numerical model of the fragmentation rheometer; this model has been conceived for the purpose of getting a versatile and trustworthy tool capable to simulate the effects of dynamic fragmentation with reference to both laboratory rheometric tests (the numerical model does not have the structural limitations of the real one) and real low friction phenomena. The numerical model results are presented and commented; pros and cons are reported as well. The model performances have proved good and worthy of further developments.
The theses is concluded by a chapter (5) with the final remarks and conclusions of the whole study, with some future research perspectives opened by this research.
Two Appendices (A, B) are attached at the end of the Reference listing: Appendix A contains some more photographs and construction sketches of the high fragmentation rheometer with an extended set of resulted graphs. Appendix B contains more information and results of the numerical model of the rheometer with some examples of PFC (Particle Flow Code) and FISH (programming language embedded within the code) as it has been used to build the rheometer model.

RIASSUNTO

Questo studio tratta delle valanghe di roccia, cioè delle grandi frane rapide caratterizzate da volumi maggiori di (in media) da 2 a 10 milioni di metri cubi, con velocità dell'ordine delle decine di metri al secondo e costituiscono uno dei fenomeni naturali dal più elevato potere distruttivo.
Lo scopo di questa ricerca è di fornire un contributo alla conoscenza delle valanghe di roccia, mettendo a disposizione della comunità scientifica un nuovo contributo su alcuni aspetti del loro comportamento che non sono stati ancora completamente chiariti.
In particolare l'oggetto del presente lavoro è costituito dalla fase di trasporto di questi fenomeni, dato che presentano delle caratteristiche del moto che costituiscono uno degli interrogativi più discussi nell'attuale dibattito internazionale di argomento geologico e nessuna delle varie teorie avanzate finora a questo proposito è stata completamente accettata dalla comunità scientifica.
L'aspetto più strano del comportamento delle valanghe di roccia è che la distanza coperta durante la loro fase di trasporto risulta molto maggiore di quella che ci si aspetterebbe dalle normali leggi dell'attrito di Coulomb che, d'altro canto, funzionano in maniera soddisfacente con frane di volumetria inferiore; quasto comportamento può essere chiamato ipermobilità delle valanghe di roccia.
Nel primo capitolo della tesi viene presentata un'introduzione generale alla tematica delle valanghe di roccia ed ai relativi problemi collegati ed è seguita da una descrizione degli scopi del lavoro e dall'indicazione schematica della metodologia seguita.
Il secondo capitolo contiene una sintesi dello stato dell'arte delle conoscenze sulle valanghe di roccia a livello internazionale ed in particolare sul lungo dibattito sulle cause, la meccanica e le caratteristiche generali, comprese le varie teorie avanzate per spiegare il comportamento a basso attrito, nonché le relazioni proposte per la previsione della massima distanza raggiungibile da questi fenomeni in fase di deposizione.
Sempre nel secondo capitolo è contenuto un paragrafo che prende in considerazione la teoria, recentemente presentata, della frammentazione dinamica come possibile causa di alcuni fenomeni geologici caratterizzati da coefficienti di attrito particolarmente bassi, fra cui l'ipermobilità delle valanghe di roccia.
In chiusura di questo capitolo vengono presentati, come esempi della possibile influenza che la frammentazione dinamica può avere nella fase di trasporto delle grandi frane rapide, due casi reali di valanghe di roccia ed un caso di scivolamento di un grande blocco di roccia, tutti e tre questi eventi hanno avuto luogo in Nuova Zelanda.

Il terzo capitolo tratta della parte di lavoro svolto in laboratorio: con l'obiettivo di trovare delle evidenze sperimentali dell'effettiva influenza che la frammentazione di ganuli di roccia può avere nei citati fenomeni a basso attrito, è stato progettato e costruito un reometro ad alta pressione in grado di provocare la rottura di granuli di roccia posti in moto rotazionale (taglio). Vengono descritte le caratteristiche di questo apparato sperimentale di nuova concezione, le difficoltà costruttive, le sue possibilità e le relative limitazioni. Vengoni poi presentati i risultati conseguiti con gli esperimenti fatti con diversi tipi di rocce e con varie condizioni iniziali di pressione di confinamento e velocità di deformazione; tali risultati sono descritti e commentati soprattutto con riferimento al moto delle valanghe di roccia.
Il capitolo 4 è dedicato allo sviluppo di un modello numerico del reometro ad alta pressione, tale modello è costruito tramite il metodo degli elementi distinti (DEM) ed è stato concepito con lo scopo di avere a disposizione uno strumento versatile ed affidabile in grado di simulare gli effetti della frammentazione dinamica sia nei test di laboratorio (per cui il modello numerico non ha le limitazioni strutturali del vero reometro) sia per quanto riguarda i fenomeni naturali. I risultati del reometro numerico sono riportati con relativi commenti. Il modello è risultato soddisfacente e meritevole di futuro ulteriore sviluppo.
La tesi si conclude con un breve capitolo (il 5°) in cui sono riportati in sintesi i risultati conseguiti e le conclusioni generali del lavoro, con menzione dei possibili sviluppi successivi aperti da questa ricerca.
Dopo la bibliografia sono state inserite due appendici:
l'appendice A è relativa al lavoro di laboratorio e contiene disegni relativi alla progettazione del reometro a frammentazione, qualche ulteriore fotografia ed una selezione dei grafici risultanti dai test eseguiti;
l'appendice B contiene disegni e grafici relativi alla modellazione numerica del reometro, sono riportati, a titolo di esempio, alcuni listati del codice in PFC (Particle Flow Code) e FISH (linguaggio di programmazione inserito in PFC) utilizzati della predisposizione del modello.

THE HYPERMOBILITY OF ROCK AVALANCHES

Qual è quella ruina che nel fianco
di qua da Trento l'Adice percosse,
o per tremoto o per sostegno manco,

che da cima del monte, onde si mosse,
al piano è sì la roccia discoscesa,
ch'alcuna via darebbe a chi sù fosse:

[Such as that ruin is which in the flank
Smote, on this side of Trent, the Adige,
Either by earthquake or by failing stay,

For from the mountain's top, from which it moved,
Unto the plain the cliff is shattered so,
No path would give to him who was above;]

Dante Alighieri, Divina Commedia, Inferno, XII, 4-9

1. INTRODUCTION

1.1 General concepts

Rock avalanches are among the most impressive and powerful natural phenomena and, with their capacity to devastate the landscape and human works, have always been feared, despite their rarity; even Dante Alighieri, almost seven hundred years ago, in his Comedy, wrote about the famous Lavini di Marco rock avalanche (located near Trento, North Italy), which is still subject of study by earth scientists (e.g. Cuman, 2007).

The literature on rock avalanches is rather vast, comprising various arguments, from description of real cases, to studies of causes and triggering mechanisms, to transport and emplacement mechanics, to statistical investigations aimed at the possibility of runout forecast.
In the last few decades, rock avalanches are receiving increasing attention from scientists around the world. The reasons for this augmented interest are to be found in the increasing anthropic pressure on mountain environment, for tourism and development (e.g. ski fields, trans-mountain highways, oil and gas pipelines, hydropower reservoirs etc.), in many mountainous areas around the world; all these areas are potentially exposed to landslide risk. Rock avalanches, with their high destructive potential (both directly and indirectly through valley damming) have therefore become of great interest. However scientists' attention to these phenomena is also driven by pure scientific interest, given the puzzling, intriguing behaviour shown by rock avalanches.

While small landslides are generally well understood geologic phenomena which travel according to the balance of gravity and internal and basal friction, farther, with a total covered distance (runout) that can exceed 30 times the vertical drop, whereas the runout of smaller landslides is typically between 2 and 3 times the vertical drop.

The very low apparent friction in the motion of rock avalanches, also called “hypermobility” or, with reference to the slide volume, “size effect”, has generated long debates, because of the indisputable evidence of the phenomenon and because of its relevance to the possibility of prediction of the extent of the area potentially exposed to rock avalanche hazard. Unfortunately these large and destructive events are intrinsically difficult to study since data about the conditions at the time of fall, about the motion phase and about the deposition are extremely hard to get and, given their rarity, often prehistoric events are studied, where not even the original pre-

event topography of the area is known. So, almost every author who wants to study one of these big landslides has to do rough estimations even of the most important parameters like volumes, not to speak of velocities or energy dissipation. All this gives a wide field of "supposition freedom" in which every scholar can follow his or her intuitions for the interpretation of the phenomenon and, in case, for the creation of a new theory.

So, the intrinsic difficulty and complexity related to rock avalanches are second only to the interest that their destructive grandiosity exerts on experts around the world.
In order to explain and consequently to predict (at least at the level of a rough estimation) the maximum extent of the potential reach of the deposit coming from some slope instability, many different approaches have been proposed from purely statistical relations to different physical mechanisms.
These possible mechanisms are able to explain, at least in part, the long runout of some real cases of rock avalanche but fail to be a general explanation for the phenomenon and have been subject to many criticisms by other scientists.

1.2 Thesis aims

The aim of the present work is to describe the problem of low friction in gravitational phenomena (with reference to the wide literature on the matter), to review the mechanisms previously proposed and to examine with special detail the recent proposal of dynamic fragmentation as a mechanism capable of causing low friction at the base of a flowing rock mass.
With reference to this latter mechanism, the block slide phenomenon will be also taken into consideration; it is the case of a large block of rock that slides on a rock surface at a speed that is much higher than that it is possible to achieve under gravity from normal rock-on-rock sliding friction, i.e. again a question of exceptionally low friction.

The previous literature on this problem will be critically reviewed and the related low friction theories will be described together with the real cases of rock avalanches that stimulated these theories and with the most relevant criticisms that have been raised.

The study will describe in particular two real cases of rock avalanches and one case of block sliding that have been recently presented by some authors to introduce the dynamic fragmentation as a mechanism able to explain low friction in some relevant geologic processes.

The behaviour of a fragmenting shearing granular mass has been little studied so far and so there is still much to be understood.
As a contribution to fill this knowledge gap an experimental work was conducted by means of an innovative high pressure rheometer, purposely designed that is able to fragment rock grains during shearing. The basic idea is to reproduce in laboratory the motion of the rock granules at the base of a rock avalanche and to give data and information on the rheology of a shearing fragmenting volume of granular rock.

To verify further the fragmentation-low friction theory, also a numerical model of the fragmentation rheometer has been built by means of a two-dimensional particle code (PFC^{2D}) which has already been employed by no more than a few authors to simulate successfully the behaviour of various rock assembly. The numerical modelling is especially useful, once its capability to reproduce the real phenomenon has been proved, to simulate many different conditions that would be impossible in laboratory with the real apparatus (e.g. to apply external pressure much higher than the maximum possible for structural resistance reasons, in the real machine and the same with regard to shear rate and so on).
Once the model has been satisfactory implemented and its sensitivity opportunely checked, it will be possible to use it to study possible behaviour and motion conditions for real cases in which the dynamic fragmentation plays a not negligible role.

1.3 General methodology

The adopted methodology is the "classic" one: starting from the definition of the problem that is the subject of the study, it was critically outlined through the literature review.
Then, to keep the theory linked to the reality of nature, three real cases, relevant to the general interest of this research, are presented.
Since it is obviously not possible to study the detail of the rheology at the base of a real rock avalanche while it is travelling, the presented novel low friction theory is checked by means of laboratory work; this was definitely the most challenging and most demanding in terms of work time part of the study but it was a "necessary" step in the economy of the research.
Finally a numerical model has been implemented for the simulation of the laboratory tests; the necessity and utility of a trustworthy numerical model is given by the fact that it can be subjected to boundary conditions that are not possible with the real apparatus.
The chosen discrete elements model has already been proven to be reliable in modelling several geologic and geotechnical applications related to this thesis main topic; a parametric study of the model behaviour for different boundary conditions was done in order to check its sensitivity and capability to match the actual rheometer behaviour.

2. THE HYPERMOBILITY QUESTION

2.1 Literature review

2.1.1 General description of rock avalanches features

The unusually long runout of very large rock slides, called also “Sturzstrom” by the pioneer rock avalanche scholar Albert Heim, who was the first to observe and describe in details a rock avalanche (1882, quoted by Hsü, 1978): the Elm event (Switzerland, Glarus, 11 September 1881) is still not a completely understood physical phenomenon.
Since Heim, many earth scientists have approached the question from different points of view, in terms of descriptions of real cases, statistical analyses of data in the literature, and proposing physical explanations of the strange behaviour of sturzstroms.

Heim described the Elm rock avalanche deposit as similar to glaciers and, from eyewitness descriptions of the debris motion, stated that the rockfall, after a first phase in which it behaved as a rigid body, disintegrated into debris and then flowed. So he introduced his basic interpretation of a sturzstrom motion: *rockfalls do not slide, they crash, and their debris flows.* This statement is supported, among others, by Hsu (1978), and gave origin to the long debated question of “flow vs. slide” in the interpretation of the motion of rock avalanches.
In his works Heim (1882, 1932) used the term sturzstrom (literally: fall stream) to refer to the last phase of the slide in which the rock debris mass moved along the main valley on a gentle slope (i.e. the flowing stage); this word has since then been widely used by many scientists as a synonym for rock avalanche. Moreover he introduced the concept of “Fahrböschung” (travel angle) as the inclination to the horizontal of the line joining the top of the breakaway scar to the distal end of the runout deposit (Figure 2.1). The tangent of this angle is then considered (Shreve 1968) an average overall friction coefficient, the parameter which controls the motion of the sliding/flowing rock debris.
Because of the fact that a friction coefficient calculated in this way can be considered not physically correct (Hsü 1975, Davies 1982, Legros 2001), a more accurate measure would be given by the tangent of the angle of the line connecting the centres of gravity of the mass before and after the slide. However the value of the fahrböschung has been considered a measure of mobility of rock avalanches by many other authors and generally used to highlight the apparent low-friction motion for large rock avalanche. It is also worth noting that the fahrböschung is a parameter that is easy to measure by

means of a field topographic survey, while the travel angle of the centre of mass before and after the slide is more difficult and requires some difficult approximations.
Hsü emphasised that the fahrböschung line is not generally parallel to the line connecting the centres of mass of the slide mass before and after the fall, for instance, for the Elm rock avalanche the first is 16° and the second is 23°.

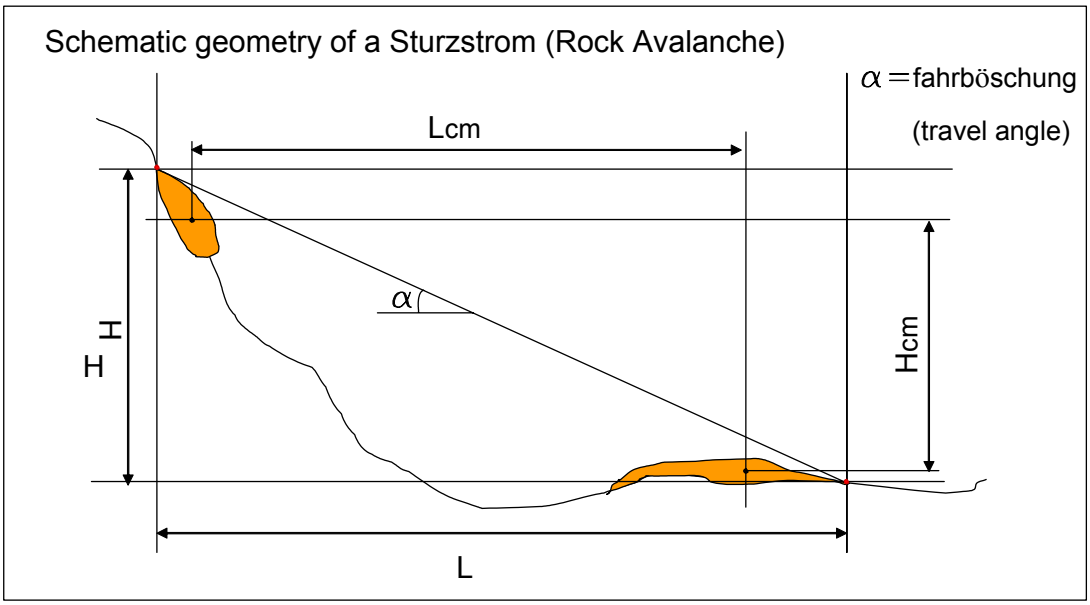

Figure 2.1 "Classical" geometrical scheme of a rock avalanche

Legros (2001) and McEwen (1989) observed nevertheless that the low friction effect of large rockslides is real, by considering as equivalent friction coefficient the tangent of the angle to the horizontal of the line connecting the centres of mass.

Following the Heim's (1882) description of the Elm sturzstrom as a flowing mass, his physicist colleague E. Müller (Heim, 1932) argued that, by analogy with the flow of a liquid, physically the fahrböschung can be analysed by considering the energy line of the motion of the flowing mass, representing at every point the kinetic energy of the flow (or the losses of the potential energy).

With reference to Figure 2.1, and following the Coulomb law of friction, we have for the apparent friction coefficient:

$$f = \tan\alpha = H/L \qquad (1)$$

where H is the total vertical drop of the rock slide and L is the horizontal projection of the travel distance. Most scholars consider the fahrböschung as α. A normal value for this coefficient is considered about 0.6, or 0.62 (tan32°)

(Hsü 1975) with reference to normal repose angle for granular materials and, by comparison between this latter value with that from a real case of sturzstrom, a measure of its hypermobility can be inferred. Hsu introduced in this way the excessive travel distance:

$$Le = L - H/\tan(32°) \qquad (2)$$

Where Le is the excessive travel distance, L and H as in eq. 1.
The physical meaning of Le is the travel of the debris mass beyond the distance one can expect from a landslide which travels with a common coefficient of friction. Hsu stated that this parameter is a more correct measure of the hypermobility of rock avalanches than the fahrböschung since the latter has no precise physical meaning and is at least inaccurate to characterize the low friction effect.
The excessive travel distance has then been used by some authors; for instance, Nicoletti and Sorriso Valvo (1991) proposed the dimensionless ratio Le/L as a mobility index.

Many authors have used data from a number of sturzstrom events to highlight sturzstrom hypermobility, generally drawing a logarithmic graph (Figure 2.2) of H/L vs. Volume. The data are generally scattered in the graph, depending on which events have been considered and on their number, but it is nevertheless obvious to observe the effect of decreasing apparent friction (H/L) with increasing volume. Hsü (1975) and Hungr (1990) commented that data scattering stating that it seems more correct to speak of a different behaviour of slides when their volume is above a few millions of m^3, rather than a systematic increase of mobility with volume; Davies and McSaveney (1999) confirmed this, showing that behaviour of large volume events is self-consistent and different from those of smaller ones..

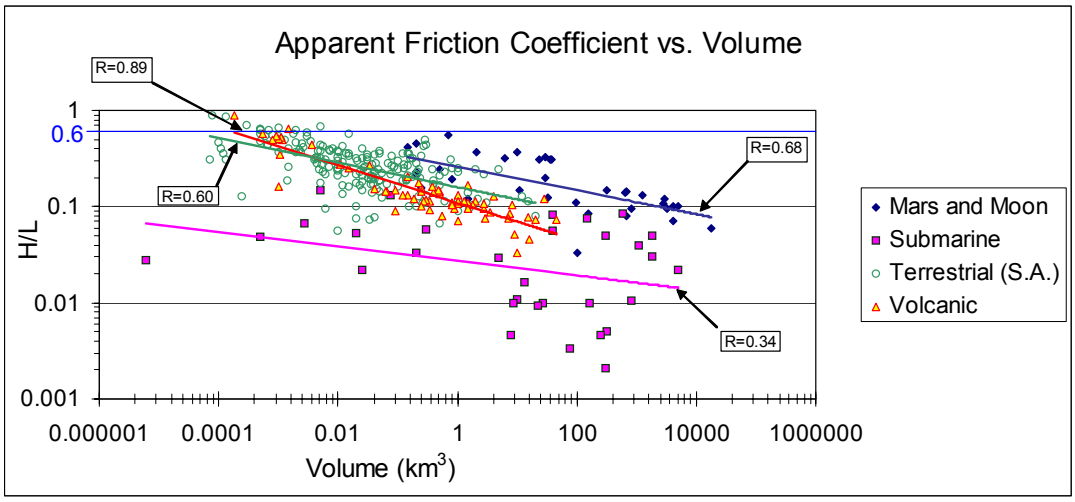

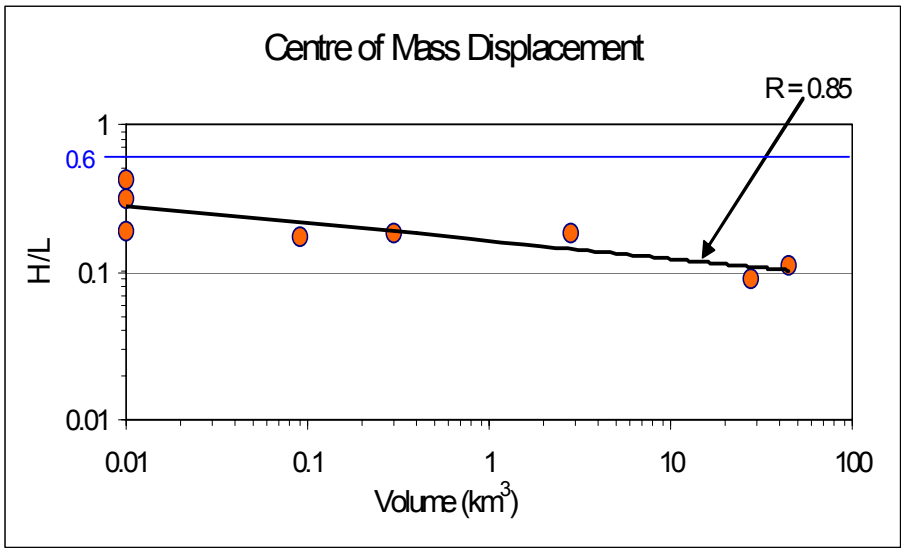

Figure 2.3 Displacement of the centre of mass of some rock avalanches. Data after Legros (2001).

Legros (2001) showed that the size effect is manifest also considering the displacement of the centre of mass of the fallen debris mass (Figure 2.3).

The first to formalize the Heim observations about sturzstroms was Scheidegger (1973) who, assuming that "the rapid motion of a small mass down a scree slope is governed by the laws of dry friction" found that rock debris avalanches travel to a maximum distance that is consistent with normal values of internal and basal friction (considering the angle of repose of rock debris: α=30°- 40° which corresponds to a friction coefficient of 0.57 - 0.83) up to a volume around 10^5 m^3 and that their behaviour changes above that value of volume becoming the maximum runout significantly higher than that the larger the volume. He did not propose a possible mechanism to explain this behaviour but, considering the data from 33 rock avalanches, calculated a regression curve between the logarithm of the friction coefficient (calculated as H/L) and the slide volume, in order to provide a tool for the prediction of maximum runout for potentially dangerous rock slopes:

$$\log(H/L)=a*\log Vol + b \qquad (3)$$

It is interesting to note that he stated that there seems to be no direct correlation between the volume and the velocity of rock avalanche, postulating otherwise a direct correlation between friction and volume; it has however to be noted that this observation is based only on 6 values (out of 33 cases) of landslide velocity, values indirectly calculated ex post facto.

Following the Scheidegger work, several other scholars, using different and more or less rich landslide data bases, proposed statistical relation for the prediction of sturzstroms runout (Hsu 1975, Li 1983, Voight et al. 1985, Nicoletti and Sorriso-Valvo 1991, Legros 2001, etc.), a general comparison among their proposed relations is given in Pollet (2004). All of them proposed an equation of a statistical regression between the apparent friction coefficient (H/L) and the landslide volume formally identical to the Scheidegger one.

The coefficients a and b of the equation 3 proposed by these authors differ for they used data from different groups of slides (the number of considered events varies from 15 to 71), introducing also volcanic slides (Voight and al. 1985, Hayashi and Self, 1992) submarine and extraterrestrial slides (Legros 2001).
A table with the resultant values for a and b (equation 3) is given by Pollet (2004) for the most prominent studies; it is possible to see that the correlation coefficient of those regressions are not very good since the scatter of data is generally wide in all the databases used and, reflecting the fact that the data come from different group of events, the values of a and b vary broadly.
A special case seems constituted by Martian slides for which McEwen (1989) found a regression with a correlation of 0.90; but Legros (2001) found 0.73 for the same data.
Thus the applicability of these equations for the assessment of the possible maximum runout of a potential rock avalanche is limited; moreover one has to add the uncertainty linked to the estimation of the possible slide volume.

To avoid this latter difficulty Nicoletti and Sorriso-Valvo (1991) propose a simple equation according to which the runout distance of large surzstroms (with volume between 5e06 and 1.6e09) ranges from 3.2 to 8 times the slide height, depending on their classification of low, moderate and high energy dissipative landslides; the same authors anyway underline that this simple relation is to be considered a rough one, valid only as a first approach.

Davies (1982) working on a sample of 14 slides with volumes ranging from 10^7 to 10^{12} m^3, argued that the length of rock avalanches deposits do not depend on the fall height, which only causes data to scatter, and obtained a regression with a correlation coefficient as high as 0.92; it is interesting to note that this is much higher than those obtained for regressions between the fahrböschung (or H/L) and the total travelled distance; on the other hand one could also observe that it is rather obvious that a debris mass of a larger volume will occupy a larger deposition area (and so a longer deposit).
Moreover he ascribed the residual scatter of data to the deposit shapes which depend on the morphology of the receiving valley and stated that, with more

and more precise data available, a family of trend lines for deposits of different shapes could be inferred.
Davies' conclusions follow the Hsu and Heim statement that the sturzstroms in the flowing stage have no "memory" of the first phase of the slide and of the fall height.

Pollet (2004) provided the most complete database about rock avalanches, gathering data from literature about 316 slides including gigantic slides on Moon and Mars and submarine ones, with volumes ranging from $6*10^3$ to $17.9*10^9$ m^3. In the relative graph H/L vs. Volume (Figure 2.2).

Other interesting observations from the wide literature on this question emerge: McEwen (1989) stated that the slope of H/L vs V correlation line for Martian rock avalanches is nearly identical to that of terrestrial slides (using Scheidegger's rock avalanches data for the latter) concluding that the effect of low friction is present in a lower gravity environment as well (gravitational acceleration on Mars is 3.72 ms^{-2}). However he observed that there is an offset between the two trend lines: at a given value of H/L, the Martian rock avalanches are on average about 50 to 100 times larger in volume than terrestrial ones (Figure 2.2).
He explained the offset stating the effect of a high yield strength of the flowing debris mass; with reference to a Bingham rheology, the slide will have a thicker deposit with a lower gravity. Moreover he said that this is a general characteristic of sturzstroms and that a size effect mechanism for rock avalanches has to be consistent with the presence of high yield strength in the flowing debris mass.
Davies and McSaveney (1999) explained the offset by the larger relief available on Mars than on Earth.

2.1.2 Proposed Mechanisms for rock avalanches long runout

Of course almost all of the scientists who have been puzzled by the rock avalanches low friction behaviour, tried to find the physical process that produces such a behaviour. Moreover many among them proposed some mechanism able to explain also other generally observed rock avalanche features, above all the retention in the deposit of the original sequential order of rock layers before the fall and the presence of ridges in the distal part of deposits, suggesting a sudden stop of the debris mass in those regions.

- Fluidization

With this term various authors meant a reduction of friction in a granular flowing mass such that it would behave similarly to a fluid. This process, occurring in the whole debris mass, would be able to explain the long runout of rock avalanches; it could however have a similar effect if it occurred only in particular regions, especially near the underlying bedrock surface. Different causes and mechanisms have been proposed for fluidization.

Heim (1882, 1932), stated that the Elm event was characterized by three distinct phases: the fall, the jump and the surge. He described the last as a flow of dry rock debris particles (sturzstrom). He observed also that the stratigraphic sequence of the rock before the fall was essentially preserved in the final configuration of the deposit, a characteristic since observed in many other rock avalanche deposits. Heim stated that the flow motion of the rock mass (once it had been disintegrated by the fall) was caused by the continuous impacts among the rock particles and this process could not be considered similar to a viscous flow of a fluid. He postulated that this peculiar process was dominant in all the large rock slides which showed a low friction, long travel character. Hsu (1975) embraced Heim's theory and observed that he postulated a grain motion that would be described by Bagnold (1954, 1956) some twenty years later in his works on turbulent flow of a dispersion of cohesionless grains. Later, Hsu (1978) deepened his position suggesting the presence of rock dust as an interstitial fluid in the grain dispersive flow, approaching in this way the Bagnold (1954, 1956) theory: the rock dust would keep the granules in suspension reducing the energy dissipation due to friction.
Davies (1982) proposed mechanical fluidization as a mechanism similar to that introduced by Heim and Hsu, stating (quoting Bagnold experiments as well) a dilation of the grain mass due to high impulsive contact pressure and the consequent reduction of internal friction. This mechanism is produced by high energy and high shear rate, concentrated in the region near the contact of the sliding mass with the stationary underlying rock bed. In this way the upper part of the rock mass remains essentially unsheared with the

consequence of preservation of the retention of sequential order. The reduction of the mass velocity under a critical value should abruptly diminish the degree of dilation in the shearing layer leading to a sudden stop of the front of the landslide; the following part of the slide will be forced to stop by the already still distal part giving origin to the lateral and transversal ridges often present in the most advanced part of sturzstroms deposits.
Mechanical fluidization has been adopted (sometimes with some variation) by a few other authors to explain several cases of real rock avalanches (Körner 1977, Voight 1978, Mc Saveney 1978). Schneider and Fisher (1998) studying an ancient volcano in Central France, stated the applicability of this mechanism to large volcanic debris avalanche.
Hungr (1990), however, questioned this mechanism stating the lack of theoretical demonstration and that there is no field evidence nor laboratory definitive proof of such a behaviour.
McSaveney (1978), in his very detailed study on the Sherman Glacier rock avalanche, suggested the existence of mechanical fluidization due to ground vibrations from the earthquake that triggered the slide; he suggested a kind of hybrid motion mechanism for the 10.1×10^6 m^3 debris mass: a sliding motion on the snow covered glacier surface with a friction as low as 0.1, above which the fluidized rock fragmented particles were in laminar motion; he noted the presence of a "crust" of undeforming material on the slide surface; this "carapace" would come from the Bingham rheology (presence of a shear strength) he adopted for the flowing mass to explain the deposition features of that sturzstrom, in particular the presence of large amount of weathered mountain surface as the surface of the rock avalanche deposit (Shreve 1966).

In addition to grain dispersive impact flow (with or without rock dust), fluidization can be the result of different (at least partially) mechanical causes: trapped air, pressurized water vapour, and acoustic vibrations.

- Air cushion theory
Shreve (1959, 1968a, 1968b) proposed a compressed air cushion as a frictionless layer at the bottom of the slide, above this cushion the slide would ride like a hovercraft (Davies 1992). Studying the Blackhawk slide in California (and later the Sherman Glacier rock avalanche in Alaska), he stated that a large amount of air was trapped beneath the rock mass as it "jumped" at high velocity over a morphological step, then compressed to generate a lubrication layer on which the rock sheet easily slid on the lower gentle slope. He asserted that this peculiar kind of motion explains all of the principal physical features of the slide deposition lobe, in particular the preservation of the original sequential order of the rock formations. For a while this theory was considered very promising, even if some doubts were raised about the possibility that the air cushion theory could well explain the Blackhawk slide

deposit features (Johnson 1978). This mechanism and the trapped air fluidization (Kent 1966) were almost abandoned when sturzstrom-like deposits were recognised on the airless surface of the Moon (Guest, 1971; Howard, 1973) even if Legros (2001) argued that terrestrial-like rock avalanches are extremely rare on the Moon and some of them are associated with impact craters and so the avalanche material could have been transported as impact ejecta as well.

- Fluidization by trapped air (Kent 1966): an upward flow of compressed air, trapped by the rock mass during the initial stage of the fall, keep the debris in a dilated state, so the friction among the rock clasts is reduced and this permits the slide to travel for long distances.
For the two authors the mechanism is able to explain the fluidization of the mass and is supported by deposit morphology and by filed evidence and witnesses experience of high pressure air blast associated to recent rock avalanche events (Frank and Madison Canyon slides). This theory has been widely questioned (Hungr 1981, Hungr and Morgenstern 1984, Cassie et al. 1988) since the body of a rock avalanche is far from a condition of airproof compactness and the compressed air, if present, would escape quickly through the moving debris mass; moreover there is lack of physical evidence for fluidization (Cruden and Hungr 1986) in real cases and in laboratory experiments.

A variation of this theory foresees the presence of water vapour generated by the presence of pore water and by the heat due to friction (Habib 1973, Pautre et al. 1974) along the sliding surface; Habib demonstrated that in presence of high pressure from the rock body and a sliding speed higher that a critical value, the possible pore water vaporizes. As in the case of air basal lubrication this mechanism requires a compact rock mass to prevent water vapour to escape, and moreover it implies the assumption of a very high thickness of the shearing block to ensure the high pressure necessary for water vaporization. Finally, there is no record of any substantiating field evidence.

Erismann (1979, 1986) introduced the concept of self-lubrication as the most promising explanation of the size effect showed by rock avalanches. His idea starts from some evidence of rock melts (frictionites) on the sliding surface of the Koefels landslide (Oetztal, Austria) and observed that the heat generated on the sliding plane is proportional to the mass thickness and so it looks reasonable as a size effect physical cause; moreover the bad heat conductivity of rock should ease the melting process. For calcareous rock avalanches Erismann (stating the Flims giant landslide as an example) proposed the high temperature tribological dissociation of rock as a possible

mechanism. The latter process falls into the gas lubrication group since the dissociation of $CaCO_3$ produces gaseous CO_2 ($CaCO_3 \rightarrow CaO + CO_2$). The difficulties in this case are the same of water vapour generation and basal air lubrication, i.e. gas proof sliding mass, lateral constraints, lack of field evidence (Hungr 1990).

-Other mechanisms
Other authors proposed different mechanisms, often, but not only, constituted by a hybrid combination of two or more previously presented mechanisms.

Nicoletti and Sorriso Valvo (1991) studying a sample of 40 rock avalanches, proposed "geomorphic controls" as the main explanation for rock avalanches mobility. They considered three general categories of geomorphic controls: channelling by lateral constraints, free lateral and downward spreading, and frontal impacting (as on the opposite slope of a valley). Consequently they called the first type of control as "low energy dissipative", the second and the third as "moderate" and "high" energy dissipative controls. Following this scheme, the mobility of sturzstroms decreases from the first to the last type.

Evans (1995) studying the rock avalanches in the Canadian Cordillera, and noticing that most of them shows enhanced mobility, stated the possible presence of different mechanisms acting separately or together as well. For the landslides which did not flow/slide on glaciated terrain (e.g. the famous Frank slide), he proposed the fluidization of valley fill under undrained loading conditions as the most probable low friction mechanism. Otherwise he said that for debris avalanche on glaciers, low basal friction sliding is realistic and the mobility can in this case be enhanced by the melting of ice and snow due to load pressure and frictional heating. He admitted also the possibility that lateral moraines can channelize the debris mass and so reducing the energy loss (as proposed by Nicoletti and Sorriso Valvo, 1991).

Watson and Wright (1967) with reference to an old (about 10.000 years) event, the gigantic (volume of 30 km^3) Saidmarreh landslide in Iran, rejected as improbable and with lack of field evidences the air cushion mechanism and also water lubrication, previously proposed by Harrison and Falcon (1938) for the Saidmarreh landslide. Instead they stated a low friction sliding on the gypsum bedrock of the valley, further eased by pulverized marl.

Erismann (1985) defending his proposal for self-lubrication by rock melting, described as possible low friction mechanisms for landslides also rolling (presence of clasts able to rotate at the base of the sliding mass, so acting as roll bearings) and bouncing of the mass on the sliding surface irregularities. He stated the energy economy of these mechanisms that can act together,

but concluded that they can have a role only for small volumes of rock since large ones would induce immediate crushing of the "rollers" and bouncing can have a role only occasionally and for some event (e.g. the Huascaran slide).

Campbell and his co-authors (1995) with a study on computer simulation of rock avalanches by means of a large number of circular particles stated that the apparent friction coefficient is an increasing function of shear rate and that larger slides travel with higher thickness and so with lower shear rate; combining these two statements they explained the size effect of sturzstrom, even if they admitted that no current granular flow theory predicts such behaviour. So, at last, they invoked an unknown rheological behaviour following which rock avalanches travel in a *transitional regime between rapid and quasistatic flow* motion. At the end this hypothesis seems rather weak.

Another transport mechanism is described by Pollet and Schneider (2004) who, studying the giant prehistoric Flims sturzstrom deposit, observed a particular texture of the material in the proximal and median axis regions. The fabric is a well recognizable structure of surfaces following the original sedimentary bedding of limestone and, according to authors, this structure suggests a slab on slab transport mechanism with finely fragmented fault-like gouge between sliding surfaces, this gouge formation assures high dilatancy and a consequent reduction of friction. The authors admitted that this particular transport mechanism is difficult to be generalized, volcanic sturzstroms, for instance, usually do not show a stratified structure.

In this wide field of alternative theories, crossed criticisms, frequent scepticism, in one thing the whole set of authors who worked on the behaviour of rock avalanches seems to agree: none of the proposed mechanisms is completely satisfying in explaining such a strange runout behaviour.
So, as for every natural mystery, the interest is great: it is necessary to go on with the research in this field!

2.2 A recent proposal: dynamic fragmentation

Davies and McSaveney (1999, 2002, 2006) studying rock avalanches deposits, observed that the material is pervasively fragmented (Figure 2.8), with smaller clasts in the lower part of deposits, often immersed in a matrix constituted of finely comminuted rock granules. Even apparently intact boulders and outcrops in deposits at a close inspection result highly fragmented (Campbell et al. 1995, Schneider and Fisher 1998, Watson and Wright, 1967, etc.), Shreve (1959,1968a) called "3D jigsaw puzzle effect" this configuration of not much deformed shattered rock. So, the observation of various degree of fragmentation is almost ubiquitous in field descriptions of rock avalanche deposits and, even if some of scholars (Genevois, 2007) think that the fragmentation process is mostly concentrated in the first stage of the fall, all of them acknowledge that fragmentation is a fundamental process in sturzstroms.
Starting from the consideration that none of the previously proposed rock avalanche hypermobility mechanisms is completely satisfying, Davies and McSaveney studied the effect on sturzstroms mobility of dynamic fragmentation, given its general importance in the process.

Schneider et al. (1999) studying the deposit features of the ancient Flims (Switzerland) giant rock avalanche, stressed the important role of rock comminution in the emplacement mechanism, in particular they emphasized the dilatancy effect produced by dynamic fragmentation with a resulting reduction in apparent friction. Pollet and Schneider (2004) in the already described slab-on-slab mechanism proposal for the runout of the same rock avalanche, again gave to fragmentation an important role, but they, introducing the dispersive inflation concept, used fragmentation as a step in the complex slab-on-slab transport mechanism. They acknowledged that this model is applicable only to sub horizontal stratified rock (Pollet et al., 2005).

Otherwise Davies and McSaveney stated that dynamic fragmentation is a necessary and sufficient condition for long runout, even if they admitted that it is not the only process contributing to runout being granular flow another necessary condition. So, dynamic fragmentation would have a prominent role in sturzstroms long runout and also in other geologic phenomena like long-runout, low angle block slides and fault ruptures, phenomena that require low friction to explain observations.

The dynamic fragmentation basic mechanism is described as follows: under the motion conditions relative to one of those low friction phenomena, the flowing grains of rock tend to form grain bridges (or arches) which are chains of particles aligned in the direction of the maximum compressive stress of the

flowing mass (45° to the motion direction). The compressive stress is transmitted through the contact between grains during motion, until the failing of the bridge. The formation of grain bridges in granular flow is a well recognized characteristic of this type of motion (Sammis and Stacey, 1994; Liu et al., 1995; Neddermann, 1992). A bridge can fail for buckling (slip or rotation of any grain) or when the weakest grain in the bridge is stressed over its strength (Sammis et al., 1987). In this case, prior to failing, a grain of intact unjointed rock is stressed and the consequent deformation imply a storage of elastic energy in the particle (Figure 2.4) until, when the rock strength is exceeded, it breaks releasing the stored energy about half of which (Grady and Kipp, 1987) is converted to kinetic energy of the resulting fragments. This emission of energy can be explosive (Figure 2.5). The effect on the surroundings is an isotropic dispersive stress and the resultant of the fragment momenta with respect to the original centre of mass is null.
The elastic energy (W) stored in a strained unit volume of rock and released by failure is given by:

$W = Q^2/2E$ (Herget 1988).

Where Q is the rock strength and E is the Young elasticity modulus.

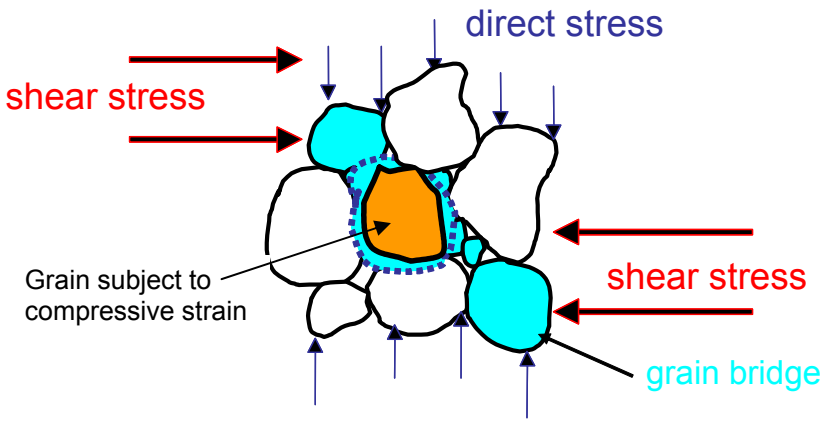

Figure 2.4 Graphical illustration of the effects of high confinement pressure and high shear rate on a flow of granular material.

In static (or quasi-static) condition a stressed rock sample begins to break when its unconfined compressive strength (UCS) is reached, but in presence of dynamic conditions, a rapidly loaded rock fails when its Hugoniot elastic limit (HEL) is exceeded. The HEL is normally higher than the UCS and for a brittle rock it is around the order of 1 GPa (Melosh, 1997), so the released energy can be around a value of this order.
Davies and McSaveney (2006) stressed that the dynamic fragmentation is different than collapse, being the latter a process of rupture of a piece of rock along pre-existing joints with no energy release, given the low strength of a joint. In the case of rock avalanches most of the fragmentation process that takes place just after the initial collapse of the rock mass is of this type, while dynamic fragmentation mostly characterizes the following runout motion.

During the runout the process of dynamic fragmentation generates an internal dispersive stress in the longitudinal direction that makes the debris mass spread to a greater extent than would occur without fragmentation (Davies et al, 1999). This resultant spreading effect produces the extended distal runout observed in rock-avalanche deposits, and also reduces the runout of debris in the proximal region of the deposit.
One-dimensional numerical modelling (Davies and McSaveney, 2002) supports the hypotheses that simultaneous fragmentation of about one grain in 200 is sufficient to explain the deposit shapes of the Falling Mountain and Acheron rock avalanches in New Zealand.
The fragmentation hypotheses for sturzstroms long runout is related to the size of the slide (size effect) since only in presence of a high confining (overburden) and shearing stresses dynamic fragmentation can take place and generate its friction reduction effect; so its process is most effective in the basal region of the flowing mass, while it is much less present in the higher part, where overburden stresses are lower and grain bridges can easily yield by buckling. This is in agreement with field observation of rock avalanche deposits; for instance the Falling Mountain one shows a superficial layer 10 m thick where the rock material is much less fragmented (Dunning, 2004); and the presence of such a "carapace" of coarse, less fragmented rock is a ubiquitous feature of rock-avalanche deposits.

To link the dynamic fragmentation theory to the field, some real cases from New Zealand, two rock avalanches, Falling Mountain and Acheron (Figure 2.6) and an association of a block slide and a rock avalanche are presented as they are good examples of how dynamic fragmentation can explain low friction phenomena.

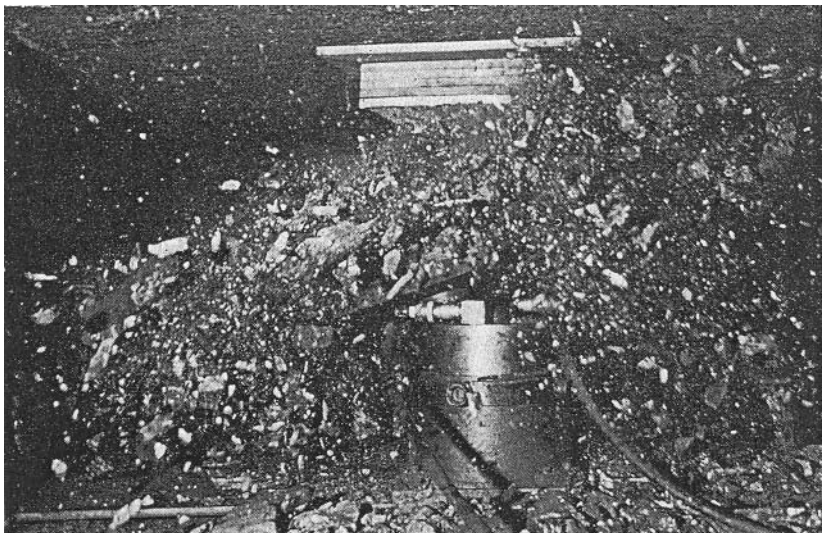

Figure 2,5. Explosion of a coal specimen during an on-site unconfined compressive test, from Bieniawski (1968).

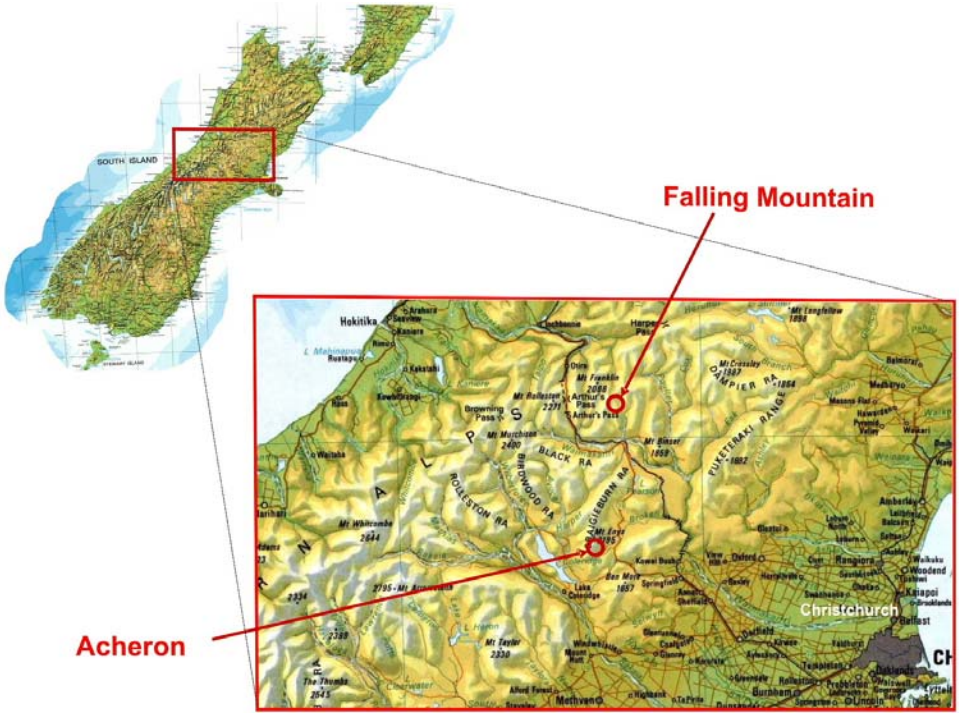

Figure 2.6 Localization of Falling Mountain and Acheron rock avalanches, New Zealand South Island

Figure 2.7 Oblique view of the Falling Mountain rock avalanche area. It is possible to see the scar, the deposit, the run-up and the long runout where the deposit has been heavily incised by the local stream. Photograph by Lloyd Homer.

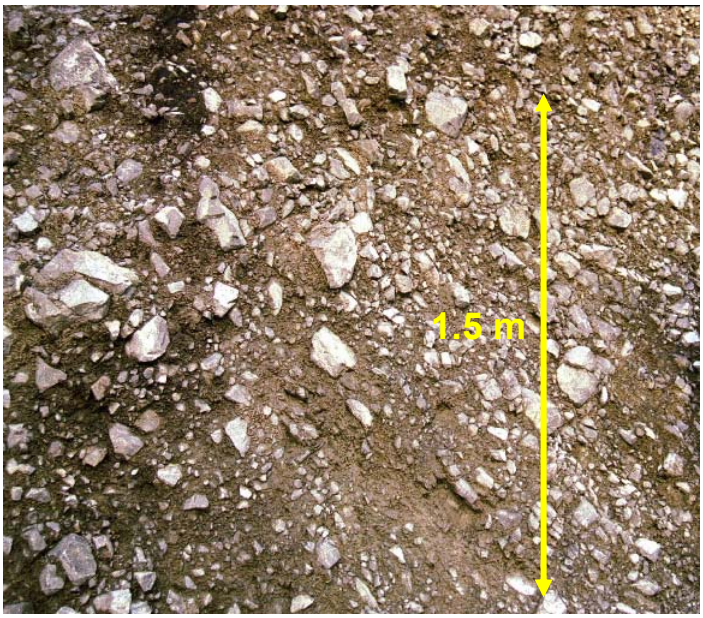

Figure 2.8 Highly fragmented clasts in fine matrix in the incised Falling Mountain sturzstrom deposit (modified from Davies and McSaveney, 2002).

2.3 The Falling Mountain rock avalanche

The Falling Mountain rock avalanche is a mid-sized sturzstrom of about 55 millions of cubic metres that presents all the "classical" characteristics of rock avalanches: long runout of 6.5 km (from top scar to distal end of deposit), a fahrboshüng of 14.8 degrees and a final deposit volume of 65 millions m^3.
It was triggered by the 1929 Arthur's pass earthquake and detached from the 1901 m a.s.l. summit of Falling Mountain (the name was given later!); most part of its western face fell down, climbed up for 250 m on the opposite valley slope and then ran down the main valley (Figure 2.7 and 2.9).

The highly fragmented clasts that is possible to observe in the deposit of this rock avalanche deposit (Figure 2.8) suggested to Davies and MsSaveney (2002) that dynamic fragmentation played a fundamental role in the emplacement of this landslide.
They observed also that on top of the deposit there is a layer (the "carapace") of much less fragmented pieces of rock and this layer has an average thickness of about 10 m (Dunning, 2004).
They stated that the fragmentation dispersive pressure reduced generally the shear resistance of the flowing mass but its most relevant effect was due to its longitudinal component which enhanced the downward motion of the debris mass; while the vertical component kept the material dilated but its effect was much less important and, being the avalanche laterally confined in a narrow valley, the transversal component had no effect on the emplacement mechanism. In the carapace the fragmentation was much less effective, given the low confining load.

Davies and McSaveney (in progress) applied the one-dimensional DAN model (Hungr 1995) taking into account the different apparent friction coefficient active in different regions of the avalanche mass, due to shear banding and fragmentation: they supposed that the friction coefficient goes from 0.1 at the base of the flow to an ordinary (no fragmentation) value of 0.7 just below the carapace. In this way they obtain a good simulation of the avalanche runout.
A positive correlation between fragmentation and runout distance for these phenomena was also highlighted by McSaveney et al. (2000) making a comparison between this rock avalanche deposit features and those of a nearby smaller landslide (South Ashburton slide) of some 300,000 m^3 of deposit volume which had no long runout, remaining most of fallen rock at the toe of the slope and where there is no pervasive fragmentation of clasts in the deposit.

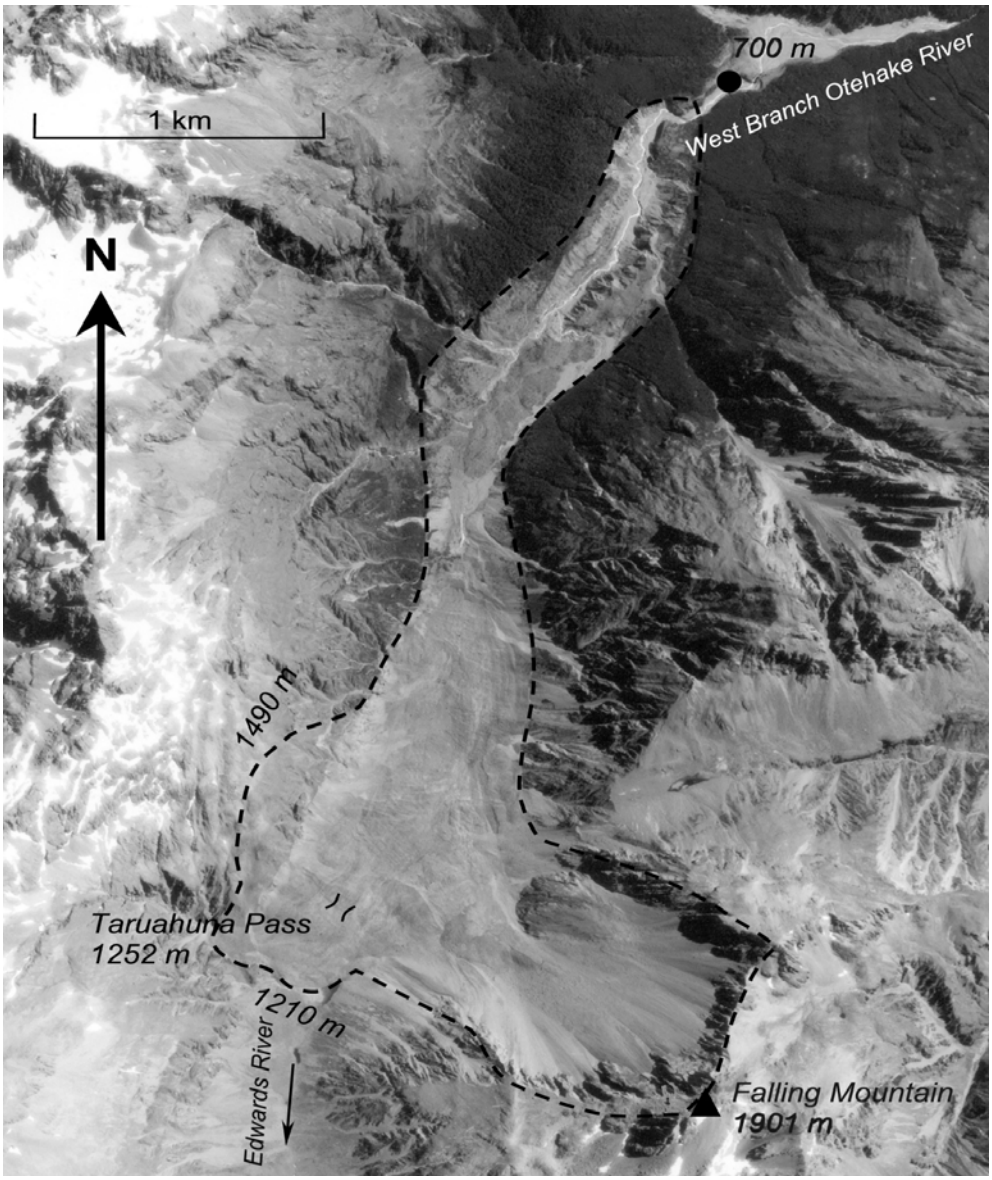

Figure 2.9 Aerial vertical view of Falling Mountain landslide, the dashed line outlines the source scar and deposit (modified from Davies and McSaveney, 2002).

2.4 The Acheron rock avalanche

The Acheron rock avalanche is a prehistoric (with respect to New Zealand written history) event of some 1100 years BP (by radiocarbon dating, Smith, 2004) and its deposit is placed in Canterbury, mid-east region of New Zealand South Island (Figure 2.6). It has a volume of 10^7 m^3 with a runout distance of 3.5 km and a total vertical drop of about 700 m (Figure 2.11).
The proximity of a system of active faults makes suspect of an earthquake triggering.
The deposit is well preserved and some incisions (especially in the distal region) permit to observe that, like in the case of the Falling Mountain rock avalanche, the deposit is mostly composed by intensely fragmented greywacke rock (highly compacted sandstone), and so it is possible to deduce that dynamic fragmentation had an important role during the landslide emplacement (Smith et al., 2005).

The detachment scar is on the East face of Red Hill mountain and its highest point is at about 1500 m a.s.l., (Figure 2.10) the rock mass flowed eastward until it impacted the toe of the opposite valley slope; here it ran up and turned sharply (about 75°) South and then arrived to a valley narrowing where the debris mass had another run-up on the right side of the valley (opposite to the first run-up) then it continued to flow for almost 1.7 km. The height of the two run-ups was of about 60-80 m.

Smith et al. (2005) performed also a dynamic one-dimensional numerical simulation of this rock avalanche event using the DAN (Dynamic ANalysis) model (Hungr, 1995; Hungr and Evans, 1996) and obtained a satisfactory reconstruction of the sturzstrom runout deposition. Using a realistic internal friction angle of 27° (the same of the repose angle of the scree now present on the avalanche scar), they simulated the dispersive pressure due to the dynamic fragmentation by analogy with an opportune setting of earth pressure coefficients, calculated by means of back analysis.
The maximum velocity calculated by the DAN model was of 45 ms^{-1}, while the velocity calculated from the two run-ups (by means of the simple Torricelli's formula: $v=(2gH)^{0.5}$, where g is gravity and H the run-up height) was of 39 and 40 ms^{-1}, which can be considered a good match.

Figure 2.10 Acheron rock avalanche source scar (red dashed line) partially covered with snow.

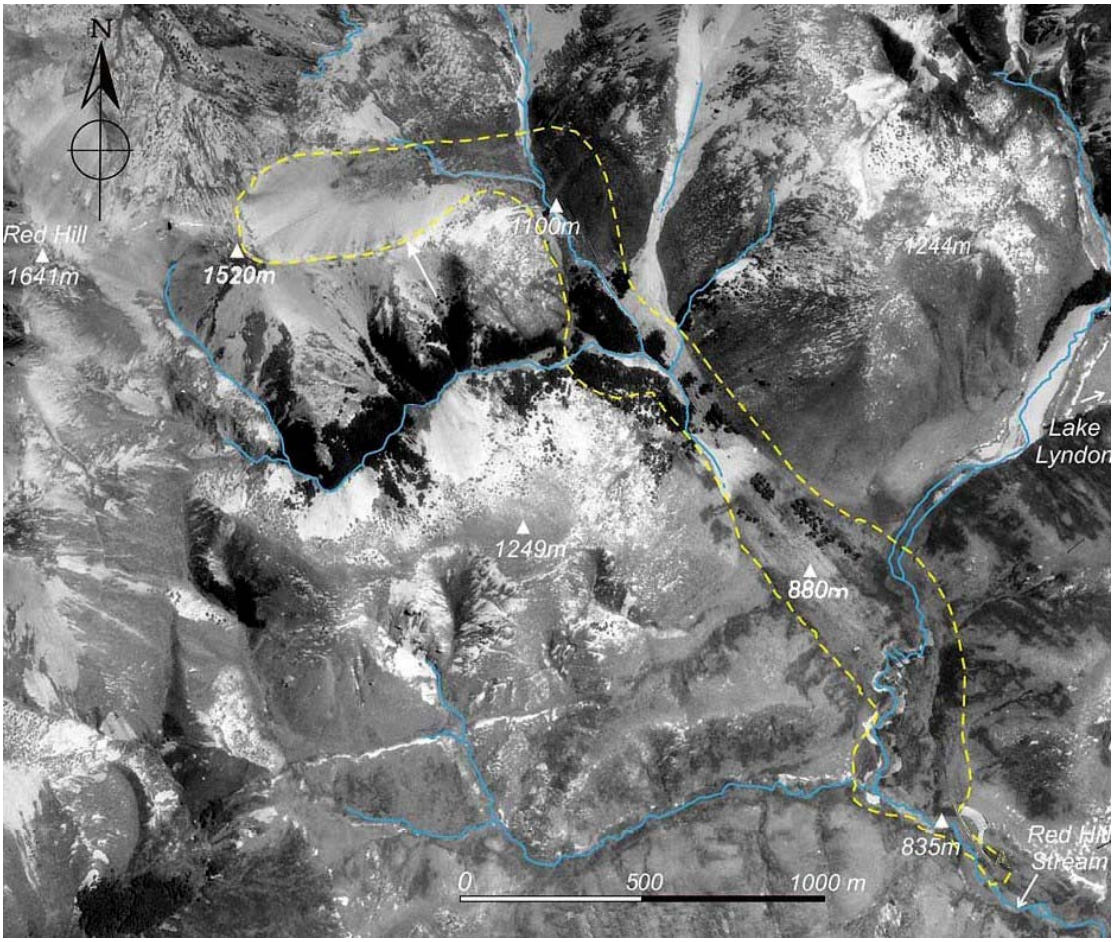

Figure 2.11 Aerial view of the Acheron rock avalanche, scar and runout path are outlined by the yellow dash line (modified from Smith et al. 2005).

Figure 2.12 Acheron rock avalanche, photograph of the lower part of deposit, the red dashed line shows the deposit limit (modified from Smith et al. 2005).

2.5 The Waikaremoana Block Slide

A particular type of low friction landslides is constituted by block slides: large and mostly intact blocks of rock that travel for a long distance on low gradient sliding planes at an unexpectedly high velocity. These phenomena for their very low friction character are closely related to sturzstroms but somehow, in their macroscopic simplicity, even more intriguing than rock avalanches' long runout.
Some studied cases of this kind of very low friction phenomena are from the USA: the Bearpaw Mountains slide (Gukwa and Kehle, 1978), the Heart Mountain slide (Prostka, 1978), Horse Creek and South Creek slides (Beutner, 1972), these block landslides are very large (volumes of order of cubic kilometres) and travelled for long distances (order of tens of kilometres) on very low gradient sliding surfaces (typically around 2° to 5°).

As in the case of rock avalanches long runout, many hypotheses have been proposed to explain this behaviour with different physical mechanisms, some of them already proposed for sturzstroms: high pore water pressure, pressurized gas (water vapour or air) layer, low residual strength of basal layers and, for the gigantic size of some of these slide, also seismic and tectonic activity.

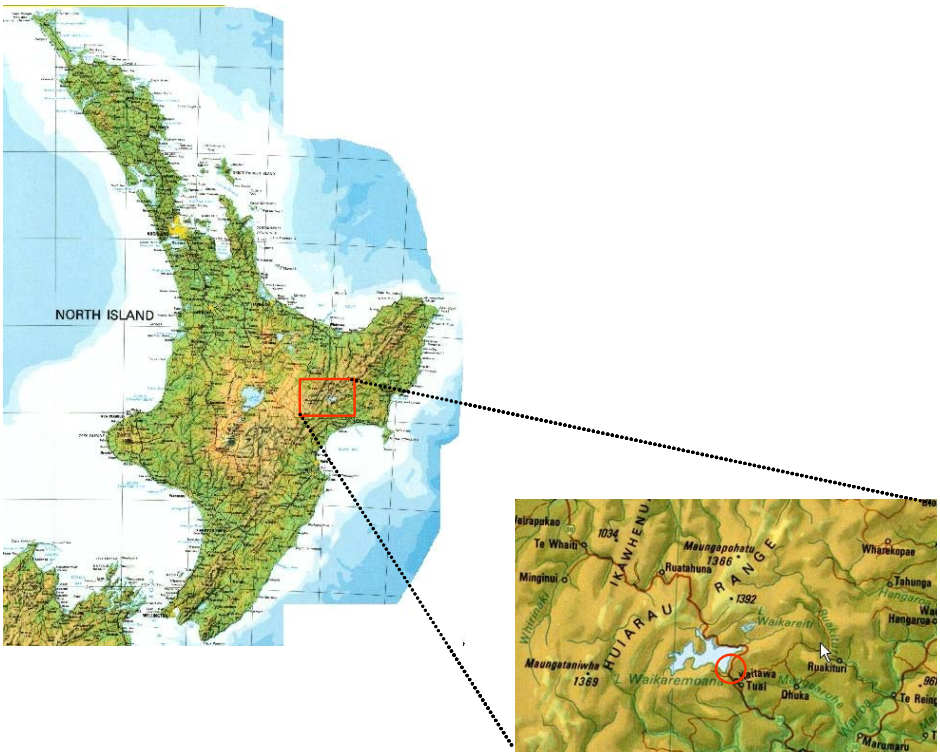

Figure 2.13 Localization of the Waikaremoana slide

And, again, none of the advanced explanations have been widely accepted. Since these slides are prehistoric, there is even not general agreement on the type of movement of these phenomena, if fast with high velocities or as slow creep over a long time.
A few decades ago a slide of this type was recognized in the North-East region of New Zealand North Island, the Waikaremoana slide (Figure 2.13) which originated the same name lake and is intriguingly constituted by an association of a block slide and a rock avalanche (Read 1979, Read et al., 1992, Beetham et al., 2002).
This large block of rock (about 3 km long, 1.8 km wide with an average thickness of 175 m) slid down with a displacement of 2 km about 2000 years ago, and was probably caused by an earthquake; the average gradient of the sliding plane is around 6.5 degrees (Davies et al. 2006), (Figure 2.14 and 2.15).

The deposit of this large event is constituted by a rock avalanche deposit of about 0.8 km^3 of rock debris (partially submerged by the lake water) and by a nearly intact block of rock of 1.4 km^3. This two different deposits had been previously thought originated by two separated events, but Davies et al. (2006) showed, also by means of a physical model, that the two events were simultaneous.
In the interpretation of the quoted authors, the slide, probably triggered by an earthquake (the area is tectonically very active) made the slope fall and a big block glided at a speed as high as 26 ms^{-1} (Beetham, 1983) while the lower part of the slope collapsed as mass of rock debris, pushed from back by the giant sliding block. At the end of its run the block impacted on the opposite slope pushing the rock avalanche mass ahead to form a debris mound 150 m high that presents evident impact pressure ridges. The rest of the rock avalanche debris deposited in two lateral tongues, one of which is covered by the lake water.
By means of their physical model Davies et al. (2006) calculated a higher maximum velocity for the block of about 40 ms^{-1} and this result permitted them to conclude that the 150 m debris mound could effectively have been created by the block push at the end of its run.

With regard to the required low friction to explain the fast motion of the rock block, Beetham (1983) made three hypotheses: the presence on the sliding surface of a thin layer of a material with very low shear strength, the action of high pore-water pressure and the formation of highly pressurized water vapour due to heat generated by friction in the first instants of movement of the block.

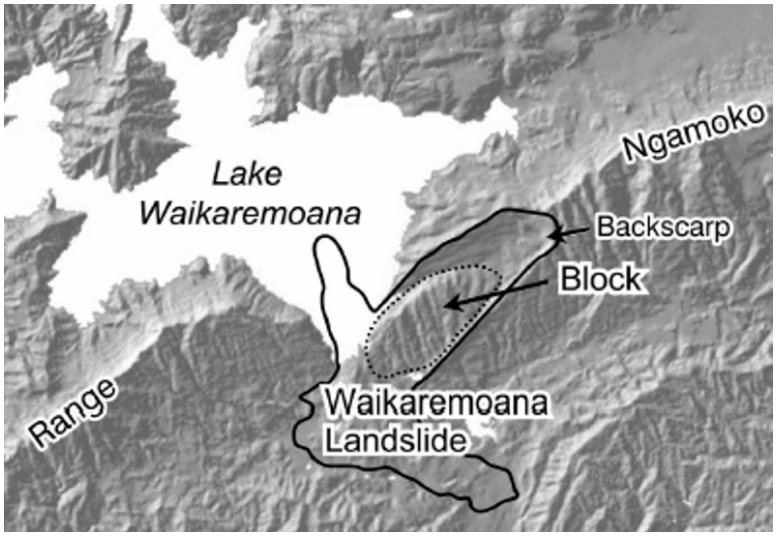

Figure 2.14 Schematic map of the Waikaremoana slide (particular from Davies et al. 2006)

Davies et al. (2006) stated that the three possible mechanisms proposed by Beetham were unrealistic or improbable, and presented, as a more satisfactory mechanism the dynamic fragmentation in the granular layer which is still present between the block and the sliding plane.
Their idea is that the shearing movement produced pervasive fragmentation in the rock grain layer beneath the block; since the layer is thin, the produced fragmentation dispersive pressure acted directly on the confining rock surfaces reducing the direct stress due to the bock weight, the shear resistance was consequently lowered, remaining the component of the block weight along the sliding plane unaffected.
A support for the fragmentation hypotheses came from the found of a 30 cm thick layer of finely comminuted material (silt-sized) on the expected sliding surface by means of a cored drill hole.

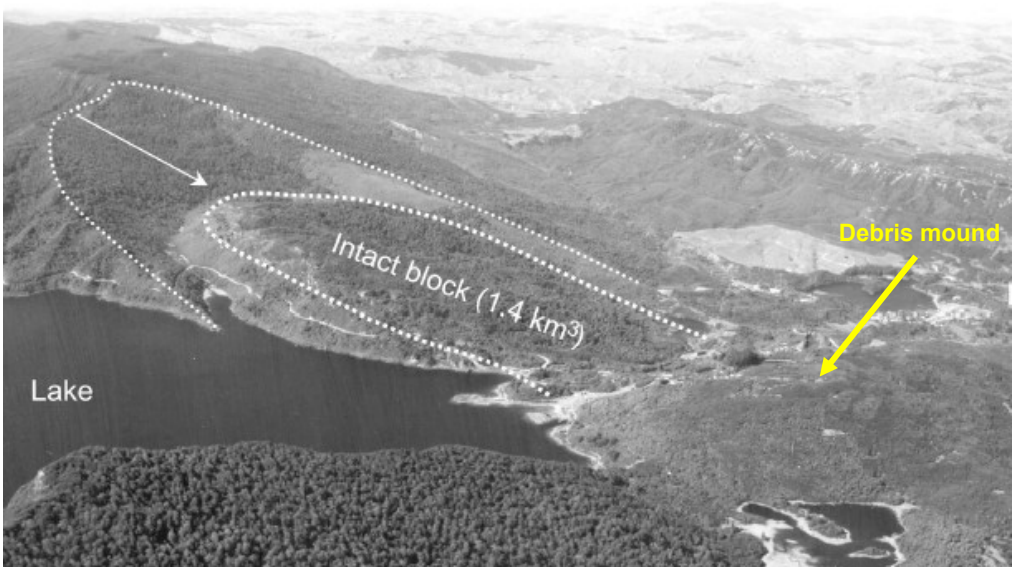

Figure 2.15 Oblique aerial view of the Waikaremoana slide (modified particular from Davies et al. 2006). Photograph by Lloyd Homer.

3. EXPERIMENTAL WORK

3.1 Introduction

In order to obtain some laboratory evidence of the role of fragmentation on the runout of rock avalanches and also on other low friction geologic phenomena, and to investigate the rheology of fragmenting material, a specially designed rheometer has been built (Davies et al., 2005).
Since the very beginning, this project looked challenging: rheometers are widely used in laboratories around the world but none was ever built capable of breaking rock granules and resisting pressures higher than 100 kPa.
High pressure shear experiments are performed by scientists who study low friction geologic phenomena (especially the slip-weakening in faults during earthquakes) by means of laboratory tests use high pressure shear boxes in which rock on rock shear is performed with limited strain, with no consideration for the fragmentation process, even if gouge is formed during the test (e.g. G. Di Toro et al., 2004).

3.2 The Fragmentation Rheometer

The problems to solve were many and consequently the design and the construction have been intensive and time-consuming processes: high resistance steel and special high speed/high load bearings had to be used. At the end, even if the basic concept on which the machine is based is rather simple (to shear granular material under high confining pressure), the resulting apparatus is quite mechanically complex; a drawing of the resulting apparatus is reproduced in Figure 3.1.

The idea is to try to reproduce the internal stress conditions of a large rock avalanche; high direct and shear stresses are applied to the granular rock sample, causing the fragmentation of the particles during shearing. So it was the starting of a new research field: the laboratory study of the rheology of fragmenting rock particles. The aim was to get a better understanding of the motion of large masses of rocks where fragmentation is a ubiquitous process.

Following the basic shape of a "classic" cone-and-plate rheometer (Deganutti and Scotton, 1997) the new rheometer consists of a steel cylinder with a cone-shaped sloping (9 degrees) floor. The cylinder is rotated relative to a circular stationary cover plate (lid) which is put on the sample and is free to move vertically. So, the sample space is a cylindrical annulus with a trapezoid

section. The average depth of the sample cell is 7 cm, the width in radial direction is 5 cm (sketches with sizes in Appendix A, figure A.1, A.2).

Rheometer working scheme: a vertical load is applied to the lid by means of a loading arm (Figure 3.2) at the end of which a weight is suspended.

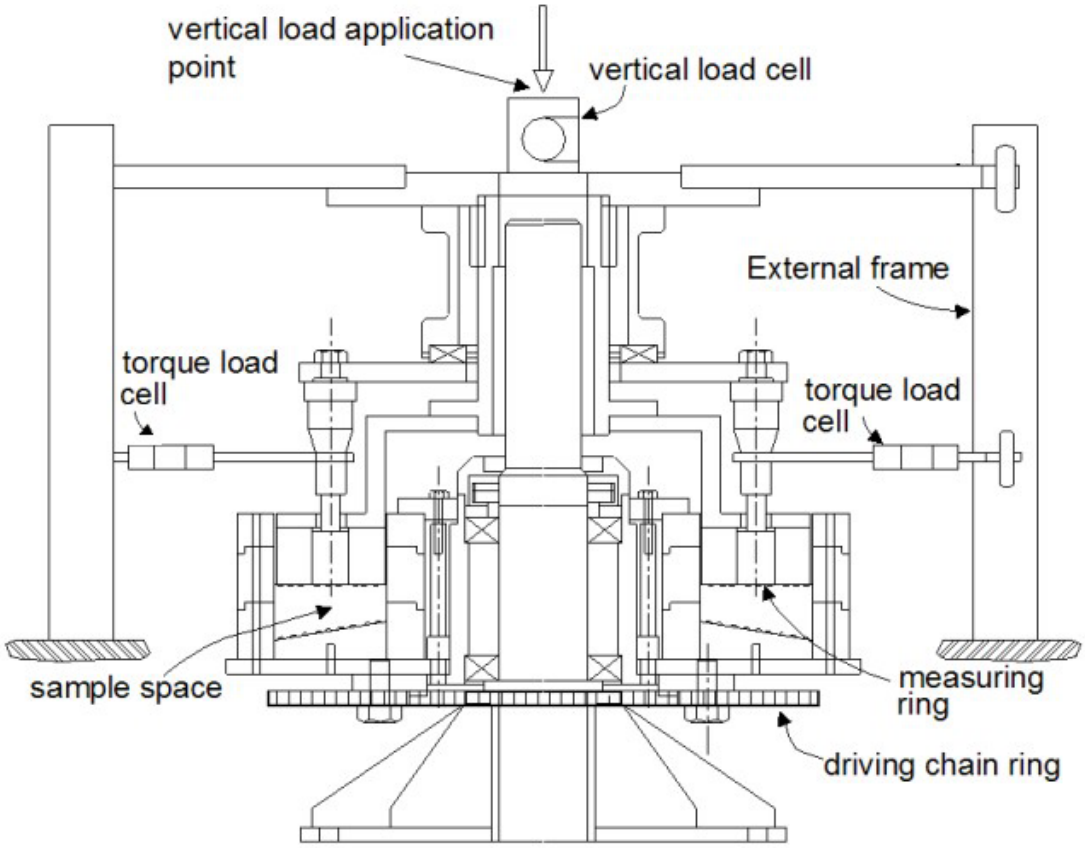

Figure 3.1 Fragmentation Rheometer mechanical scheme.

A load cell placed between the vertical load application point and the cover plate measures the direct load and hence stress during tests. A central annular ring in the cover plate is free to rotate independently; the reaction torque due to the frictional drag of the shearing material on the cover plate is measured (Figure 3.2) by means of two load cells mounted on steel arms connected to the annulus (measuring ring) (Figure 3.3).

The geometry of the “bowl” (sample space) was aimed to reduce possible secondary (i.e. radial) movements of the rock particles while shearing, assuring a reasonably constant shear rate and hence shear stress in the column of material that is under the measuring annulus.

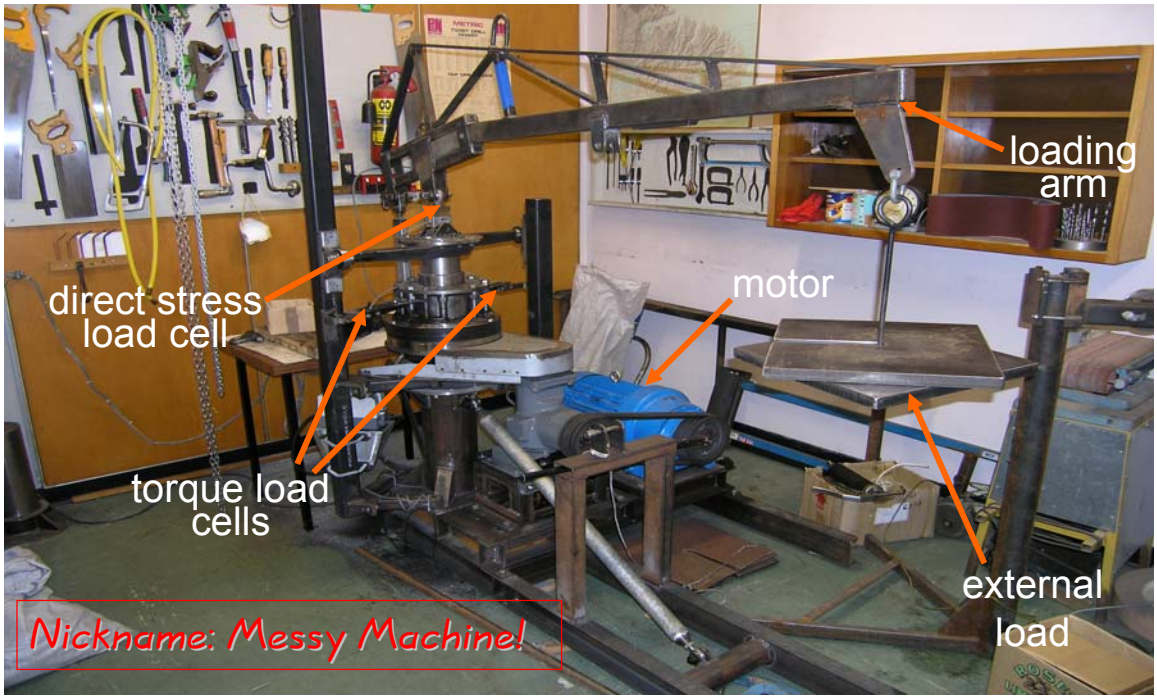

Figure 3.2 General fragmentation rheometer apparatus set-up

A particular building problem arose from the necessity of provide a certain roughness on the floor and on the inner side of the cover plate in order to prevent slippage of the material at the bottom and in contact with the cover plate. A 4 mm roughness was adopted (Figure 3.3) using rivets.

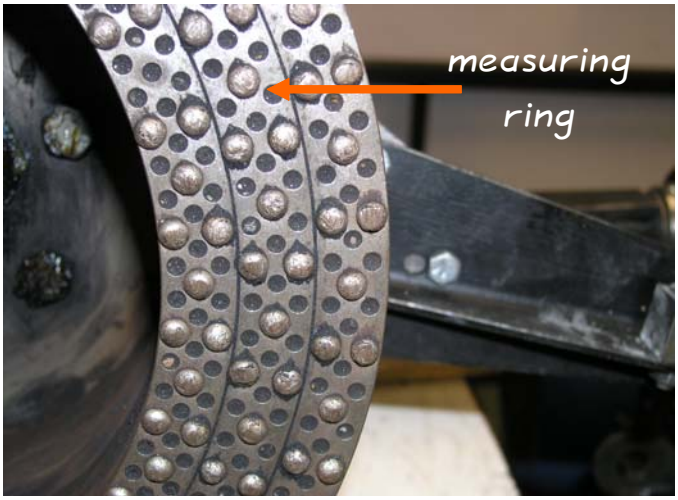

Figure 3.3 Inner side of the rheometer cover plate (lid) and particular of the measuring ring and of the rivets roughness.

Another problem to be solved was that of the rock dust generated by fragmentation which could enter the small clearance gaps between rotating and stationary parts of the rheometer and between the measuring annulus and the other parts (inner and outer rings) of the cover. This latter problem was solved by pumping grease into the small clearances through grease nipples; the grease reduces the friction between the surfaces of the two rings and prevents the rock dust entering the small clearances.
Some rock dust could anyway escape from the clearance between the cover plate and the rotating cylinder (bowl) this was not a big experimental problem, but it was enough for the apparatus to be nicknamed "messy machine" at the Geological Sciences Department of University of Canterbury (New Zealand)!

The three load cells were connected to a PC system through a wiring board, an acquisition card and software Advantech GeniDAQ. Data were recorded at the highest rate that was possible by the adopted data logging hardware-software system (33 Hz, sample time=0.03 s).

A set of first trial tests were done to test the mechanical soundness of the apparatus and several modifications were made afterwards: change of motor with a more powerful one, the substitution of the transmission system, from a belt one (which had shown a tendency to slippage) to a double chain system and of the gear box with a more robust one, that was necessary after a gear breakage during a high load test.
Eventually the calibration of the load cells was done, the acquisition software was set up and the apparatus was ready to work.
This apparatus was designed and built at Lincoln University, the tests have been conducted at Lincoln University and University of Canterbury.

3.3 The Tests

To perform a single test was quite a long process, from breaking and sieving the rough pieces of rock to get the required initial size of rock particles, to greasing the measuring ring, to applying the load, to operating the data logging software and the final operations after every test (vacuum emptying of the sample cell, weighting and sieving the fragmented sample). A test required about 3-4 hours to complete. In Appendix A the check list of test operative procedure is reported.

A critical experimental condition was the start of a test and especially the load application: since a hydraulic jack was used to lower the loaded cover plate onto the sample, the time during which the sample itself was experiencing increasing load was a function of the applied load; in the resulting stress data it was difficult to distinguish the "retarding effect" due to the loading time taken by the jack from the initial and most important phase of the fragmentation effect.
We also tried to do some tests starting the rheometer rotation with the loaded cover plate completely lowered on the sample but the required starting torque was very high so a strong mechanical stress occurred in the driving system with very loud noise and huge oscillations of the loading arm; so this way to start a test was abandoned (Appendix A, figure A.12).
To reduce as much as possible the effect of the load application time, the lid was just raised to the minimum height permitting the free rotation of the bowl, so the lower side of the cover plate was about 1 mm above the sample.

Different rock materials were tested, with different loads and different grain sizes: coal, limestone, argillite, glass, rock salt.

External loads of 25, 50, 100 and 150 kg (corresponding to a load of about 200 to 1250 kg on the rheometer lid) were applied.

Grain size: after having tested samples of various sizes, the following sizes have been chosen to standardize the tests: 2 to 4 mm, 4 to 8 mm and 8 to 16 mm, also in consideration of the dimensions of the sample test space. Occasionally bigger grain sizes were tested (up to 40 mm).

After the first tests it was noticeable that not all the sample was sheared during the test, in fact the usual configuration in the "bowl" after a test was constituted by an upper layer of finely fragmented material, beneath which there was a layer of more or less intact rock granules, down to the bowl floor, the interstices of the intact grains were filled with fragmented material (Figure 3.4).

The fragmented fraction of the sample was generally between 10% and 65% by weight, depending on rock strength and on external load.

Figure 3.4 Situation of the sample (in this case coal granules) after a test: a layer of unfragmented material remains in contact with the bowl floor, while a thin layer of coal dust coats the sample.

The tests were performed at three different rotation velocities: in the first series the rotation speed of the rheometer was of 13.8 revolutions per minute (1.44 rad/s); then the rotation speed was almost doubled having been increased to 25.5 rev/min (2.67 rad/s) and for the third series of tests the angular velocity was further increased to a value as high as 108.5 rev/min (11.36 rad/sec) in order to test the dependency of the recorded shear stress on the shear rate.

Afterwards with the term friction and friction angle, the apparent measured friction effect (calculated as the ratio of shear and direct stresses) is meant; in this measure different processes are involved that affect motion resistance (friction among grains, friction between grains and boundaries, fragmentation effects…) and therefore the term is useful but not physically correct; this terminology assumption is similar to that of considering the ratio H/L as a general "over all" friction coefficient for rock avalanches (Chapter 2).

3.4 First stage of fragmentation rheometry: preliminary tests

First of all it was possible to observe, upon repetition of tests in the same experimental conditions, that the tests results were reproducible.
From the graphs of stresses vs. time it was possible to infer that most of the fragmentation (in this phase the dispersive stress due to fragmentation reduced the direct stress on the sample, reducing consequently the friction) took place in the first moments of a test, probably in less than a complete revolution of the bowl, especially with high loads. In fact generally the lowest values of the friction angle (calculated as the arctangent of the ratio of shear and direct stress) was recorded at the very beginning of tests (after a time of about a few tenths of second). A similar behaviour has been seen by G. Di Toro et al. (2004) during rock on rock shearing lab tests, even at low shear velocities and much smaller scale.
As already said, it was not possible to separate the effect of sample loading, which involves reduction of pore space by compaction, from that of fragmentation, which involves also creation of new pore space within originally intact particles. However, one would still expect the shear and direct stresses to vary together during loading, while the rheo tests showed a low ratio of the two; so it looks reasonable to assume that the variation of friction recorded is real.

When the loading of the sample was complete probably an important part (sometimes most of it) of the fragmentation had already taken place.
For this quick process, the shear rate in the sample was not constant as not all the material was sheared and the depth of the effectively shearing grains changed quickly due to fragmentation, so the shear rate values went from 10-20 s^{-1} at the very beginning of a test to 50 s^{-1} (to 200 s^{-1} with the higher rotation speed) and to even higher values when only a very shallow layer of finely comminuted material, with no further fragmentation, was shearing.
This can be considered a shear band behaviour, often described as a characteristic of real granular flows (Mueth et al., 2000; Davies and McSaveney *in progress*).

Since, as said, the most of the fragmentation occurred in the first moments of shearing, the data recording rate limit of 33 Hz was an impediment to a deeper study of that important phase of fragmentation rheometry. As an improvement of the apparatus for the continuation of the fragmentation research a higher rate acquisition system is necessary.

The argillite we tested was quite a hard rock and we had not significant fragmentation (Figure 3.5); after a quick initial phase of a few sample times (matter of some hundredths of a second) in which low friction values were

recorded, the friction goes up to normal values (Figure 3.7). As a result of the non-fragmenting behaviour, argillite average friction angles resulted between 35 and 45 degrees, similar to those measured in unloaded condition by means of a tilting plane. The initial low friction behaviour is probably due to rearrangements of particles and some "smoothing" of their surface (rounded granules and rock dust was found in the bowl after the test).

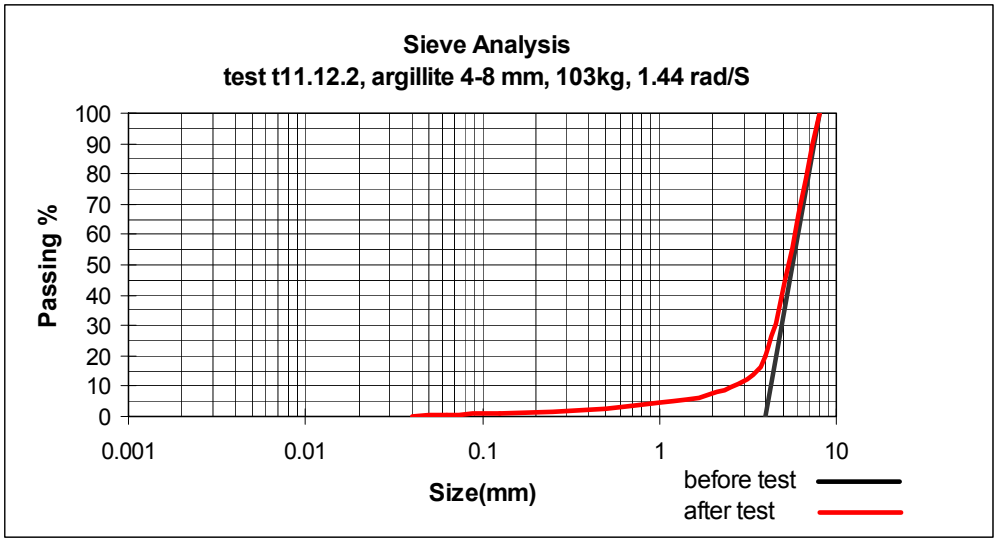

Figure 3.5 Sieve analysis before and after a hard rock test, the comminution rate is very small (about 20%).

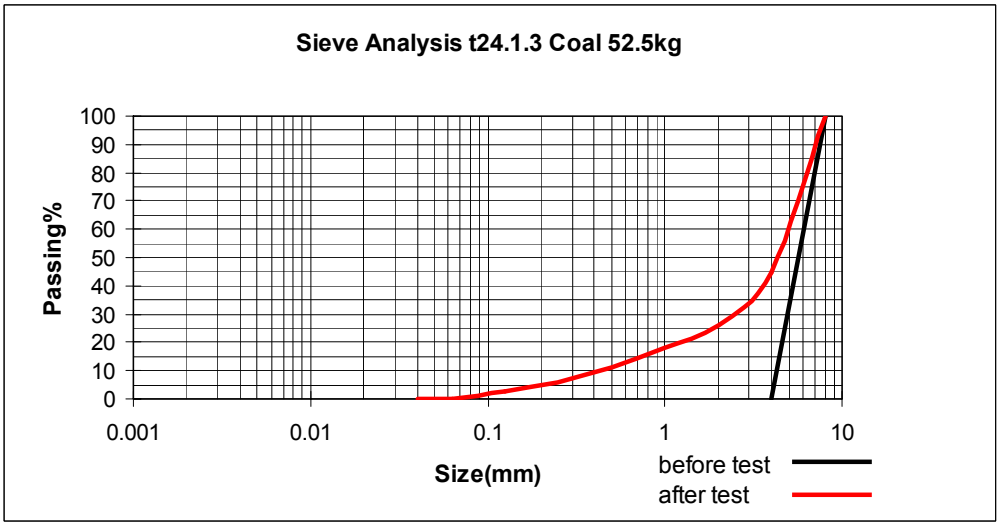

Figure 3.6 Sieve analysis for a coal test, the fragmentation rate is about 45%.

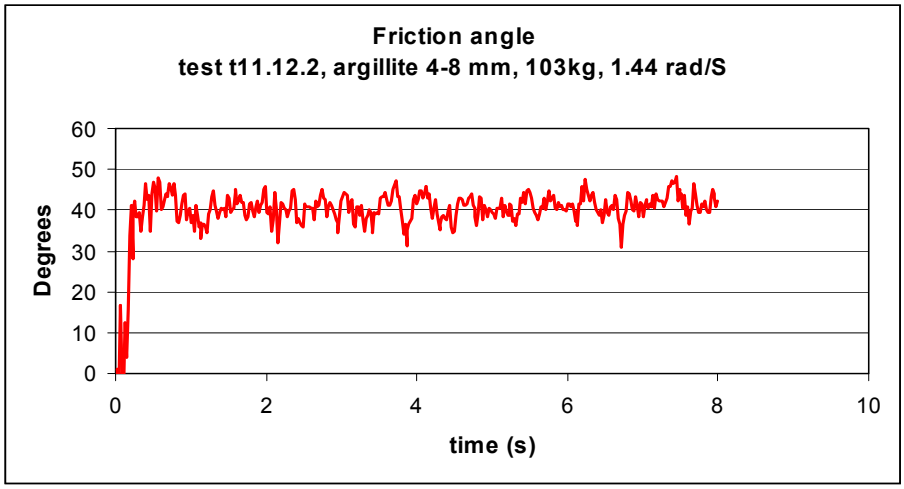

Figure 3.7 Friction angle vs. time as a result of a rheo test with argillite.

With coal the results of tests were different, since the material is brittle and less hard than argillite, the fragmentation is effective (Figure 3.6) and starts almost immediately when the plate touches the sample and a few values of the friction angle as low as 5 to 15 degrees are recorded.
During this starting stage these low friction values are due to the combined effects of rearrangements of particles (initially they are in a loose state) and fragmentation; then it is possible to note (Figure 3.8) an increasing shear stress with time, probably due to the fact that the rearrangement of particles has no more effect while the low friction effect (Figure 3.9) of fragmentation is

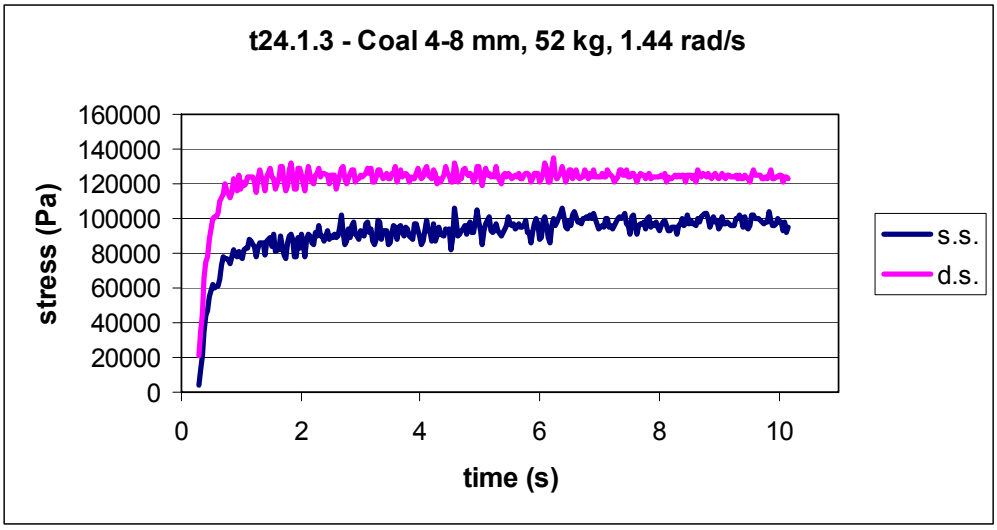

Figure 3.8 Typical shear and direct stresses vs. time graph for coal, most of the fragmentation takes place in the first two seconds of the test; s.s.=shear stress, d.s.=direct stress.

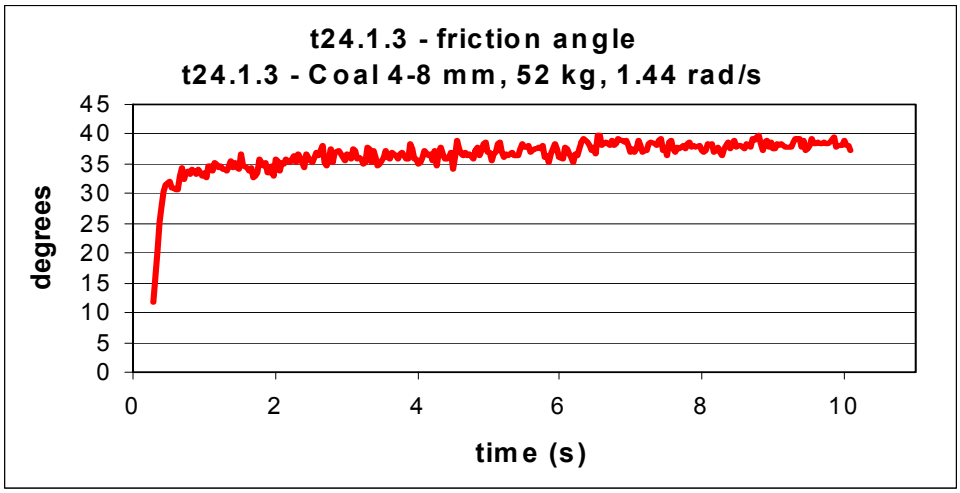

Figure 3.9 Friction angle values for coal in the same test conditions as in Fig. 3.8.

still present and progressively becoming less important along with the reduced amount of particles available for fragmentation and, at the same time, that there is an increasing volume of pulverized coal which can play a damping role on fragmentation kinetic energy (as said, after test the upper layer was constituted by very fine coal dust). The percentage of the fragmented material goes from 40% to 70%, depending, of course, on the applied load.
The tests with limestone granules (from a local quarry) gave results similar to those of argillite (Appendix A, figure A.7) with the difference of the production of a higher amount of fine rock dust during the tests, since this type of rock was less hard than argillite. The limestone rock dust did not come from fragmentation but rather from a process of "surface grinding", the granules clearly appeared rounded after a test; this process had not influence on the recorded friction.

The behaviour of glass chips (from a glass recycling firm) was more or less the same as coal, but with a smaller fragmented fraction (around 30%) and an average lower friction during the tests with a friction angle of about 25°- 27° (values recorded for glass chips 2 to 4 mm, figure A.8 in Appendix A), values which were significantly lower than those measured, for glass particles of the same size, in unfragmenting conditions, by means of a tilting plane (obtained values of 35 to 37 degrees).

The smaller fragmented fraction can depend on the shape of the glass chips, which were rather flattish, more similar to small lenses than to grains, and on the low surface roughness. The low recorded friction could also be a consequence of the fact that glass is a homogeneous material and its strength does not vary from place to place as rock does. So, the fragmentation of glass is normally more energetic than rocks, since cracks propagate much more rapidly through the whole of a fragment. So it looks reasonable to think that fragmentation pressures would be consistently higher.

3.5 Second stage of rheometric research.

Because the increase (by about a factor 2) of the rotation velocity of the rheometer cylinder (and consequently of the shear rate) did not give the expected rise in fragmentation rate (friction angles similar to that of not fragmenting materials), in the second stage a considerable increase of the rotation velocity (from 2.67 to 11.36 rad/s) was achieved with some major modifications of the experimental apparatus. Other changes included a substantial strengthening of the containing frame (to reduce the experienced vibrations at the highest loads).

From the point of view of the tested rock materials, it appeared that the apparatus was only able to fragment coal at a significant rate. So the second stage of research concentrated on this material, with a short series of tests with rock salt granules.

To know better the mechanical characteristics of the coal that was available for tests (it was Giles Creek coal from the West Coast of the South Island of New Zealand) in this second stage of rheometric study a series of point load tests were performed on a number of specimens of various dimensions. The measured point load strength was very variable, ranging from 0.5 to 2.1 MPa, on the basis of about 80 tests, with no evident relation with the specimen dimensions.
Obviously the coal was anisotropic and non-homogenous presenting flaws and joints at any size; during the point load tests some lumps broke in a "soft" way, others with an explosion of numerous fragments. Anyway the average behaviour of the Giles Creek Coal when loaded over its strength was that of brittle failure (Bieniawski, 1968); and so it was an acceptable "candidate" for fragmentation tests.
Looking for another brittle and not too strong rock material, rock salt was tested as well; point load tests gave an average strength a little higher than coal, going from 1.2 to 2.0 MPa. The failure type was always less "energetic" than that of coal (there were no explosive breakages).

Three sizes of coal (2-4 mm, 4-8 mm, 8-16 mm) were tested in the rheometer at three different external loads (50, 100 and 150 kg, corresponding to a load on the lid of 470, 865 and 1255 kg and a direct stress of about 120, 220 and 320 kPa on the sample)).

The effect of fragmentation in this series of tests at high shear rate can be described as follows: there is (as in the tests with lower shear rate) high fragmentation (low friction angle) at the beginning of tests, then the fragmentation (Figures 3.10, 3.11) goes on at a slower rate for a while

(variable with load and sample size) as the sample is compacting with fine particles filling voids among bigger ones. Friction increases until the fine fraction packs between the lid roughness rivets (Figure 3.12), reducing their effectiveness and the inner side of the cover plate becomes a progressively flatter surface that slides on the compacted layer below with a reduction of friction that lasts for a few seconds (the duration of this phase highly depends on test conditions) and then the friction angle becomes constant; this is a situation of almost pure sliding with no more shearing material.
This behaviour is clearly visible in the "coal 4-8 mm, 100 kg" friction angle vs. time graph (Figure 3.11), while with a lower load (50 kg) the friction reduction after a maximum is not evident (Appendix A, figure A.9); with grains of the same size and a 150 kg load the maximum in friction is reached in a shorter time than in the 100 kg test and the following friction reduction is more pronounced (Appendix A, figure A.10). In the latter test there is more "noise" in the data, due to higher load and the consequent mechanical disturbance (especially vibrations of the loading bracket).

The results of the high shear rate tests for smaller particles (2-4 mm) showed a similar behaviour with a lower friction maximum which was attained in a longer time; it is reasonable to think that for smaller particles, given the apparatus limitations, there is a lower comminution possibility; this trend for 2-4 mm coal grains was very similar for different loads (Figure 3.13).

With big grains (8-16 mm) a higher scatter of data was observed at all external loads, it is my impression that this scatter was due to the larger voids created by the big grains failure, while the behaviour described for the 4-8 mm particles was still evident but it was "compressed" in a much smaller time range (Appendix A, figure A.11) of about 0.4 - 0.5 seconds and the "peak" friction was around rhe same values as with smaller particles.

With rock salt only a few tests with rather large chunks (16 to 32 mm) have been performed. The results of these tests were quite different than those with coal (Figure 3.14): it is possible to observe a large scatter of data, especially in the first moments of the test, due, as in the case of large (8-16 mm) particles of coal, to the big chunks used, fragmentation of which produced high but localized fragmentation pressure and a high degree of compaction for big voids shrinkage; unlike coal, however, the average friction angle after the initial peak was significantly low, resulting between 20 and 30 degrees.

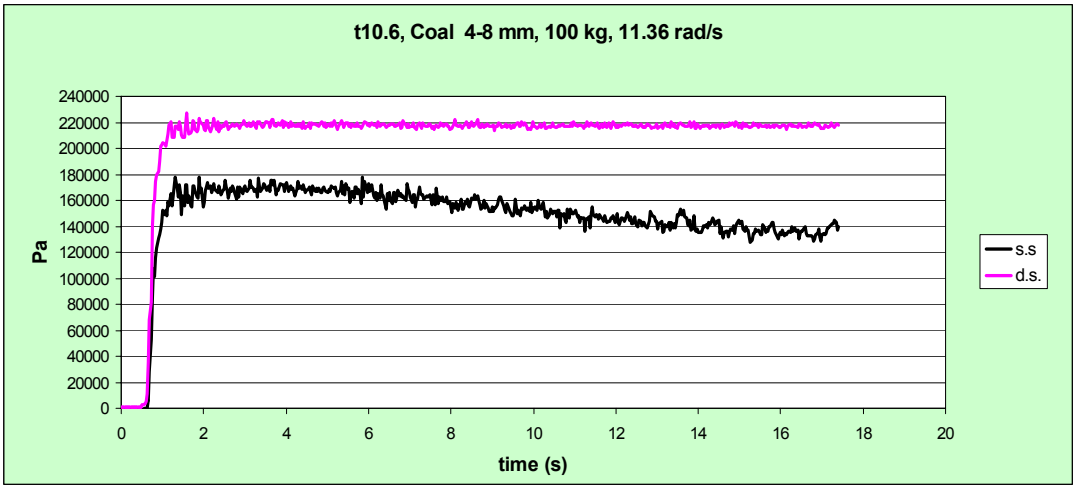

Figure 3.10 Shear and direct stresses in a high shear rate test with coal

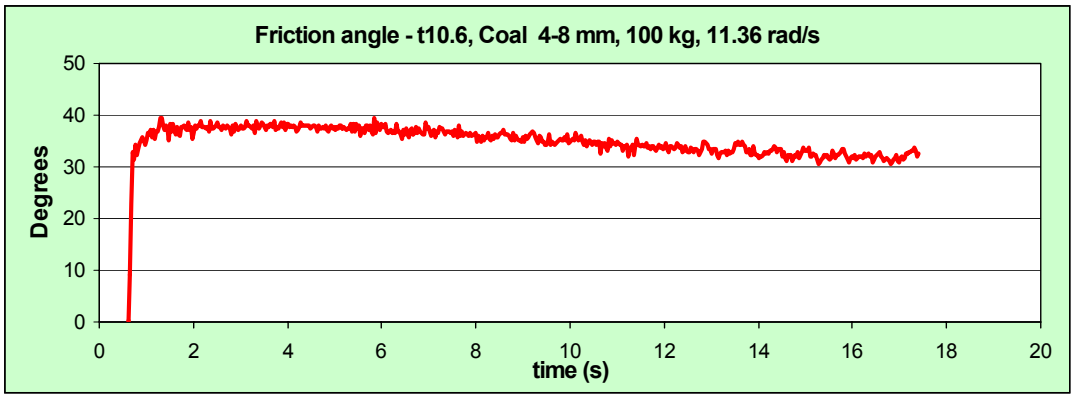

Figure 3.11 Friction angle for the same test of Fig. 4.10

Figure 3.12 Compacted coal dust on the inner side of the cover plate after a test

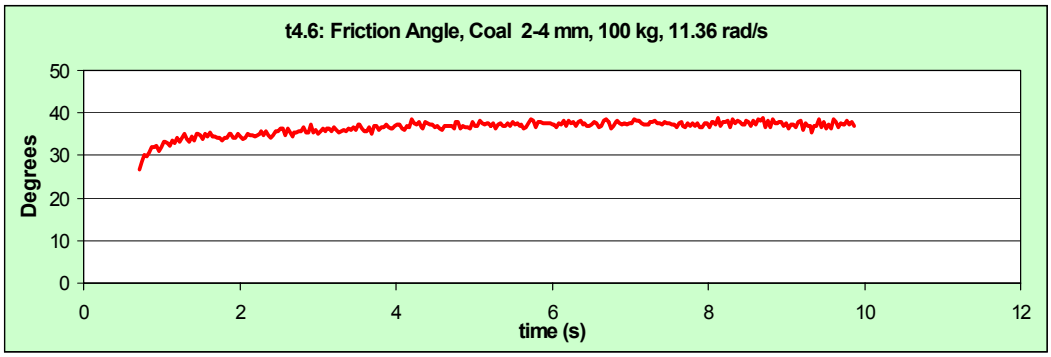

Figure 3.13 Friction angle graph for a test with small coal particles

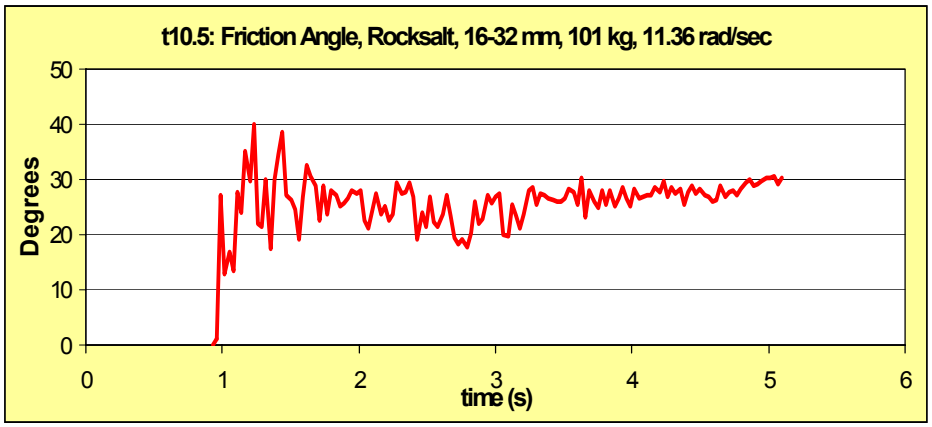

Figure 3.14 Friction angle graph for rock salt

3.6 Other type of fragmentation experiments

As a collateral "branch" of this research on fragmentation, a series of quasi-static and of highly dynamic fragmentation tests of hard rock pebbles have been performed. For the first type of experiments a high pressure apparatus for unconfined axial load tests was used with argillite and greywacke (highly compacted sandstone) specimens; the dimensions of the pebbles was around 50 to 80 mm.
The dynamic tests were performed by means of a falling weight of about 5 kg that was released from a height of 2 m and made fall on a rock lump. During both the experiments video film was taken with a high speed video camera (200 frames per second) in order to measure the speed (kinetic energy) of the resulting fragments.
With the quasi-static breaking tests the failure of the rock specimens was energetic with a loud noise (especially with greywacke) and major cracks opened but with no explosive features, only small fragments detached from the lump. The measured velocities for those fragments in video shots were not very high, being between 1 to 5 m/s.

The breakage induced by the falling weight was much more dramatic with hard greywacke pebbles completely shattered in small fragments which flew away at velocities from 1 to 13 m/s, with peaks as high as 26 m/s (maximum). So it looks that the released fragmentation energy is closely related to the loading rate, an effect that was also perceptible in the rheometric tests as the shear rate increased after the augmentation of the rheometer rotation speed from 2.6 to 12.4 rad/s.

3.7 General observations on the rheometric tests.

The rheometer proved capable of effective fragmentation of brittle and not very hard granular materials as coal, rock salt and glass; harder rock grains are only superficially ground with production of rock dust without fragmentation.

The tests are reproducible, same external conditions of confinement pressure, rotation velocity, rock type and grain size yield very similar data for stresses and friction.

The induced shear rate in the sample is not constant, it depends on test conditions and varies with time during a test (since fragmentation reduces the depth of shearing material); moreover on the cell floor always a layer of intact

particles remains. This latter situation is probably due also to a wall effect of the cylindrical cell.
This situation is similar to the shear bands which are present in real fragmenting granular flows.

Most of the fragmentation takes place in the first moments of a test; the comparison between non-fragmentation tests (hard rock) and tests with fragmentation (coal) permits to observe an initial sharp increase of friction in the first case, while friction increases slowly (i.e. with a longer phase of low friction) in the second. It is reasonable to conclude that this evident difference is due to the fragmentation pressure since breaking of grains is the only process difference between the two situations. The pure friction among grains does not play an important role since the "peak" friction angle in the two cases is about the same (40°).

The duration of the first low (and increasing) friction stage, which ends with a maximum in friction, decreases with load, with grain size and, obviously, with the rotation velocity; the following friction reduction phase is generally decidedly longer and its duration until a constant friction is attained, is related to load, grain size and rotation speed in the same way as the initial friction increasing stage.

The observed macroscopic behaviour in our tests was similar to that recorded in other studies on high pressure shear tests on fault gouge, even if with lower shear rate and higher direct stress (Mizoguchi et al. 2007); their experiments highlighted a lowering of friction with increasing of shear rate while in out tests we saw that the increment of the shear rate just makes quicker the observed processes.

4. NUMERICAL MODELLING

4.1 Introduction

In order to try to illustrate further the dynamic fragmentation process, a numerical model of the high pressure rheometer has been implemented. Starting from the consideration of the interesting and useful applications of discrete particle computer simulations about the behaviour of rock avalanches transport mechanisms that have already been presented by some authors (e. g. Staron, 2000; Cleary and Campbell, 1993), to build this model a similar approach has been chosen: the distinct element method (DEM) and the code PFC (Particle Flow Code, from Itasca Consulting Group) was adopted.

Born as a tool to study the behaviour of granular material in motion, PFC can model directly a physical phenomenon that is related to the motion and interaction of granular particles.
It is also possible to build a granular material composed by particles of chosen shape by bonding any number of elementary particles together. In this way new objects are created and can move independently from the others and also break down or not, depending on the logic used in their constructions (clusters or clumps).

4.2 Theory

Every single distinct element (particle) is free to move independently of the others and all interact only at contact points; particles are non deformable, but support a "virtual deformation" concentrated at the contact point (and not over a finite area that would be in the case of contact between deformable bodies). In this case the particles can overlap and the contact point is assumed placed in the overlap region, in central position along the line connecting the two particle centres (point C in Figure 4.1).
The normal force F_n at this point is calculated by PFC by means of the force-displacement law (Hooks law):

$$F_n=K_n a \qquad (1)$$

in which K_n is the characteristic normal stiffness of the particle and a is the overlap distance (virtual deformation) as in Figure (4.1).
With regards to shear force, the calculation is made with reference to displacement difference: the change of the shear force during one time step is

$$\Delta F_s = k_s \Delta a_s \qquad (2)$$

where k_s is the shear stiffness of the particle and Δa_s is the displacement difference (or incremental displacement); K_s is conceptually different to K_n since the latter relates total displacement and force, while K_s refers to incremental displacement. The new shear contact force is then calculated as the sum of the last shear force with its change over the time step.

Finally, the new position of a particle is calculated by integrating twice the Newton II° Principle:

$$F_i = m \frac{d^2 x_j}{dt^2} \qquad (3)$$

where x_i is the displacement of the i_{th} particle over one time step, F_i is the resultant of force vectors acting on the same particle and m its mass. An equation formally similar is solved for rotational motion.
Of course, equations (1), (2) and (3) refer to force and displacement vectors.

These full dynamic equations of motion are solved following an explicit centered finite difference scheme (Cundall and Strack, 1979; Calvetti et al., 2000). The time step is chosen very small for the purpose of limiting calculation disturbances to the immediate particle neighbours. It is assumed that particle velocities and accelerations are constant within each time step. This scheme is useful given its ability to model dynamic problems accurately and efficiently; it allows dynamic waves to propagate through the simulated continuum (rock) in a realistic way (Hazzard et al., 2000).

Bonding a certain number of particles each other, PFC can model a brittle solid, by bonding every particle to its neighbour; the resulting assembly can be considered a solid that has realistic properties (elasticity, strength) and is capable of breaking when the internal bonds strength is overcome.

Since PFC is a particle code, it is not possible to create an initial arbitrary shape of compacted particles, because there is not a sole way to fill a given volume with circular particles. A chosen volume delimited with defined walls has to be initially filled with balls (or disks) which can freely overlap and then the particles are allowed to acquire a compacted state, with the possibility to increase the particle radius in order to get the required porosity. Analogously, one has not the possibility to specify the initial stress state: the contact forces depend on the relative positions of particles.
Moreover, the freedom to choose boundaries of arbitrary shape is "paid" with a more complicated setting of boundary conditions.

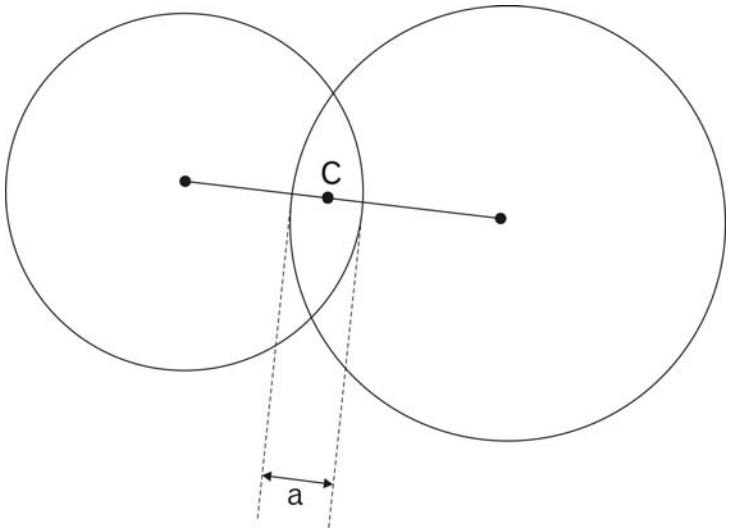

Figure 4.1 Contact between two elementary particles.

So, to model a solid continuum with PFC is a process that involves a certain amount of trial and error procedure, because the match of real geometry and behaviour adjusting size and micromechanical parameters of the elementary particles is not easy.

4.3 PFC^{2D} model of the fragmentation rheometer

The discrete element approach has already been successfully applied to model different geological processes like shear banding in granular flows (Antonellini and Pollard, 1995), faults slipping during earthquakes (Mora and Place, 1998) and even rock explosion (Donzé et al., 1996).
In particular Hazzard et al. (2000) demonstrated the ability of PFC to simulate failure of competent rock under compression and the relative emission of energy upon formation of cracks and fractures.
As in the case of the real rheometer with the term friction and friction angle the apparent measured friction effect (calculated as the ratio of shear and direct stresses) is meant; as previously stated, in this measure different processes are involved that affect motion resistance and therefore the term use is justified but somehow "illegal".

4.3.1 Model description.

To simulate the fragmentation rheometer, PFC in two dimensions (PFC^{2D}) has been used: the rock material is represented as a large set of circular disks of uniform thickness.
The adopted code works in two dimensions, while the actual rheometric fragmentation tests are (obviously!) tri-dimensional; as a consequence, our model represents what happens in a tangential vertical section placed in mid position under the measuring ring of the rheometer. This ideal section would be a plane rectangle, while in the real case particles move along curved (circular) trajectories, but the considered section is small and besides, the fragmentation process that we need to simulate is not different if grain paths are curved or rectilinear; so it was considered that this assumption (which is necessary since the used code is two-dimensional) permits an acceptable model of the real situation.

Moreover, since in the real rheometer the sample is composed by a number of grains that are continuously sheared and fragmented by the rotation of the apparatus, we had to find a way to permit a recirculation of the material in our two-dimensional model. So a circular ring has been "built", it is constituted by two concentric circular walls with 5.1 cm of clearance in between (the average sample cell depth under the measuring ring of the real rheometer); this ring lies on a plane which is vertical and tangent to the circular trajectories of the grains in the real rheometer, in central position with respect to the measuring annulus; therefore the rotation axis of the model is orthogonal to that of the actual rheometer (Figure 4.2).

Initially the space between the two circular walls was filled with as many as 20,500 disks with diameters randomly distributed between 1.2 and 1.8 mm (Figure 4.3); this small range of elementary disk diameter was chosen for calculation stability reasons. At this stage the disks are chaotically disposed between the two walls, they overlap freely and there are wide voids (Figure 4.3).
Then a porosity as low as 0.2 was chosen to get a rather compacted assembly and the particle radii have been multiplied by an appropriate factor to get the wanted porosity. Then the particles have been allowed to expand.

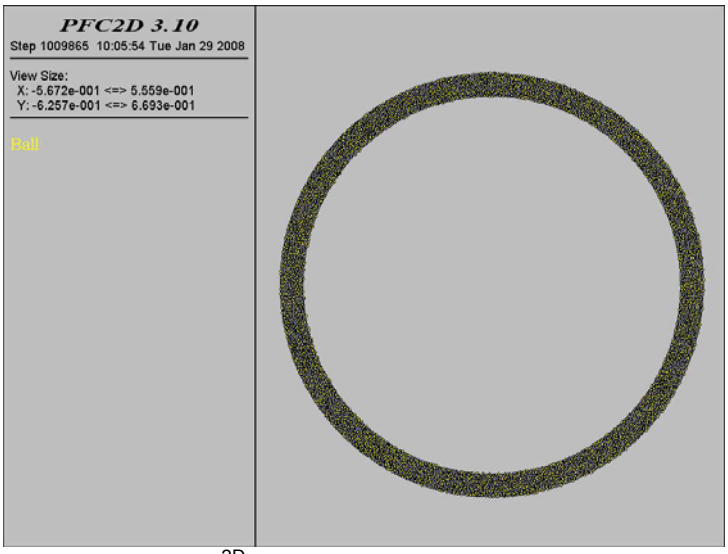

Figure 4.2 PFC^{2D} model of the fragmentation rheometer: two circular walls and 20,500 elementary disks.

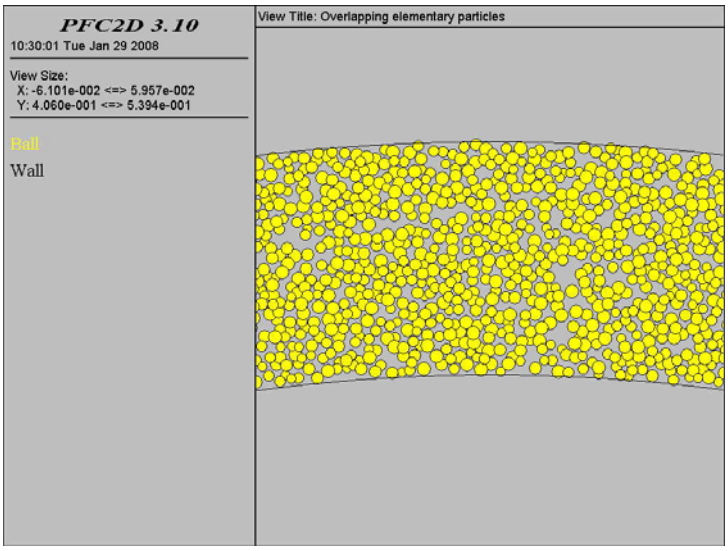

Figure 4.3 Initial configuration of elementary elements (enlarged particular).

and relax for as many as one million cycles of calculation. At the end the model was completely relaxed (no overlapping of particles) with unbalanced forces reduced to the order of 10^{-6} N.

The non-slip condition on roof and bottom (obtained with rivets in the real rheometer) was achieved by a very high friction coefficient (10) between disks and circular walls. The friction among disks was set to 0.5.

A difficulty arose because PFC elementary rounded particles (disks) do not break and in order to simulate the fragmentation process we developed a special procedure using the PFC embedded programming language FISH, and a set of clusters of elementary disks was built. In a cluster the disks are bonded together at contact points, the strength of bonds is chosen in relation to the real strength of the simulated rock (coal): 1.5 to 2 MPa, depending on elementary particle size. Two sizes of clusters have been built: 1000 of them with and average diameter around 1.5 to 2 cm and an average of 20 elementary disks per cluster and a set of as many as 3000 clusters with an average diameter of 1 cm with an average number of about 7 elementary disks per cluster (Figure 4.5). Every cluster is independent from the others. The clusters were created when the whole set of particles had settled down after 1 million cycles at a confining pressure of 100 kPa and 320 kPa (two sets of them were created with the purpose to check the effects of the confining pressure on clusters building and their behaviour during simulations).

The actual rock grains are thus represented by clusters of chosen size which can break when the stress induced by the external load and by the motion

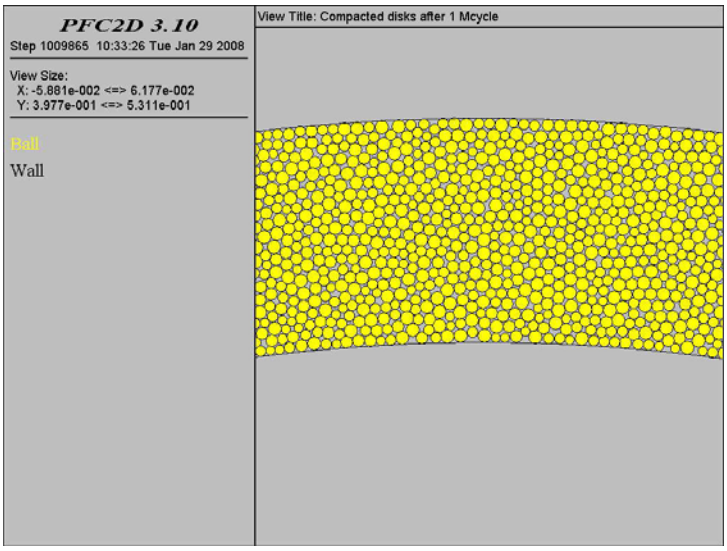

Figure 4.4 Disks configuration after espansion and compaction obteined after 10^6 calculation cycles.

exceeds the intra-cluster bond strength.
This way to simulate a rock body as a two-dimension assembly of bonded circular disks has already proved successful (Hazzard et al., 2000).
The values for disks stiffness and clusters bond strength have been chosen by similar models (Calvetti et al. 2000) keeping into consideration the real values (point load tests) of the rocks that had been tested with the real rheometer; some correction is necessary, Hazzard et al. (2000) demonstrated that, since the PFC disk model is an abstraction with respect to the real rock internal structure, it is always necessary to adjust the real values of rock mechanical parameters in order to get the most realistic behaviour of the PFC model.

It is evident that the fractal character of fragmentation (Davies and McSaveney, 2006) is not reproduced in the model since the PFC elementary particles cannot break and they are smaller than the clusters by only an order

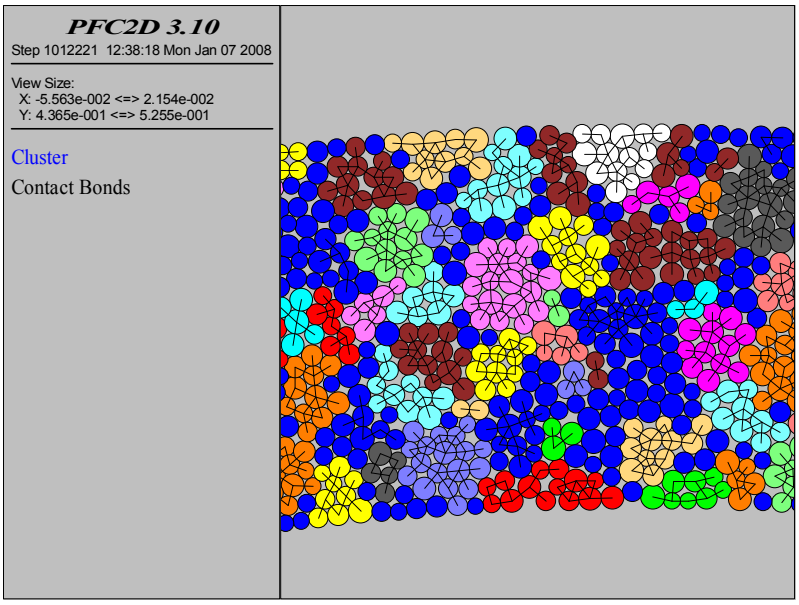

Figure 4.5 Grain clusters and relative contact bonds.

of magnitude, which can therefore break three or four times before being comminuted to elementary unbreakable particles. Of course it would be possible to build a model with many more particles (PFC does not have a limit in the number of particles) and then to create clusters composed of a lot of elements but calculation times would become correspondingly longer. However this is the first attempt at numerical simulation of the effects of grain fragmentation in a granular flow, so this is an open field for future research.

Once the clusters had been created, the external load was applied to the outer confining circular wall and a numerical servomechanism was applied to the wall so that its movements, due to the forces acting on it (the outer wall

simulated the rheometer cover plate) during the test were automatically updated at every cycle of calculation, while the external confining load remained constant.

The implementation of the "numerical rheometer" required extensive code-writing both in PFC commands and in FISH language with a series of trial-and-error runs to establish the set of numerical parameters which permitted an acceptable model behaviour.

The whole numerical model was composed of:
- a module for the model geometry (walls and disks definitions: mechanical properties, grain size and porosity);
- a module for the test control (data monitoring, definitions of control functions, initialization of boundary conditions, data storage) ;
- a module for building clusters and for bonds breakages monitoring.

For each numerical test the following parameters were stored, at a frequency of a value every 10 calculation cycles (time steps):

- direct stress on the outer wall
- direct stress on the inner wall
- shear stress on the outer wall
- shear stress on the inner wall
- torque for both walls
- time
- number of contact bonds broken by tensile stress
- number of contact bonds broken by shear stress

Normally a single test was run for 10^6 cycles corresponding to a real time of about 1.6 seconds. (as said above, the time step is automatically chosen by PFC). With a modern personal computer it took 20 to 24 hours for a test simulation (but even much more time for some particular conditions). The duration of the numerical tests was chosen as a compromise between the expected significance of a run and computation time.

Many tests have been performed changing the boundary conditions and the model fundamental parameters (confining pressure, cluster dimensions, particle friction etc.); among these, the damping coefficient has proved to be important for the capacity of the model to simulate the fragmentation process. PFC foresees the set up of this coefficient in order to prevent unrealistic propagation of waves through the sample, also in real rocks stress waves are subjected to some attenuation, this attenuation is small in brittle rock (Hazzard et al., 2000). Moreover PFC is very sensitive to the setting of this parameter

and therefore it is a fundamental task to determine what level of numerical damping makes the model behave in a realistic manner. The damping factor is also important for calculation stability, in order to control abnormal propagation of shock waves through the sample; thus this model parameter has to be determined by trial and error, also to check the related sensitivity of the model.

4.3.2 Numerical Rheometric tests

A fundamental difference between the real rheometer and the numerical one was the time step: real rheometric data of shear and direct stresses were acquired at a rate of 33 Hz, i.e. with a sample time of 30 ms (this was discussed in the rheometer lab work chapter earlier in this thesis) while the time step of the numerical model was automatically set by PFC to the very small value of about 1.17×10^{-6} seconds, and, because of the code's intrinsic structure, it was not possible to change it. This time step varied up to a few per cent between tests depending on test conditions.
We have already said that, from the actual rheometer test results, most part of the fragmentation process took place in the first instants of a test and that the low data acquisition rate was an apparatus limitation to a deeper understanding of the fragmentation rheology.
Now, with the numerical time step so small, the high data recording rate allows us to see in detail the dynamics of the initial stress and strain; the problem is that we cannot compare those numerical data with the real one simply because we have too few of the latter! (The PFC model yields more than 15,000 data for every real rheometer datum!).
This is another good reason for improving the rheometer data logging system.

The PFC model of the rheometer has been proven capable to simulate realistically some features observed in the real fragmentation rheometer: for instance grain bridges (Figure 4.7) which are a well recognized feature of granular flows (Howell and Behringer, 1999) and in figure 4.6 it is possible to see that at the end of a test (1.2 seconds of model time) near the external circular wall there are many free disks, resulting from the successive fragmentation (bonds rupture) of the clusters which were near the rotating wall, a similar configuration was found by Abe and Mair (2005) using a tri-dimensional numerical model of granular flow based on a different numerical code. This is also very similar to the situation after a test with the prototype rheometer in which effective fragmentation took place only in the upper layer of the sample. The number of the free particles is almost independent of the damping factor, while it is sensitive to the confining pressure, their number was obviously greater the higher the external load.

As for the model initial and boundary conditions imposed for the various tests performed:
- one thousand (called large afterwards) clusters and three thousand (small) particle clusters configurations;
- 100 kPa and 320 kPa have been used as applied external load;

- the tests with an applied load of 320 kPa were performed both with clusters created with a 320 kPa preloaded set of compacted elements and with a preload of 100 kPa;
- the rotation was impressed to the outer wall with linear increments from zero to 12 rad s^{-1} in 20,000 cycles (equivalent to 0.023 seconds); for some tests the gradual linear increment was applied to the external load (ramp_sigma), over the same time interval;
- damping factors of 0.7, 0.1, 0.05 and 0.01 have been used (the lower the damping factor, the lower the damping effect);
- "special tests" were performed with just free elementary particles (no clusters) and with very strong clusters, in order to see the model behaviour with unbreakable particles and with no rotating particles.

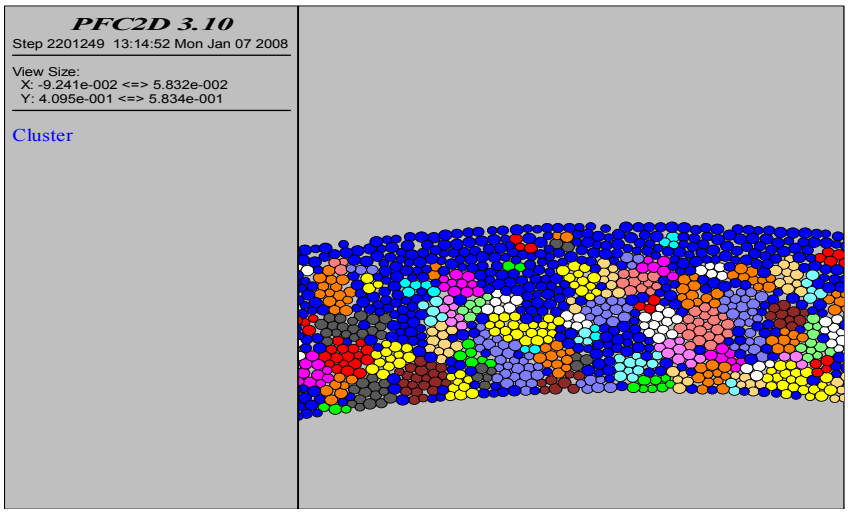

Figure 4.6 Configuration of the PFC rheometric model at the end of a test (1 million calculation cycles, 1.2 seconds, 320 kPa of confinement pressure, blue disks = free).

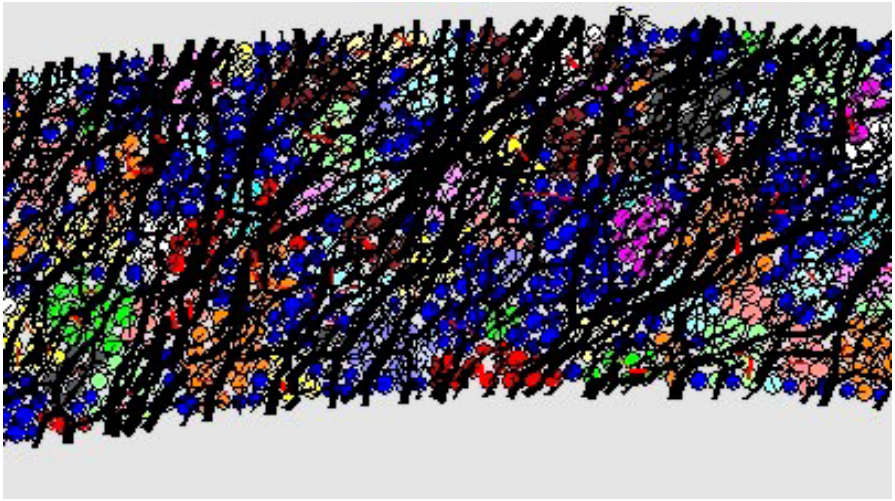

Figure 4.7 Grain bridges at the beginning of a test; at every contact between two disks a black segment represents the local contact force, the thickness of the segment is proportional to the modulus of the force.

4.4 Numerical rheometer results

4.4.1 General observations

As already said, the simulations were run for 10^6 cycles, for a total model time of 1.2 seconds, this can seem an incongruence, since the real rheometric tests had been run for about 10 seconds; this choice was made after the first preliminary simulations from which it was evident that there was an important difference of time scale between the prototype rheometer and the numerical one: the processes in the PFC model took place in a much shorter time than in the real rheometer, even if the same (relative to the 2nd stage of lab rheometry) rotation velocity had been used (12 rad s^{-1}) .

For this reason the graphs of stresses and friction relative to the initial part of tests are presented here for a time span of 0.1 second, while in the broken bonds graphs the time span covers the whole test duration.

While the direct stress shows always small oscillations around the imposed value of the applied load, in all tests an initial peak in shear stress and, consequently, in friction, was recorded (Figure 4.8 and 4.9); the value of this ubiquitous initial shear stress/friction peak depended on the test boundary/initial conditions.
This effect was seen also in the real rheometric tests, even if with a much greater delay with respect to the start of the test and with a much less pronounced.

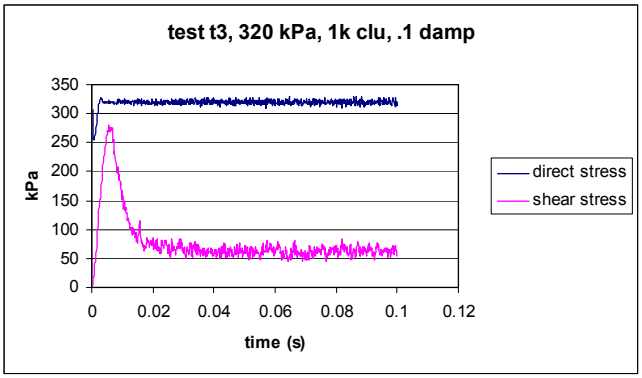

Figure 4.8 Typical graph of shear and direct stresses vs. time.

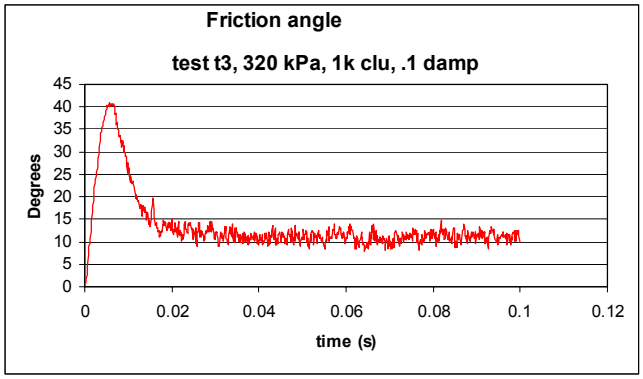

Figure 4.9 Friction vs. time for the same test as figure 4.8

A similar behaviour was also recorded in other high pressure laboratory friction tests, also with granular material (Di Toro et al., 2004; Chambon et al., 2006; Mizoguchi et al., 2007).

It's my opinion that this behaviour is mostly due to an inertial effect of the resting material which has been sharply put in movement under a high confining stress; it could be possible to speak of an apparent static friction coefficient that would be higher than the corresponding dynamic one.
It is interesting to note that the initial friction peak happens in the real apparatus between 1 and 10 seconds (and sometimes more) after the start of a test, while in the numerical model it is always recorded the first 2 hundredths of second. It looks to me that the above described inertial effect is very strong and acts immediately in the PFC model, while it is "cut down" by the instantaneous crushing action that takes place at the beginning of a test with the real rheometer. This can be seen as another friction reduction effect of fragmentation.
This effect is not well simulated in the model because its "fragmentation efficiency" is limited by the relative large size of the unbreakable elementary particles, i.e. the modelled fragmentation is not fractal.
Another reason could be the fact that the initial transient dynamics of prototype rheometer and its numerical model is (obviously) different: with the real rheometer the fragmentation starts instantaneously at the lowering of the loaded lid on the sample and so its effects are contemporary to the inertial effects, though in the PFC model the inertial effect is sharp and takes place at the very beginning of the rotation, while the clusters breakage is slower and, as said, somewhat less energetic and its effects are more present in the descending phase of the shear stress afters its initial peak.

Another effect coming from this general limitation of the PFC model that underlines a difference in behaviour between model and prototype is constituted by the low values of the friction angle after the initial peak, in fact the friction goes down to values (generally between 10° to 25°) that are lower

than those seen in the real case and than they oscillate around an average value that is more or less constant for the rest of the test.
This effect is due to the fact that the elementary, unbreakable particles are circular disks and are therefore able to rotate, especially when in contact with the rotating external wall, where very high wall-ball friction was imposed (to simulate the rivets roughness). Once the clusters are broken their disks are free to rotate, keeping the friction on the outer wall low.

4.4.2 Discussion of model results

- Effects of Cluster size: the initial shear stress and friction peak is higher with big clusters (48° vs. 41° for apparent friction angle) the shear stress peak is even higher than the direct stress and this is, again, an effect due to the high inertia of big clusters and for an intrinsic higher "robustness" coming from the fact that larger clusters can build larger (and so stronger) grain bridges and are less free to move and rotate compared to smaller clusters. This explains also the higher number of total broken bonds (which simulate a fracture in a rock grain) recorded at the end of a test for small clusters than with the large ones (with a difference of 60%: 2900 vs. 1800) this was true both for bonds broken when their normal strength was exceeded and in shear strength yielding. With big clusters the "residual friction" after the initial peak is lower and the descending branch of shear stress and friction curves is steeper than in the case of small clusters; this feature comes probably from the fact that the fracture of a large cluster produces a higher number of free particles that can carry and transfer to the surroundings some kinetic energy and are also a "low friction source" in the phase of residual friction. (Appendix B, figure B.1 to B.3).

- Effects of increased load: the change from 100 kPa to 320 kPa generated an interesting effect: while the stresses are obviously higher for the higher load, the peak friction angle is higher (48°) with 100 kPa of confining pressure, moreover when the model with 320 kPa load was previously loaded and left to settle (before the creation of clusters), the friction is even lower (37°), while it was 41° with the model preloaded to 100 kPa. There is no difference in the residual friction (Appendix B, figure B.1, B.4 and B.5, relative to tests t2, t3 and t3b). This behaviour may appear strange but it could be explained as an effect of a fragmentation pressure, as with higher load the fragmentation intensity is higher.
As far as the broken bonds are concerned, with 320 kPa of confinement the number of broken bonds is obviously higher than with 100 kPa and the difference is more marked for shear breakages, it appears that the effects of breakages on friction are more noticeable for tensile bonds yielding.

(Appendix B, figure B.3 and B.6, tests t2, t3 and t3b). This behaviour was seen both with large and small clusters with the only difference being that with small clusters the residual friction was also higher (about 2°- 3°) with 100 kPa of load. (Appendix B, tests t4 and t5b, figure B.2 and B.7).

- A different behaviour was recorded when the external load was applied through a linear increment over 20,000 steps (ramp-sigma); this way to start a test is more similar to the real one in which the rheometer bowl was made rotate and then the loaded lid was lowered on the rotating sample. Of course the shear stress peak, still present, is much lower (around a half) than in the case of a simulation in the same conditions and gradual linear steps applied to the rotation velocity: 41 kPa vs. 80 kPa for an external load of 100 kPa; the residual friction is, as expected, the same; this behaviour, with regards to the shear stress trend, is more similar to the behaviour of the real rheometer. (Appendix B, figure B.8 and B.9). In the test with "ramp_sigma" (test t10) the friction angle has a very high "spike" at the very beginning of the test of just two data: this effect has no physical meaning and is due to calculation inaccuracy in a moment in which both direct and shear stresses are as low as a few Pa.
The successive "real" friction peak has almost the same maximum value (40°) in the two tests with and without "ramp_sigma" but in the first case it is sharper and it does not coincide with the shear stress peak (which is retarded) and moreover presents more "disturbances" and the peak is reached more or less at the same time as in the test without "ramp_sigma", irrespective of the fact that at the time the confining pressure is only 10 kPa, this confirms the friction initial peak as an inertial effect.
With regards to broken bonds, it is interesting to note that while the total number of broken bonds is almost the same at the end of the two tests, in the "ramp_sigma" test there are less tensile breakages and more shear ones, with differences within 10% (Figure B.10).
When "ramp sigma" was used with 320 kPa of confinement the shear stress peak was, as already observed, lower than the corresponding test with normal load application and 100 kPa, and, since the 100 kPa "ramp_sigma" shear stress peak was already low, with 320 kPa it almost disappears (Appendix B, figure B.11); this is the only test in which there is almost no initial shear stress peak. On the other hand the friction peak is very high (46°) and the sharpest and the earliest of all tests.
The broken bonds shows a similar trend, with the same total number at the end of the test and the inversion of tensile and shear breakages described above.

- The last parameter effect to be discussed is the damping factor.

After the first preliminary tests, "parallel" tests have been done with the same external conditions while changing the damping factor (DF) only, from 0.1 to 0.05 to 0.01.
The effect of the damping reduction is very similar in the passage from 0.1 to 0.05 and from 0.05 to 0.01, and for 100 kPa and 320 kPa of confining pressure: always the decrease of DF implies a slight reduction in friction, both in its peak values and in residual ones (for this latter the reduction is very slight); and always the broken bonds increase (around 10% with 100 kPa and 25% with 320 kPa of confinement) and the relative importance of tensile breakages grows. (Appendix B, figure B.2 and B.12, stresses and friction relative to tests t4 and t20 and figure B3(b) and B.13, broken bonds relative to the same tests).
A very strange behaviour has been seen with low damping (DF=0.01) and 320 kPa of confinement pressure: the calculation became very slow (one week of computation time for 100,000 cycles!) and after 0.17 seconds the whole sample rotated together with the outer wall and most breakages occurred at the inner wall contact. Probably the low damping fosters the transmission of stresses through the sample making the clusters move and break even at the internal wall; the confining pressure of 100 kPa was not sufficient to produce this unrealistic behaviour.
The effects of the damping factor are rather evident, a low damping factor produces lower friction but its effects are smaller than expected.

4.4.3 Special tests

Some tests in particular conditions have been performed.

- Free elementary particles (no clusters): a test was conducted in this condition to check the behaviour of the model with no fragmentation (Appendix B, figure B.14, test t31). Since the disks are free to rotate the start inertial effect, still present, is much lower than all the tests with clusters, the maximum for the friction angle is about 23°, not much higher than its residual value of 17°, value similar to that with fragmenting clusters, an evidence that after about 0.1 seconds the motion in the model is dominated by the low friction of rotating free elementary particles, even if there is still cluster fragmentation.
It is worth to note that the residual friction is equal to that of a normal test with cluster at the same confining pressure and damping factor (e.g. test t6, figure B.8), this is a confirmation that after 0.1 second the model motion is controlled by the free particles which can move and rotate between the cluster layer and the rotating wall, in fact at this stage (after 0.1 s) of a test with cluster the

number of broken bonds increases slower than in the initial phase (Figure B.10).

- Another test performed in order to check the behaviour of a unfragmenting set of particles was done building particle clusters with very high (unrealistic) bond strength. There were no broken bonds at the end of the test and the effect was not striking: the maximum value for friction angle (39°) was the same as in a test in the same conditions and breakable clusters (Appendix B, figure B.15, test t35 and figure B.8, test t6); the only evident difference is the higher residual friction (40 vs. 23) and this could be due to the low number of loose particle in contact with the rotating wall and the unbreakable clusters were not circular and could not rotate easily (and they also stuck one each other).

- A test was conducted where the disks had been prevented from rotating (no spin) to check somehow the role of elementary circular particles rotation on the recorded shear stress on the outer wall. (Appendix B, figure B.16, test t36). The effect was remarkable: shear stress is so high to be always higher than the direct stress! Consequently the friction angle is always higher than 45°, close to 50° for the residue and its peak value is 67°: these values are not realistic and this shifting from the reality is again due to the effect of the shape and size of PFC elementary particles: round disks. Natural rock grains are never circular and can break in fractal manner with a reduction in size of many successive orders of magnitude; this limitation of PFC model in simulate the natural process of fragmentation comes mostly from this intrinsic feature of the code. In this "extreme" test the number of broken bonds is enormous: more than 10,000, and almost all of them were shear breakages; the consequent very thick layer of single particles against the rotating wall (Figure 4.10) cancels the propagation of the effects of the bonds rupture of the underlying clusters to the outer wall. (Figure B.13, test t36). This is an extreme situation: real particles are not circular but can rotate; unfortunately in PFC there is not the possibility to introduce a resistance to particle rotation that could account for the effect of the irregular shape of real particles on their spin motion.

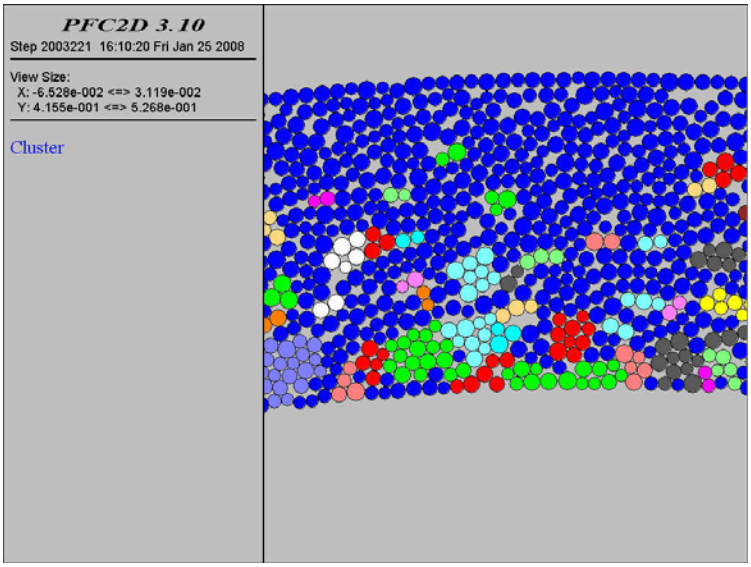

Figure 4.10 Final configuration for a test conducted with particles spin locked (blue disks = free).

4.4.4 Final remarks

Some features of the real rheometric tests were also shown by the model: the formation of a layer of elementary particles at the contact with the rotating wall; the presence of a maximum in friction early after the start of a test; and the highest fragmentation rate of a test occurs at its beginning.

Apart from some tests in very special conditions, the most noticeable feature of numerical model tests is the shear stress/friction peak at the beginning of every test; probably, as in the case of the prototype rheometer, the effects of the initial high fragmentation rate is superimposed on the inertial shear stress peak and so, it is difficult to distinguish the importance of each of the two effects.

The effect of cluster breaking is not striking, once again the low "breakability" of clusters plays an important role: the low size reduction possibility of, at most, one order of magnitude, tends to avert the model from the reality of fragmentation which can go on for several orders of magnitude.

Many aspects are worth of future development, first of all the implementation of a model with many more elementary particles, even if in this case the computation time will become a critical parameter. Another useful direction of further work will be towards a wider parametric study, involving variables that have been kept constant in the present research like ball-ball and wall-ball

friction coefficients, the density and stiffness of elementary particles, the initial porosity and son on.
Another interesting development would be the application of this type of model to real geologic phenomena, first of all rock avalanches and block glides.

Finally, passing to a tri-dimensional model would surely be a step towards simulations closer to reality (Hazzard and Mair, 2003); since it exists a 3-D version of PFC, the routines in written code for the 2-D model would be easily adaptable to a tri-dimensional model; however the computation times will be much longer.

5. GENERAL CONCLUSIONS AND FUTURE RESEARCH PERSPECTIVES

The most general aim of the present research work was to deepen the scientific knowledge on rock avalanche behaviour and to open some perspectives for further advancement of the research in this field.

The hypermobility of rock avalanches has been studied and the recent proposal of dynamic fragmentation for its explanation was taken in particular consideration.

From the analysis of the large literature on the matter came out that, while the low friction motion characteristics of these phenomena is widely recognized as an evident fact, among the many different proposed mechanisms none has been accepted as an exhaustive and satisfying explanation for those peculiar motion features.

The recently advanced dynamic fragmentation theory, starting from some previous works on rock avalanches transport mechanisms which recognized the fragmentation as a pervasive and important process, and from field observations on grain size and texture of sturzstrom deposits, is very promising as an explanation for some low friction geologic phenomena, among which, the hypermobility of rock avalanches.

The developed fragmentation rheometer has proven to be a useful laboratory instrument to study the rheology of a fragmenting flow of rock grains, which is still not widely studied and understood.
The performed tests gave a set of interesting results from which some evidence of the effects of the fragmentation in a shearing granular mass has emerged. Being a new concept apparatus, the fragmentation rheometer is promising for some new data, once some development and modifications will be made in its structure (making it able to crush rocks harder than coal) in the driving machinery (making possible a continuous change in rotation velocity) and in the data logging system (for a higher acquisition frequency).

The numerical model of the fragmentation rheometer yielded encouraging results and showed that the mathematical modelling of processes in which grain fragmentation is involved is possible using a code that is widely available.

In particular, the developed PFC model showed some interesting capabilities and also some limitations. Good points are the realistic simulation of particles

flow under confinement pressure, with grain bridges and a general behaviour in accordance with laboratory data. The limitations (behaviour differences from reality) come mostly from the code fundamental structure, being based on a set of unbreakable circular elements, bonded together or not.
With regards to the fragmentation effects, it is possible to say that some tests show a certain level of friction reduction, but, definitely, it is necessary to go on in this direction in order to exploit all the possibilities of PFC in fragmentation modelling. The construction of breakable clusters is just the first step, the first results are telling us that the numerical modelling of a fragmenting grain flow is promising and worth deeper research.

The results of the numerical model of our fragmenting rheometer are encouraging also in the direction of numerical simulation of natural phenomena in which dynamic fragmentation plays an important role.

Finally, I hope to have given a not negligible contribution to the knowledge of some aspects of rock avalanche mechanics; at the very least I am closing this thesis with sufficient enthusiasm to go on with the research on rock avalanches and their still secluded secrets.

REFERENCES

Abe, S., Mair, K. (2005); Grain fracture in 3D numerical simulations of granular shear. *Geophys. Res. Lett.*, vol. 32, L05305.

Antonellini, M. A., and Pollard, D. D. (1995); Distinct element modeling of deformation bands in sandstone. *J. Struct. Geol.*, 17, 1165–1182.

Bagnold, R. A. (1954); Experiments on a gravity-free dispersion of large solid spheres in a Newtonian fluid under shear. *Proceedings of Royal Society of London*, Ser.A 225:49-63.

Bagnold, R. A. (1956); The flow of cohesionless grains in fluids. *Proceedings of Royal Society of London,* Ser A, 249: 235-297.

Beetham, R.D. (1983); Seismicity and landsliding with special attention to New Zealand. Unpublished MSc Thesis, University of London.

Beetham, R.D., Read, S.A.L., and McSaveney M.J. (2002); Four extremely large landslides in New Zealand. In: *Landslides*, (Rybar, Stemberk, Wagner, Swets and Zeitlinger eds.); Lisse, 93-102.

Beutner, E.C. (1972); Reverse gravitative movements on earlier overthrusts, Lehmi Range, Idaho. *Bullettin Geological Society of America*, 83, p. 839-846.

Bieniawski Z.T. (1968); The effect of specimen size on compressive strength of coal. *International Journal of Rock Mechanics and Mining Sciences,* 5(4): 325–335.

Calvetti F., Crosta G., Tatarella M. (2000); Numerical simulation of dry granular flows: from the reproduction of small-scale experiments to the prediction of rock avalanches. *Rivista Italiana di Geotecnica*, 2, 21-38.

Campbell, C.S., Cleary, P.W., Hopkins, M. (1995); Large-scale landslide simulations: Global deformation, velocities and basal friction. *Journal of Geophysical Research*, vol. 100, n. B5, 8267-8283.

Chambon, G., Schmittbuhl, J., and Corfdir, A. (2006); Frictional response of a thick gouge sample: 1. Mechanical measurements and microstructures, *J. Geophys. Res.*, 111, B09308, doi:10.1029/2003JB002731.

Cleary, P.W., Campbell, C.S. (1993); Self-lubrication for long runout landslides: examination by computer simulation. *J. of Geophys. Res*. 98, 21; 911-924.

Cruden, D.M. and Hungr, O. (1986); The debris of the Frank Slide and theories of rockslide-avalanche mobility. *Canadian Journal of Earth Sciences*, vel. 23, 425-432.

Cuman, A. (2007); Rock avalanches: analysis of deposits' grain size and numerical modelling of run-out. Università di Padova, PhD thesis.

Cundall, P. A., and Strack, O. D. L. (1979); A Discrete Numerical Model for Granular Assemblies. *Géotechnique*, 29, 47-65 (1979).

Davies,T.R.H. (1982); Spreading of rock avalanches debris by mechanical fluidization. *Rock Mechanics* 15, 9-24.

Davies T.R., McSaveney M.J. (2006); Rapid rock mass flow with dynamic fragmentation: inferendes from the morphology and internal structure of rockslides and rock avalanches. In: Evans, S.G.; Scarascia Mugnozza, G.; Strom, A.; Hermanns, R.L. (Eds.) Landslides from Massive Rock Slope Failure; *Proceedings of the NATO Advanced Research Workshop on Massive Rock Slope Failure: New Models for Hazard Assessment*, Celano, Italy, 16-21 June 2002. 285-304.

Davies, T.R.H. and McSaveney, M.J. (in progress); The role of dynamic rock fragmentation in the motion of large landslides. Submitted to *Engineering Geology*.

Davies, T.R.H. and McSaveney, M.J. (2002); Dynamic simulation of the motion of fragmenting rock avalanches. *Canadian Geotechnical Journal*, vol. 39, 789-798.

Davies T.R., McSaveney M.J. (1999); Runout of dry granular avalanches. *Canadian Geotechnical Journal*, vol. 36, no. 2, April 1999, 313-320.

Davies, T.R., McSaveney, M.J. and Beetham, R. (2006), Rapid block glides – slide-surface fragmentation in New Zealand's Waikaremoana landslide. *Quarterly Journal of Engineering Geology and Hydrogeology* vol. 39, 115–129.

Davies, T.R, McSaveney, M.J., Deganutti, A.M. (2007); Dynamic fragmentation causes low rock-on-rock friction. Proc. of *1st Canada-U.S. Rock Mechanics Symposium*, Vancouver, Canada, 27-31 May 2007.

Davies, T.R., Deganutti, A.M. & McSaveney, M.J. (2005). A high-stress rheometer for fragmenting rock. In: *Picarelli,L. (ed.) Proceedings, International Conference on fast slope movements*. Naples, May 11-13, 1. Patron Editore, Bologna, 139–141.

Davies, T.R., McSaveney, M.J. and Hodgson, K.A. (1999). A fragmentation-spreading model for long-runout rock avalanches. *Canadian Geotechnical Journal*, 36: 6, 1096–1110. 1999.

Deganutti, A.M., Scotton, P., (1997). Yield stress of granular material. Proc. of "*First International Conference on Debris Flow Hazards Mitigation*" ASCE, S. Francisco August 7/9,1997; 270-278.

Di Toro, G., Goldsby, D.L., Tullis, T.E. (2004). Friction falls toward zero in quarz rock as slip velocity approaches seismic rates. *Nature* vol. 427, 29 Jan. 04, 436-439.

Donzé, F., Magnier S. A. and Bouchez J. (1996); Numerical modeling of a highly explosive source in an elastic-brittle rock mass, *J. Geophys. Res*., 101, 3103–3112.

Dunning, S.A. 2004. Rock avalanches in high mountains – A sedimentological approach. *PhD Thesis*. University of Luton, U.K.

Evans, S.G. (1995); The field behaviour of rock avalanches in the Canadian Cordillera. *International Symposium on prediction of landslide motion*, Disaster Prevention Institute, Kyoto University.

Genevois, R. 2007, Pers. comm..

Grady, D.E. and Kipp, M.E. (1987); Dynamic rock fragmentation. In *Fracture Mechanics of Rock*, Academic Press, London, UK, 429–475. 1987.

Gukwa, P.R., and Kehle, R.O. (1978); Bearpaw Mountains rockslide, Montana, U.S.A. In: *Rockslides and Avalanches*, (Voight, B. ed.) vol. 1 Development in Geotechnical Engineering, vol. 14A, 393-421; Amsterdam, Elsevier.

Guest, J.E. (1971); Geology of the far side Crater Tsiolkovsky. In: *Geology and Physics of the Moon* (Fielder, G. ed.) 93-103, Elsevier.

Habib, P. (1975); Production of gaseous pore pressure during rock slides. *Rock Mechanics* 7, 193-197.

Harrison, J.V., and Falcon, N.L. (1938); An ancient landslip at Saidmarreh, in southwestern Iran. *Journal of Geology*, vol. 46, 296-309.

Hazzard, J.F., and Mair, K. (2003); The importance of the third dimension in granular shear. *Geophys. Res. Lett*., 30(13), 1708, doi:10.1029/ 2003GL017534.

Hazzard, J.F., Young, R.P., Maxwell, S.C. (2000); Micromechanical modeling of cracking and failure in brittle rocks. *J. of Geoph. Res*., vol. 105, B7, p. 16,683–16,697.

Heim, A. (1882); Der Bergsturz von Elm. *Z. Dtsch. Geol. Ges.*, 34, 74-115.

Heim, A. (1932); Der Bergsturz und Menschenleben. Zürich, *Fretz und Wasmuth Verlag*, 218 p.

Hayashi, J.N. and Self, F. (1992); A comparison of pyroclastic flow and debris avalanche mobility. *Journal of Geophysical Research*, 97, B6, 9063-9071.

Herget, G. (1988); Stresses in rock. Balkema, Rotterdam.179 p.

Howard, K. (1973); Avalanche mode of motion: implications from lunar examples. *Science* 180, 1052-1055.

Hsü, K.J. (1975); Catastrophic debris streams (sturzstroms) generated by rockfalls. *Bull. Geol. Soc. Of America,* Vol. 86, 129-140.

Hsü, K.J. (1978); Albert Heim: Observations on landslides and relevance to modern interpretations. In: *Rockslides and Avalanches*, (Voight, B. ed.) vol. 1 Natural Phenomena, 71-93. Amsterdam, Elsevier.

Howell, D., and Behringer, R.P. (1999); Stress Fluctuations in a 2D Granular Couette Experiment: A Continuous Transition. *Physical Review Letters* 82: 5241-5244.

Hungr, O, (1995); A model for the runout analysis of rapid flow slides, debris flows, and avalanches. *Canadian Geotech J*., 32:610–623.

Hungr, O. (1990); Mobility of rock avalanches. *Report of National Research Institute for Earth Science and Disaster Prevention, Japan*. 46, 11-19.

Hungr, O. (1981); Dynamics of rock avalanches and and other types of slope movements. PhD thesis, Univ. of Alberta, Edmonton, 500 pp.

Hungr, O., and Evans, S.G. (1996); Rock avalanche runout prediction using a dynamic model. In: *Landslides, Proceedings of the 7th International Symposium on landslides*, Trondheim, Norway. Senneset K.(ed) A.A Balkema, Rotterdam, vol. 1, pp 233–238

Hungr, O. and Morgenstern, N.R. (1984); Experiments on the flow behaviour of granular material at high velocity in an open channel. *Geotecnique*, vol. 34, 405-413.

Johnson, B. (1978); Blackhawk landslide, California, USA (1978); In: *Rockslides and Avalanches*, (Voight, B. ed.) vol. 1 Natural Phenomena, 481-504. Amsterdam, Elsevier.

Kent , P.E. (1966): The transport mechanism in catastrophic rock falls. *Journal of Geology*, vol. 74, 79-83.

Kilburn, C.R.J. (2001); The flow of giant rock landslides. In: Paradoxes in Geology. Ken Hsü Special Volume, Chapter 13 (Eds. Briegel U and Xiao W-J.), Elsevier, 245-265.

Körner, H.J. (1977); Flow mechanism and resistances in the debris streams of large rock slides. *Bull. Int. Ass. Of Engineering Geology*, vol. 16, 101-104.

Legros F. (2001); The mobility of long runout landslides. *Engineering Geology*, 63, 301-331.

Li, T. (1983); A mathematical model for predicting the extent of a major rockfall. *Zeitschrift fur Geomorphologie*, Vol. 24, 473-482.

Liu, C.-H., Nagel, S.R., Schecter, D.A., Coppersmith, S.N., Majumdar, S., Narayan, O., and Witten, T.A. (1995); Force fluctuations in bead packs. *Science*, 269, 513-515.

McEwen, A.S. (1989); Mobility of large rock avalanches: evidence from Valles Marineris, Mars. *Geology*, vol. 17, 1111-1114.

McSaveney, M.J., Davies, T.R.H., and Hodgson, K.A. (2000); A contrast in deposit style and process between large and small rock avalanches. In: *Landslides in Research, Theory and Practice, Proceedings of the 8th International Symposium on Landslides*, Cardiff, Wales. Edited by E. Bromhead, N. Dixon, and M.-L. Ibsen. Thomas Telford Publishing, London, 1053–1058.

Melosh, H.J. (1997); Asteroids: Shattered but Not Dispersed. *Icarus;* vol. 129, 2, 562-564.

Mizoguchi, K., Hirose, T., Shimamoto, T., and Fukuyama, E. (2007); Reconstruction of seismic faulting by high-velocity friction experiments: An example of the 1995 Kobe earthquake. *Geophys. Res. Lett.*, vol. 34, L01308, doi:10.1029/2006GL027931.

Mora, P., and Place, D. (1998); Numerical simulation of earthquake faults with gouge: Toward a comprehensive explanation for the heat flow paradox, *J. Geophys. Res.*, 103, 21,067–21,089.

Mueth, D.M., Debregeas, G.F., Karczmar, G.S., Eng, P.J., Nagel, S.R., Jaeger, H.M. (2000); Signatures of granular microstructure in dense shear flows. *http://www.citebase.org/abstract?id=oai:arXiv.org:cond-mat/0003433.*

Nedderman, R. (1992); Statics and kinematics of granular materials. Cambridge University Press, Cambridge.

Nicoletti P.G., Sorriso-Valvo, M. (1991); Geomorphic controls of the shape and mobility of rock avalanches. *GSA Bulletin*; October 1991; v. 103; no. 10; p. 1365-1373.

Pautre, A., Sabarly, F., Schneider, B. (1974); L'effet d'échelle dans les écroulements de falaise. *C.R. 3éme Congrés ISRM, Denver*, vol. II-B, p. 859.

Pollet, N. (2004); Mouvements gravitaires rapides de grandes masses rocheuses: apports des observations de terrain à la compréhension des processus de propagation et dépôt. *PhD Thesis*, École Nationale des Ponts et Chaussées, Paris.

Pollet, N., Schneider J.-L.M. (2004); Dynamic disintegration processes accompanying transport of the Holocene Flims Sturzstrom (Swiss Alps). *Earth and Planetary Science Letters*, 221, (2004), 433-448.

Pollet, N., Cojean, R., Couture, R., Schneider J.-L.M., Strom, A.L., Voirin, C., Wassmer, P. (2005); A slab-on-slab model for the Flims rockslide (Swiss Alps). *Canadian Geotechnical Journal,* 42(2) 587-600.

Prostka, H.J. (1978); Heart Mountain fault and Absaroka volcanism, Wyoming and Montana, U.S.A. In: *Rockslides and Avalanches*, (Voight, B. ed.) vol. 1 Development in Geotechnical Engineering, vol. 14A, 423-437; Amsterdam, Elsevier.

Read, S.A.L. (1979); The Waikaremoana outlet, engineering geological studiesof factors related to leakage through the natural dam. *New Zealand Geological Survey report* EG336.

Read, S.A.L., Beetham, R.D., and Ridley P.B. (1992); Lake Waikaremoana barrier – a large landslide dam in New Zealand. Proceedings of the Sixth International Symposium on Landslides, 10-14 February, Christchurch, New Zealand (D.H. Bell ed.); 1481-1487.

Sammis, C. and Stacey, S.J. (1994); The micromechanics of friction in a granular layer. *PAGEOPH (Pure and Applied Geophysics)*, 142, 3/4., 777-794.

Sammis, C., King, G., and Biegel, R. (1987); The kinematics of gouge formation. *PAGEOPH (Pure and Applied Geophysics)*, 125: 777–812.

Scheidegger, A.E. (1973); On the prediction of the reach and velocity of catastrophic landslides. *Rock Mech*. 5, 231-236.

Schneider, J.-L., Wassmer, P., Ledésert, B. (1999); The fabric of the sturzstrom of Flims (Swiss Alps): Characteristics and implications on the transport mechanisms. *Comptes Rendus de lAcademie des Sciences Series IIA Earth and Planetary Science;* vol 328, 9, 607-613.

Schneider, J.-L., Fisher, R.V. (1998); Transport and emplacement mechanisms of large volcanic debris avalanches: evidence from the northwest sector of Cantal Volcano (France). *Journal of Volcanology and Geothermal Research,* vol. 83, 141–165.

Shreve, R.L., (1959); Geology and mechanics of the Blackhawk landslide, Lucerne Valley, California. *PhD Thesis*, Caltech, Pasadena, California, USA.

Shreve, R.L., (1968a); The Blackhawk landslide. *Geol. Soc. Am. Spec. Pap*. 108 47 pp.

Shreve, R.L., (1968b); Leakage and fluidization in air-layer lubricated avalanches. *Geol. Soc. Am. Bull.*, 79: 653-658.

Siebert, L. (1984); Large volcanic debris avalanche: characteristic of the source areas, deposits, and associated eruptions. *Journal of Volcanology and Geothermal Research*, vol. 22, 163-197.

Smith, G.M. (2004); The coseismicity and morphology of the Acheron rock avalanche deposit in the Red Hill valley New Zealand *Unpublished M.Sc. thesis, University of Canterbury*, Christchurch, New Zealand.

Smith G. M., Davies, T.R., McSaveney, M.J., Bell, D.H. (2005); The Acheron rock avalanche, Canterbury, New Zealand—morphology and dynamics. *Landslides* vol. 00, DOI: 10.1007/s10346-005-0012-1.

Staron, L. (2000); Mobility of long-runout rock flows: a discrete numerical investigation. *Geophysical Journal International*, vol. 172, 1, 455-463.
Voight, B. (1978); Lower Gros Ventre slide, Whyoming, U.S.A. In: *Rockslides and Avalanches*, (Voight, B. ed.) vol. 1 Natural Phenomena, 113-166. Amsterdam, Elsevier.

Voight B., Janda, R.J., Glicken, H. and Douglass P.M. (1985); Nature and mechanics of the Mount St Helens rockslide-avalanche of 18 May 1980. *Geotechnique* vol. 33, no3, pp. 243-273.

Watson, R.A., Wright, H.E. (1967); The Saidmarreh landslide, Iran. *Geological Society of America*, *special paper n. 123*, 115-139

APPENDIX A

Photographs, drawings and graphs relative to Chapter 3, Experimental work.

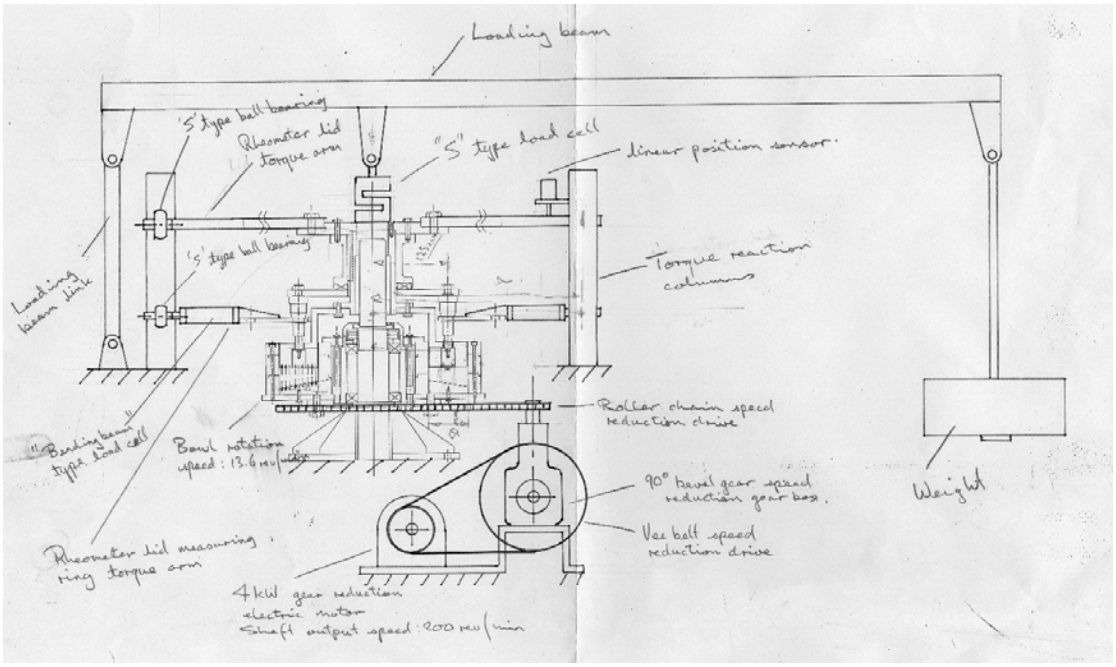

Figure A.1 Rick Diehl's "Leonardo da Vinci style" building sketch of the whole rheometric apparatus.

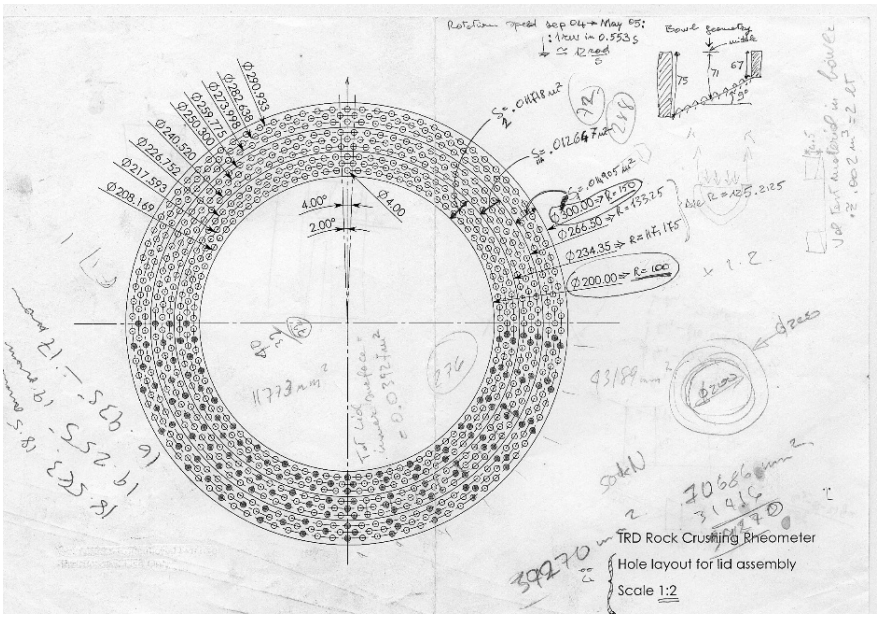

Figure A.2 Building sketch of the inner side of the rheometer's cover plate.

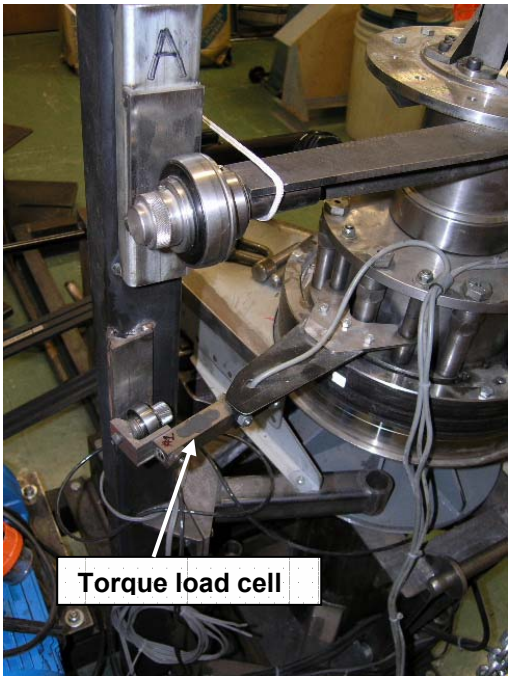

Figure A.3 Calibration of the torque load cells, particular.

Figure A.4 The rheometer after a test with coal grains.

Figure A.5 A sample of coal granules loaded in the rheometer's bowl

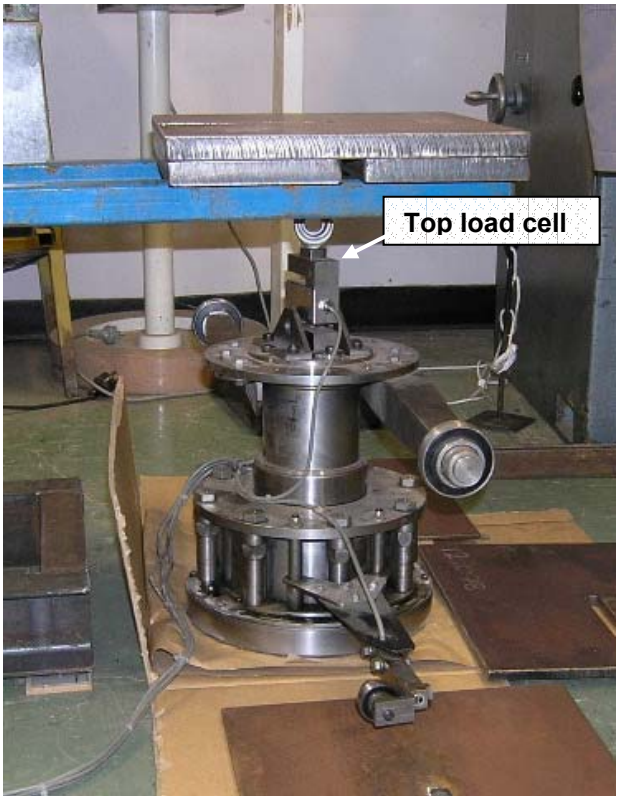

Figure A.6 Rheometer "lid": calibration of the top (direct stress) load cell

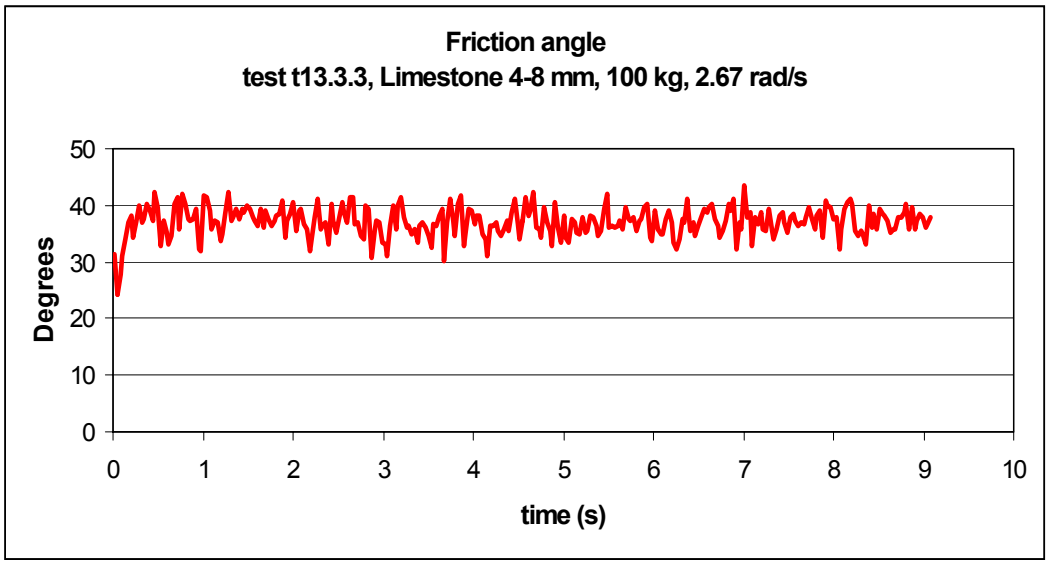

Figure A.7 Apparent friction angle graph resulting from a rheo test with limestone

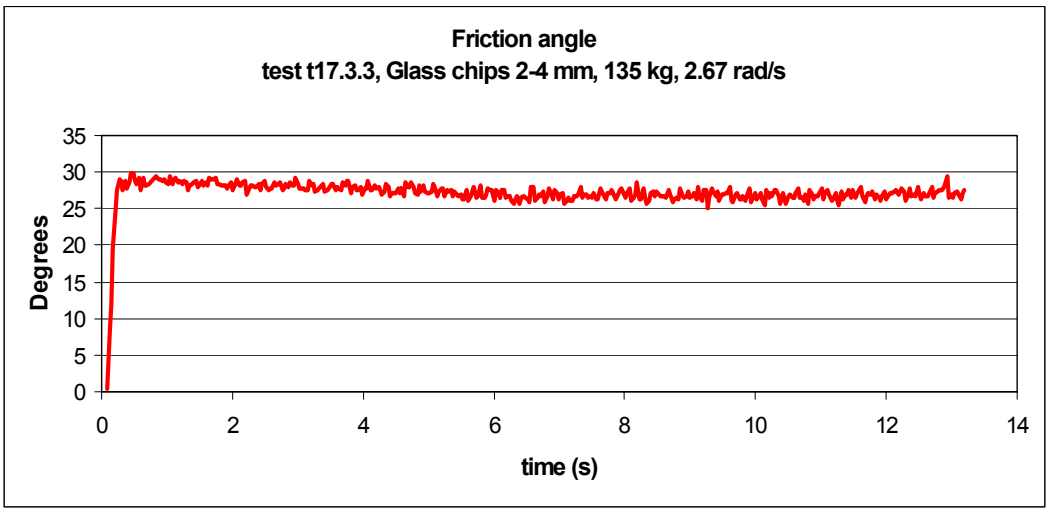

Figure A.8 Apparent friction angle for a test with glass chips.

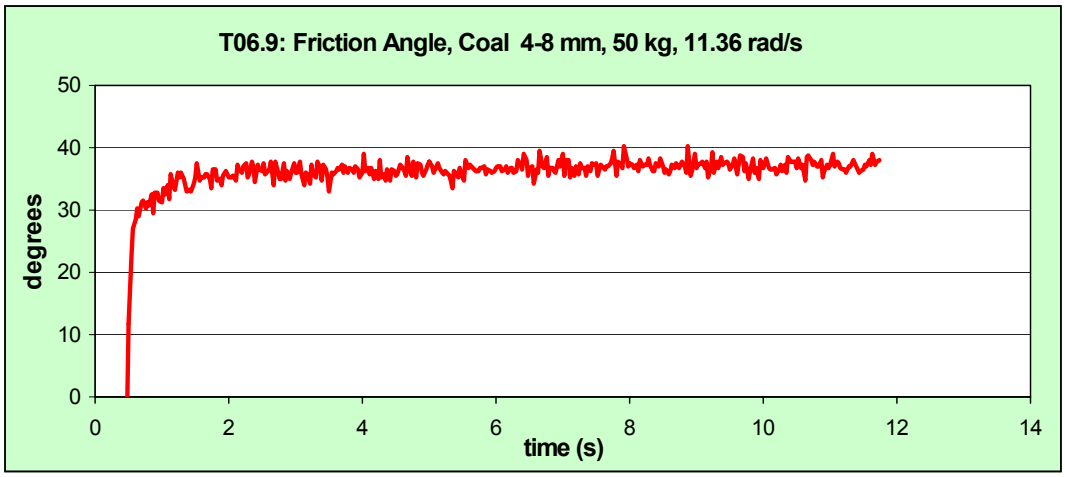

Figure A.9 Friction behaviour of a test with a low external load: there is not an evident maximum in friction

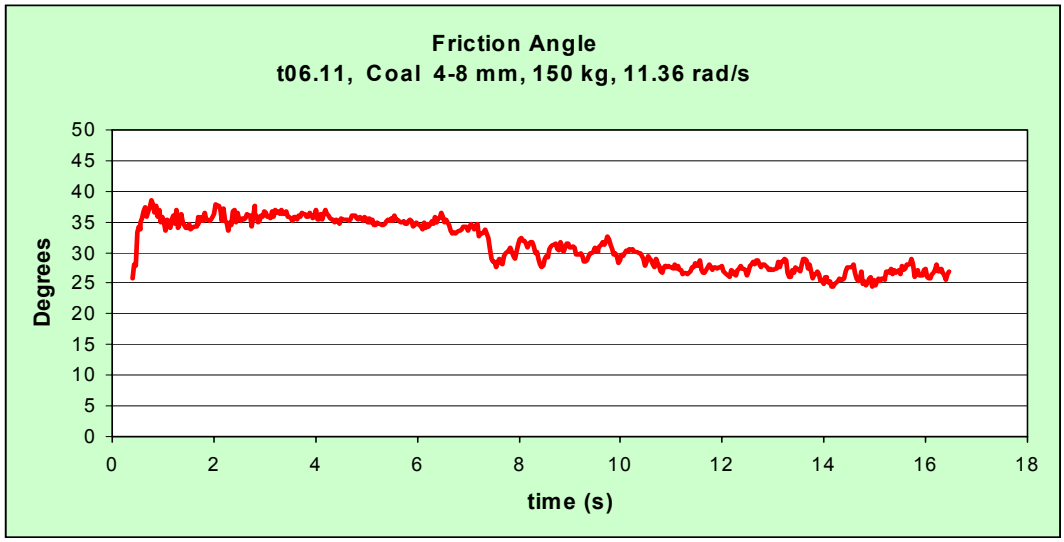

Figure A.10 Apparent friction angle for a hi-load test with small coal grains. The high graph's disturbance is due to the high confinement pressure.

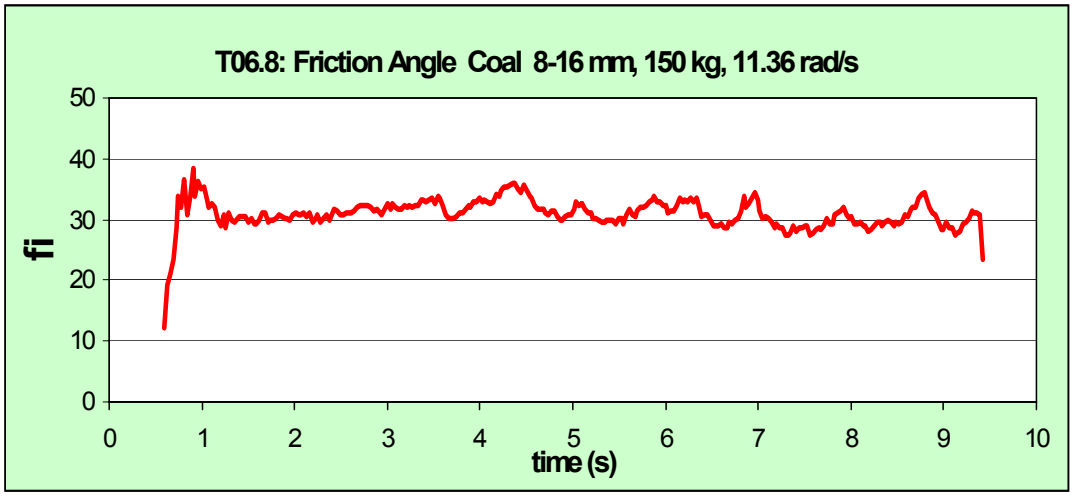

Figure A.11 Friction angle results from a test with large gains and high load.

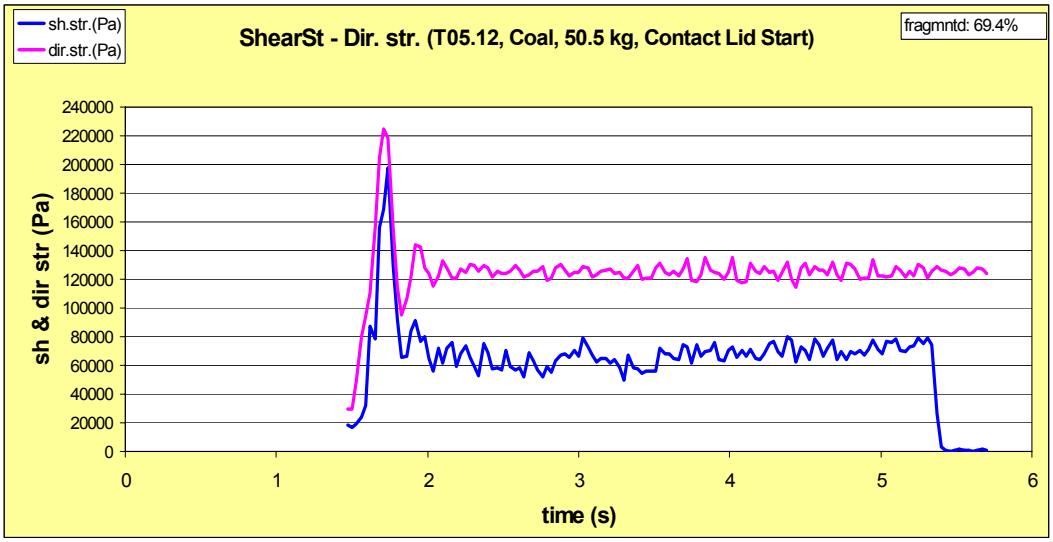

Figure A.12 Shear and direct stresses in a test in which the rotation was started with the loaded lid lowered on the sample.

Fragmentation Rheometer test operative procedure

A) Before test

1. Sieve and weigh the sample (as a measure of the rock particles bulk volume to use, fill the square tin container)
2. Clean & grease the Rheometer lid (through its grease nipples)
   2.1 Clean grease excess
3. Put the rock sample in the rheometer bowl
4. Put in the sample a 'column' of different colour rock particles (to detect the real shearing layers during the test) in correspondence of the green sign on the bowl, for this purpose use the small pipe provided
5. Lower the lid
6. Mount the loading arm
7. Apply the load
8. Measure the lid position
9. Place the jack and raise the arm with it
10. On PC: Run the Genidaq 'Strategy'
11. Switch ON the load cells electric supply (run the strategy to check the ref. Voltage (should be 12.1 to 12.2)
12. Start the engine
13. Lower the lid (by jack) as quick as possible
14. Let the test go for 10 s
15. Stop the engine
16. On PC: Stop the strategy, rename the file 'Logfile.log' with a name composed by *date, sample type, weight on arm*

B) After test

1. Measure the lid position
2. Raise the Lid
3. Check the situation of the rock sample in the bowl, upper layer, vertical distribution (opening a 'ditch' with the vacuum cleaner)
4. Control the column of the different colour particles (shearing depth)
5. Take the whole sample from the bowl and weight it
6. Sieve the sample for after test grain size analysis and fragmentation rate

APPENDIX B

B.1 Graphs relative to Chapter 4, PFC rheometer model.

Note: Stress and friction graphs are relative to initial stage of tests (0.1 s) while broken bonds graphs are relative to whole tests (1.2 s).

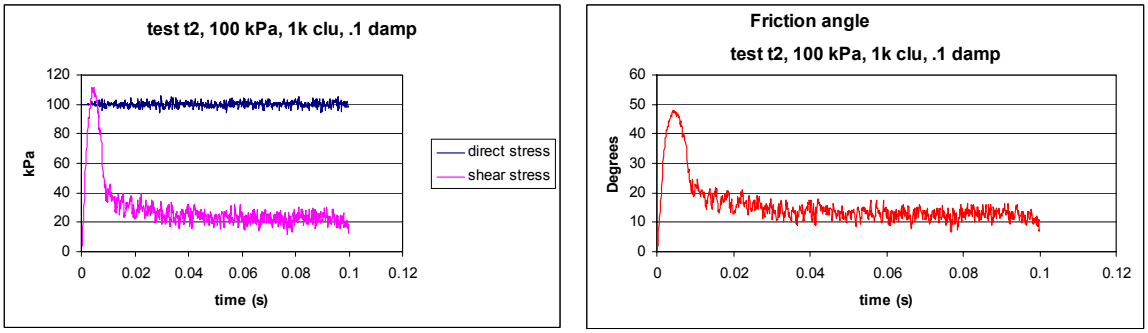

Figure B.1 Numerical rheo graphs for a test with big (1000) clusters, a confinement pressure of 100 kPa and a damping coefficient of 0.1: the friction peak is above 45°.

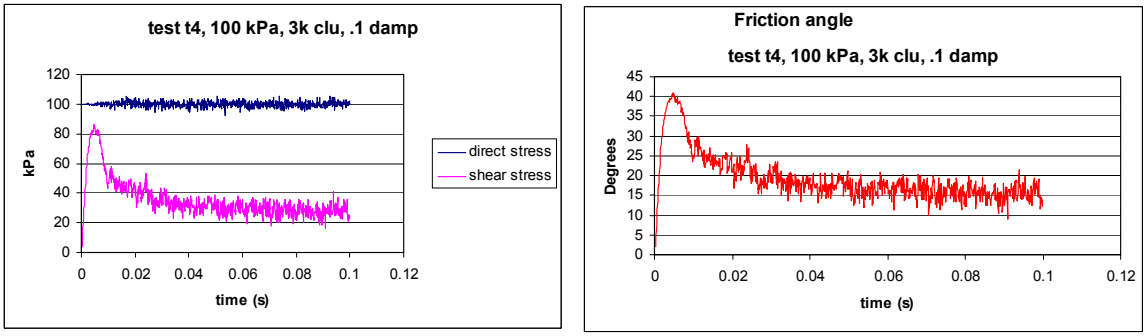

Figure B.2 Numerical rheo graphs for a test with small (3000) clusters, in the same conditions as in figure B.1: peaks are lower and the residual friction is higher.

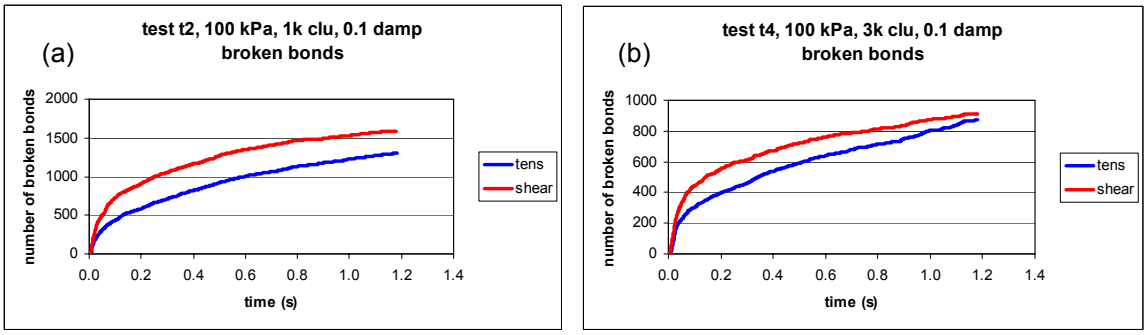

Figure B.3 Comparison between the number of broken bonds recorded for the tests with large and small clusters (figure B.1 and B.2): the number of "cracks" is significantly higher with big clusters.

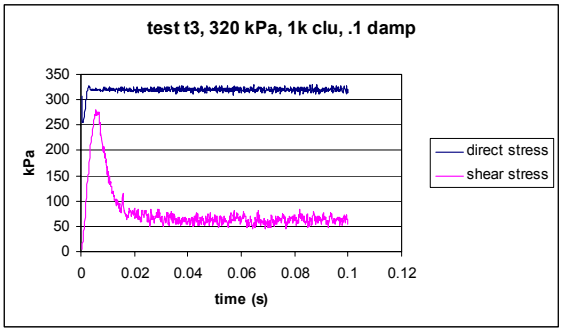

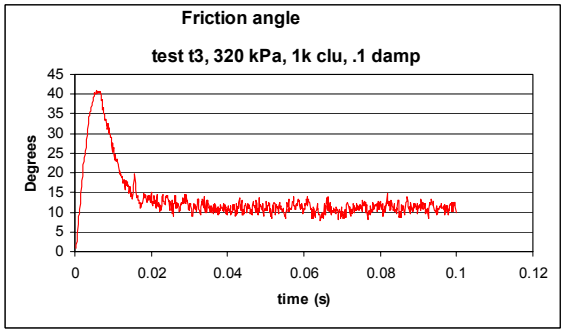

Figure B.4 Graphs for test with high load, the model was left to settle at 100 kPa, it is possible to observe the initial direct stress sharp step.

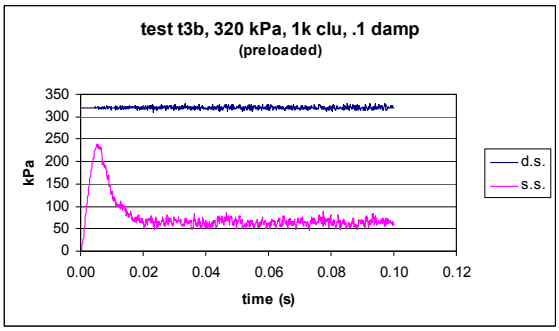

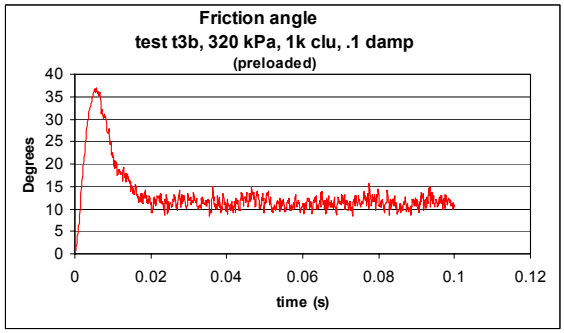

Figure B.5 Graphs for test with high load, the model was preloaded and left to settle at 320 kPa, there is no direct stress initial step; the friction peak is 11° lower than with a load of 100 kPa (test t2, figure B.1).

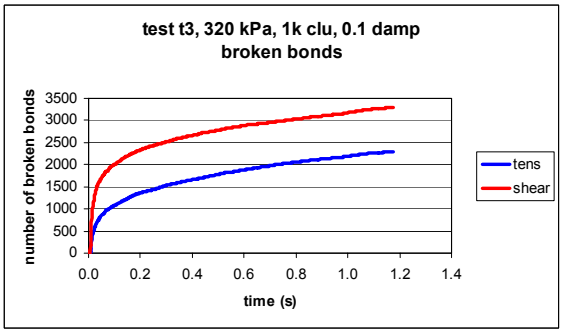

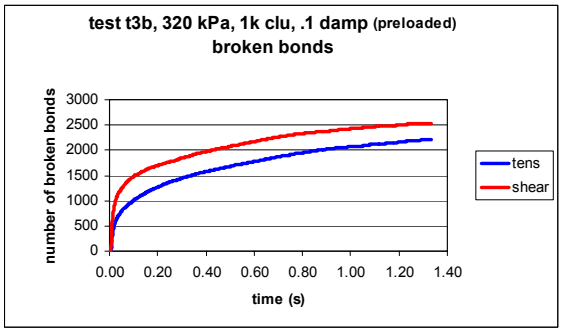

Figure B.6 Broken bonds graphs comparison between 320 kPa tests performed with models left to settle at 100 kPa and 320 kPa.

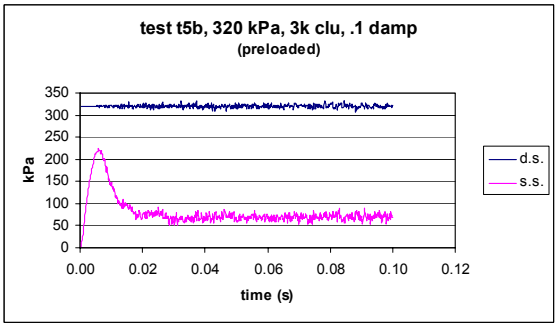

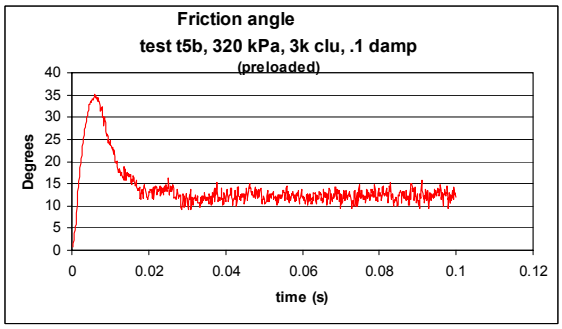

Figure B.7 Test with 320 kPa and small clusters.

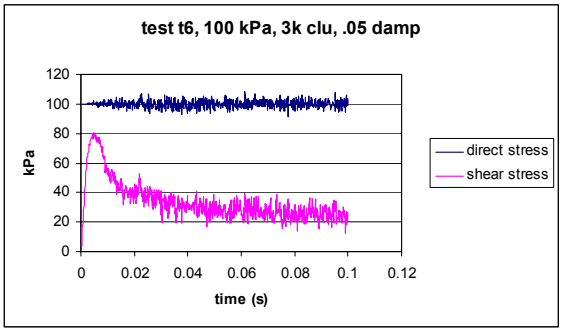

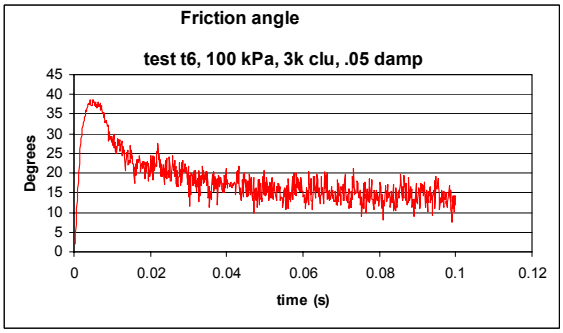

Figure B.8 Test t6: 100 kPa external load and a damping coefficient of 0.05.

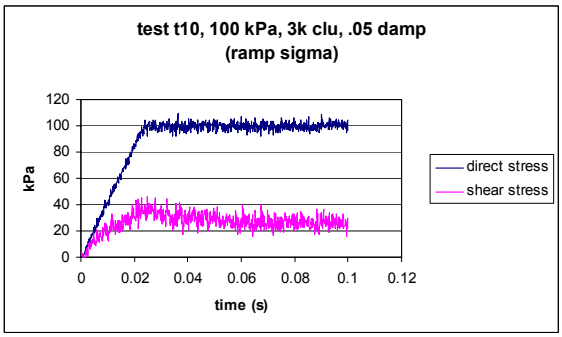

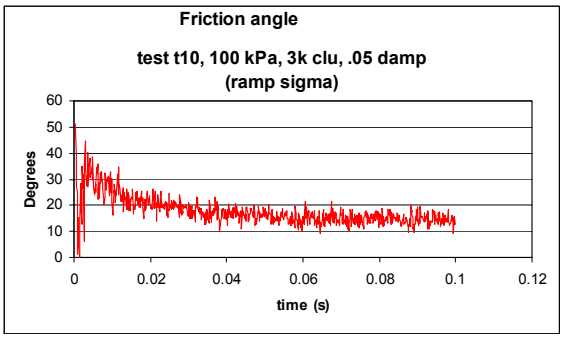

Figure B.9 Test t10: same conditions of test t6 (fig. B.9) with external load applied with 20,000 linear incremental steps.

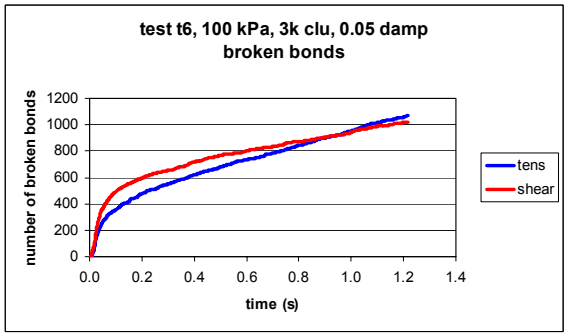

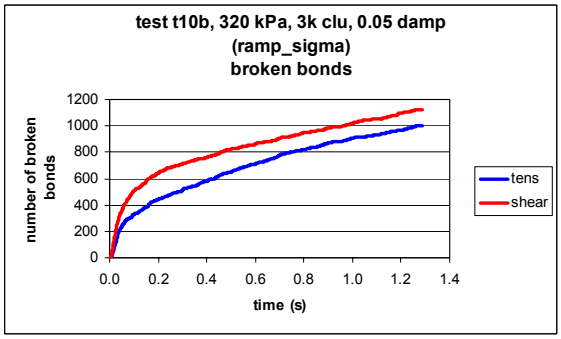

Figure B.10 Tests t6 and t10b: comparison of broken bonds trends: while the total number of the breakages are the same in the two tests, with "ramp_sigma" starting condition, a higher number of shear breakages and a lower tensile ones are recorded.

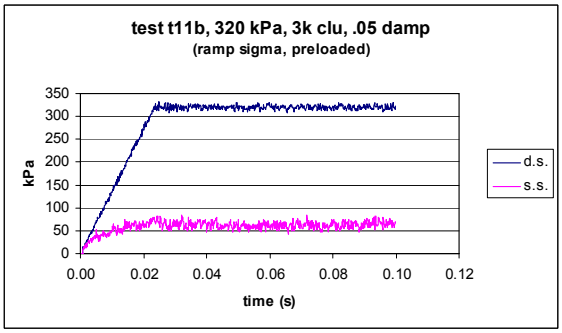

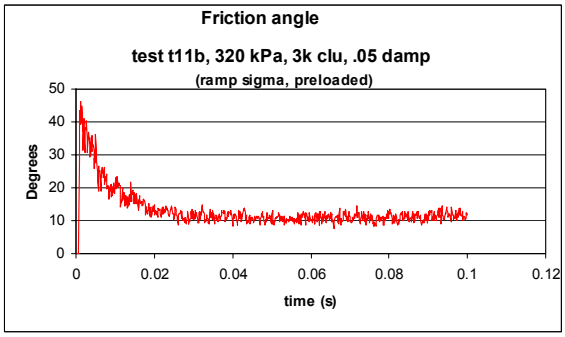

Figure B.11 Test t11b: almost no shear stress initial peak and very sharp friction peak, very low residual friction.

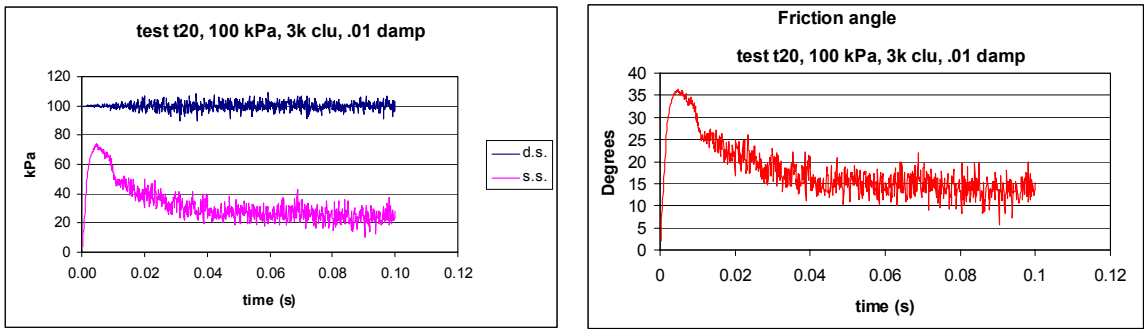

Figure B.12 Test t20: effects of low damping coefficient (0.01).

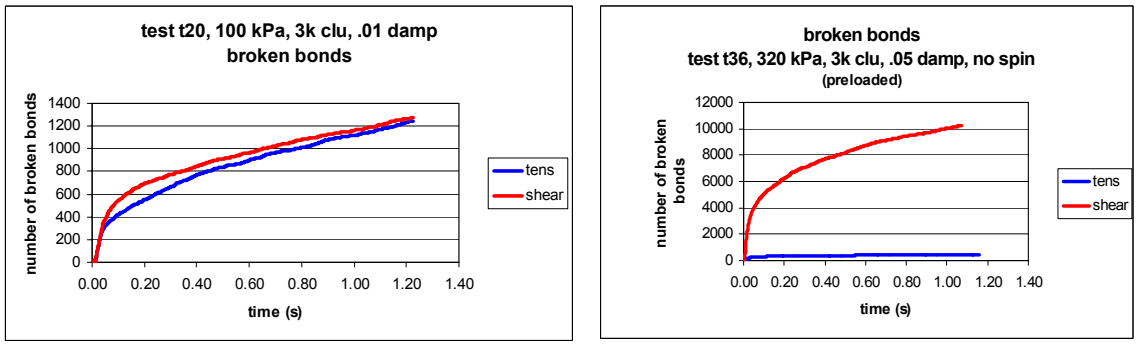

Figure B.13 Broken bonds graphs: test t20 with low damping condition and test t36 with disks rotation locked.

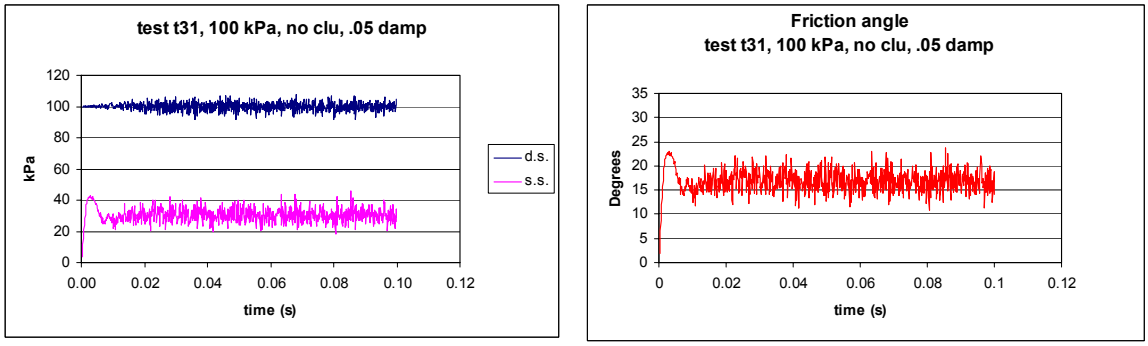

Figure B.14 Test t31: free elementary particles, no fragmentation.

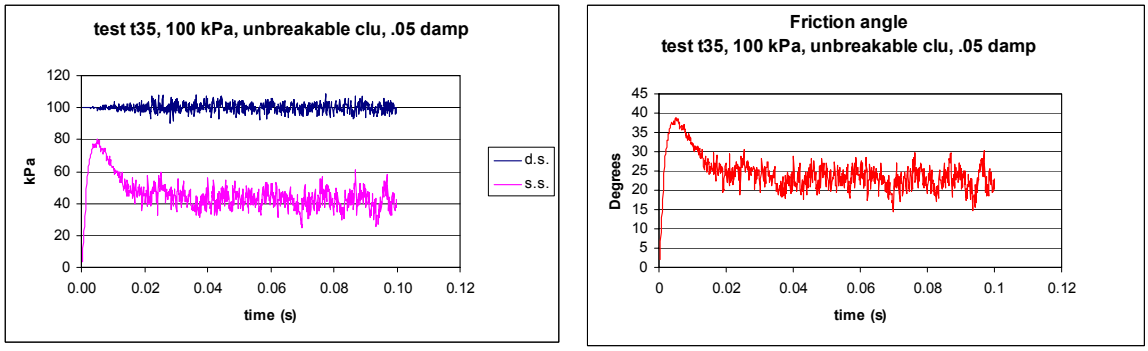

Figure B.15 Test with unbreakable clusters, the residual friction is rather high.

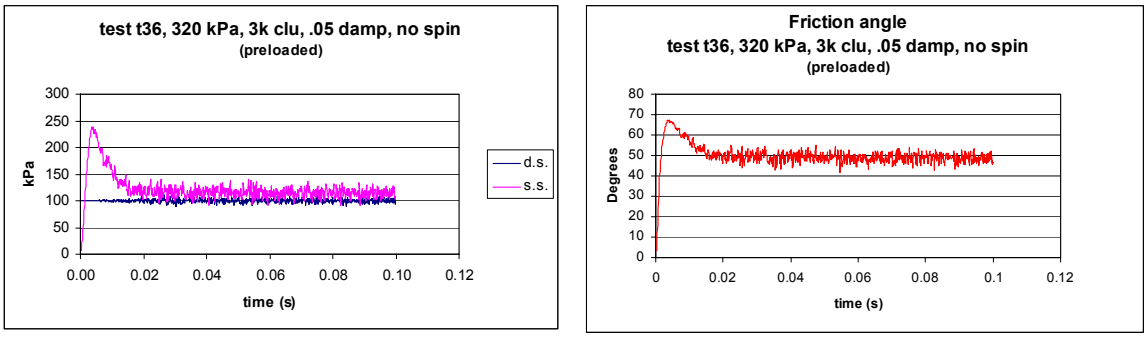

Figure B.16 Test T36: the elementary circular particles spin is locked, the friction is consequently very high.

B.2 PFC commands and FISH code examples.

B.2.1 Model construction: geometry and general mechanical settings

```
new
set disk 1.
;
call general.dat
set out_rad = .51 in_rad = .45
set wall_nstiff = 1.e5 wall_sstiff = 1.e5 wall_fric = .0
set kn_ball = 1.e5 ks_ball = 1.e5 ball_fri 0. ball_dens 1.5
set rme = .0015 rat = 1.5 poros = .2
make_walls
gen_balls
;
save initial.sav
;

def make_walls
dummy = out_rad
dummy = in_rad
dummy = wall_nstiff
dummy = wall_sstiff
dummy = wall_fric
command
  wall id 1 type circle rad out_rad kn wall_nstiff ks wall_sstiff fric wall_fric
  wall id 2 type circle rad in_rad kn wall_nstiff ks wall_sstiff fric wall_fric
end_command
end
;
def gen_balls
 ;--- input data ---
 dummy = kn_ball
 dummy = ks_ball
 dummy = ball_fri
 dummy = ball_dens
 ;--- derived data ---
 tot_vol = pi * (out_rad^2. - in_rad^2.)
 rlo     = 2. * rme / (1. + rat)
 rhi     = 2. * rme * rat / (1. + rat)
 rbar    = 0.5 * (rhi + rlo)
 mult    = 1.6   ; initial radius multiplication factor
 num     = int((1.0 - poros) * tot_vol / (pi * rbar^2))
 rlo_0   = rlo / mult
 rhi_0   = rhi / mult
 command
   gen id=1,num rad=rlo_0,rhi_0 annulus 0. 0. in_rad out_rad tries 1000000
   prop dens=ball_dens kn=kn_ball ks=ks_ball fri=ball_fri
 end_command
 get_poros
```

```
 mult = ((1.0 - poros) / (1.0 - pmeas))^(0.5)
 command
   macro zero 'ini xv 0 yv 0 spin 0'
   macro zerod 'ini xd 0 yd 0'
   ini rad mul mult
 end_command
end
;
def get_poros
 sum = 0.0
 bp  = ball_head
 loop while bp # null
   sum = sum + pi * b_rad(bp)^2.
   bp  = b_next(bp)
 end_loop
 pmeas = 1.0 - sum / (pi * (out_rad^2. - in_rad^2.))
end
;

call initial.dat
;
call control.dat
set cont_type 1 vel_iso 0. vel_rot 0. sigma_r0 10 m_mult 0.1
control
;
call monitor.dat
;
set disp hi 2;

call hist.ini
set cont_type 2 sigma_r0 sigma_r_out vel_rot 0.
control

def ini_wall
  wadd_1 = find_wall(1)
  wadd_2 = find_wall(2)
  out_rad_cur = out_rad
  spessore = out_rad - in_rad
end
ini_wall
;
def eps_ini
   out_rad_0 = out_rad_cur
   spessore_0 = spessore
   rotazione = 0
end
eps_ini

def sig_vel
   massa = m_mult * (ball_dens * pi * rbar^2.) * ((2. * pi * out_rad) / (2.* rbar))
```

```
  sigma_r = sigma_r0
  out_rad_cur = out_rad_cur + w_radvel(wadd_1) * tdel
  rad_req_for = sigma_r * (2. * pi * out_rad_cur)
  rad_cur_for = w_radfob(wadd_1)
  acc_rad = (rad_cur_for - rad_req_for) / massa
  w_radvel(wadd_1) = w_radvel(wadd_1) + acc_rad * tdel
  w_rvel(wadd_1) = vel_rot
end
def vel_vel
  out_rad_cur = out_rad_cur + w_radvel(wadd_1) * tdel
  w_radvel(wadd_1) = vel_iso
  w_rvel(wadd_1) = vel_rot
end
;
def control
  if cont_type = 1 then
    command
      set fishcall 0 remove vel_vel
      set fishcall 0 remove sig_vel
      set fishcall 0 vel_vel
    end_command
  end_if
  if cont_type = 2 then
    command
      set fishcall 0 remove vel_vel
      set fishcall 0 remove sig_vel
      set fishcall 0 sig_vel
    end_command
  end_if
end
```

B.2.2 Test control, Monitoring variable definition and storage setting

```
def monitor
 ttt = time
 spessore = (out_rad_cur - in_rad)
; sforzi
 sigma_r_out = abs(w_radfob(wadd_1)) / (2. * pi * out_rad_cur)
 sigma_r_in  = abs(w_radfob(wadd_2)) / (2. * pi * in_rad)
 tau_out = abs(w_mom(wadd_1)) / (2. * pi * out_rad_cur) / out_rad_cur
 tau_in  = abs(w_mom(wadd_2)) / (2. * pi * in_rad) / in_rad
 torque_out = w_mom(wadd_1)
 torque_in = w_mom(wadd_2)
 fri_out = atan2(tau_out,sigma_r_out)/degrad
 fri_in = atan2(tau_in,sigma_r_in)/degrad
; deformazioni
 delta_h = spessore - spessore_0
 eps_rad = delta_h / spessore_0
 rotazione = rotazione + w_rvel(wadd_1) * tdel * nstep_hist
```

```
 giri = rotazione / (2. * pi)
 gamma = rotazione * out_rad_cur / spessore
end
set nstep_hist 100
monitor
history monitor
history sigma_r_out sigma_r_in tau_out tau_in torque_out torque_in
history delta_h eps_rad rotazione giri gamma ttt
hist n nstep_hist
```

B.2.3 Clusters construction

```
def make_clusters
;definizione cluster
loop nnn (1,nclust)
  angolo = 2. * pi * urand
  posizione = in_rad + (out_rad - in_rad) * urand
  xclust = posizione * cos(angolo)
  yclust = posizione * sin(angolo)
  dclust = dclust_min + (dclust_max - dclust_min) * urand
  rclust = dclust / 2.
  bp = ball_head
  loop while bp # null
   if b_rfix(bp) = 0 then
    distx = b_x(bp) - xclust
    disty = b_y(bp) - yclust
    dist = (distx^2 + disty^2)^0.5
    if dist < rclust then
      cp= b_clist(bp)
      loop while cp # null
        if c_ball1(cp) = bp then
         bp_other = c_ball2(cp)
        else
         bp_other = c_ball1(cp)
        end_if
        if pointer_type(bp_other) = 100 then
        if b_rfix(bp_other) = 0 then
          c_nstrength(cp) = bond_ns_strong
          c_sstrength(cp) = bond_ss_strong
          count_bonds = count_bonds + 1
          b_xfix(bp_other) = 1
          b_xfix(bp) = 1
        end_if
        end_if
        if c_ball1(cp) = bp then
          cp = c_b1clist(cp)
        else
          cp = c_b2clist(cp)
        end_if
```

```
      end_loop
     end_if
    end_if
    bp = b_next(bp)
   end_loop
   bpp = ball_head
   loop while bpp # null
    if b_xfix(bpp) = 1 then
      b_rfix(bpp) = 1
      b_xfix(bpp) = 0
    endif
    bpp = b_next(bpp)
   end_loop;
end_loop
cp = contact_head
 loop while cp # null
 if c_nstrength(cp) = 1.e10 then
    c_nstrength(cp) = 0.
    c_sstrength(cp) = 0.
 end_if
 cp = c_next(cp)
end_loop
if delball = 1 then
 bpp = ball_head
 loop while bpp # null
    bnext=b_next(bpp)
    if b_rfix(bpp) = 0 then
      iii = del_ball(bpp)
   endif
   bpp = bnext
 end_loop
endif
command
  free spin
end_command
end
def real_bond
 cp = contact_head
  loop while cp # null
  if c_nstrength(cp) = bond_ns_strong then
    c_nstrength(cp) = bond_ns
    c_sstrength(cp) = bond_ss
  end_if
  cp = c_next(cp)
  end_loop
end
```